Inorganic nanoparticulate materials: Characterization and applications

1. MFNP & Optical methods

- in situ UV-vis growth monitoring
- global approach to separation and analysis
- applied NP - ligand strategies
  Eco/Life sciences:
- surface chemistry,
- plasmon, luminescence

2. Solar sector

- NP-thermodynamics/kinetics
- Photocatalysis
- Solar cells

3. ICT sector

(Information and communication technology)

- Transparent conductors
- electrochromy/electroluminescence
- planar wave guides and web amplifiers

4. Fractal approach to analysis

- introduction to fractals
- concept of fractal dimension
- examples of D_f determination

L. Spanhel

Ch 1. Optical monitoring, total analysis and tailoring

multifunctional nanoparticles MFNP (sizes << 100 nm)

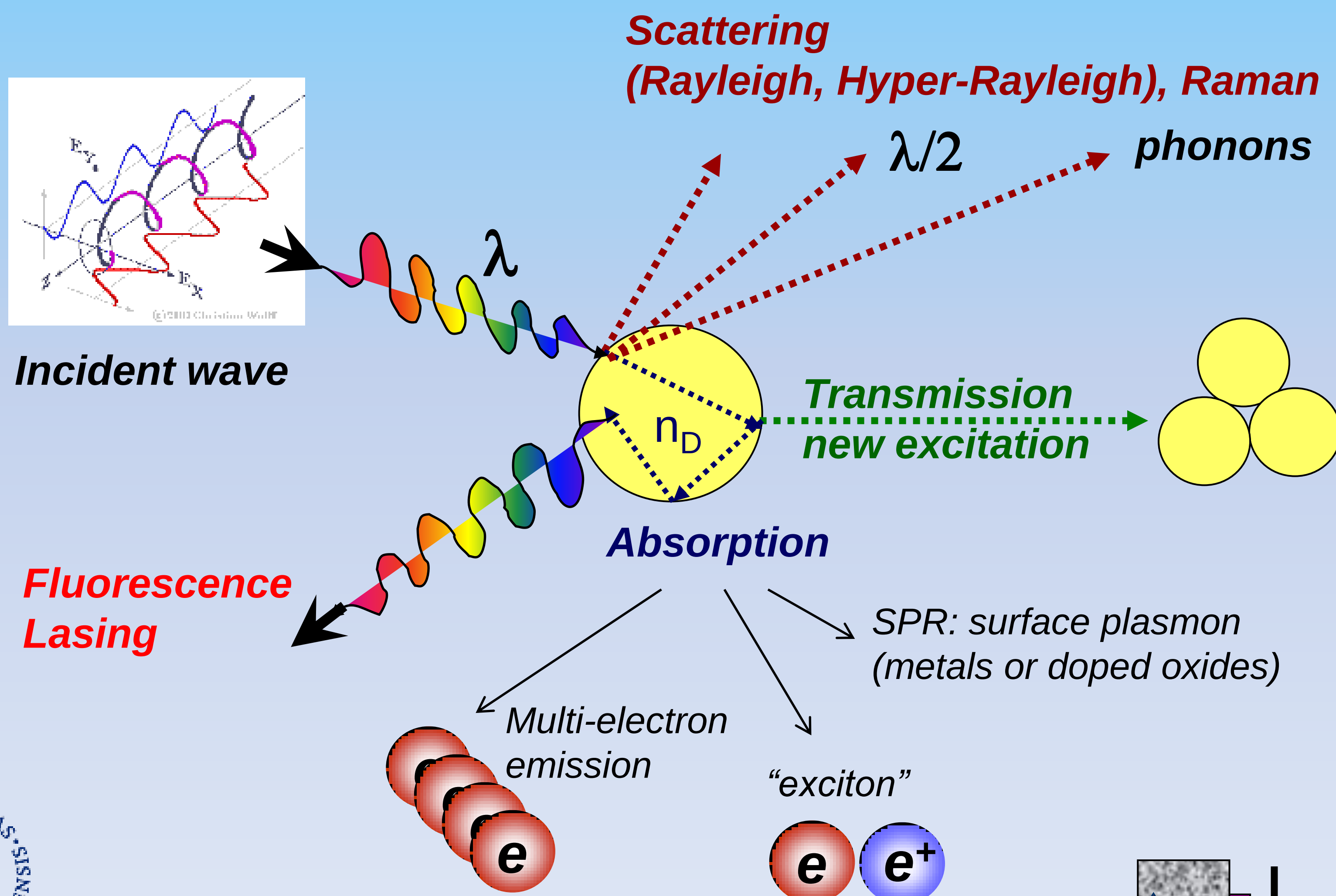

L. Spanhel

Nanostructures semi-conductrices :
Le gap optique varie avec la taille des particules!!

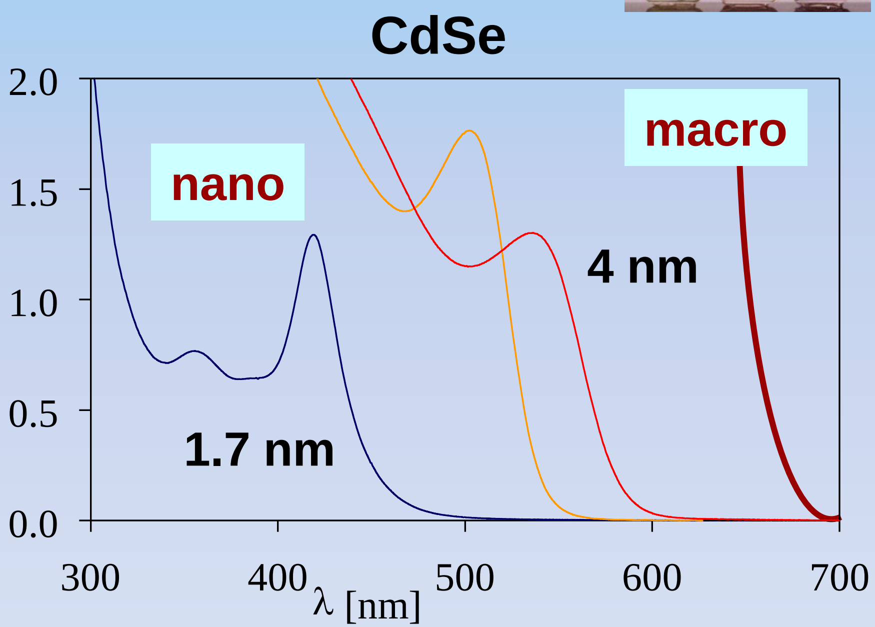

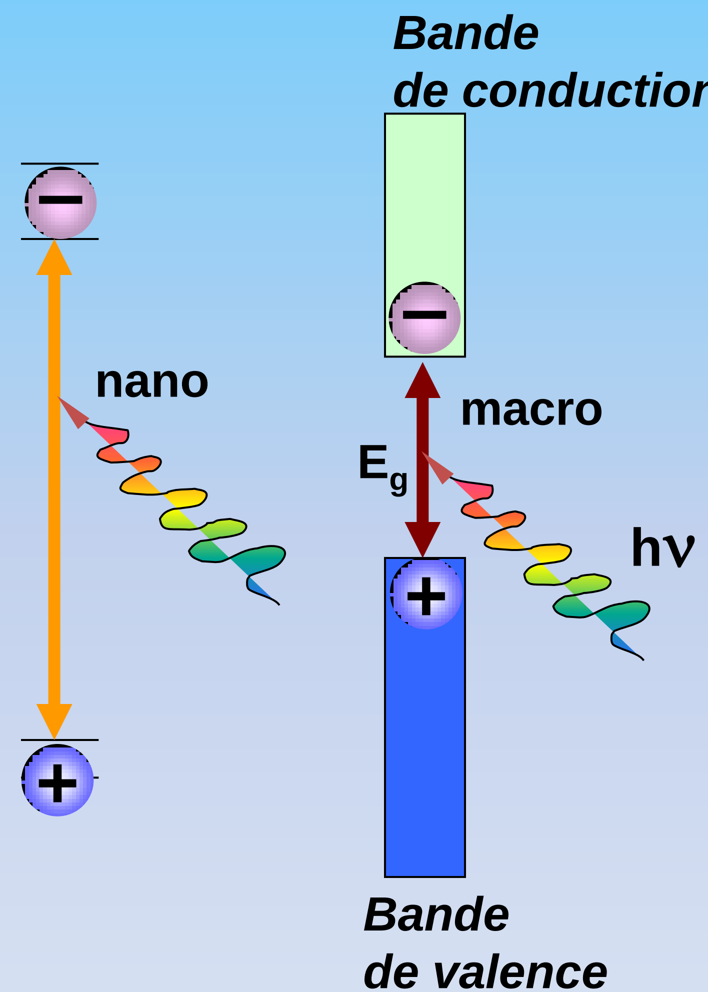

$$E(eV) \sim 1240/ \lambda\ (nm)$$

L. Spanhel

Optical absorption in ZnO et TiO_2

ZnO
size ~ 5 nm

singles

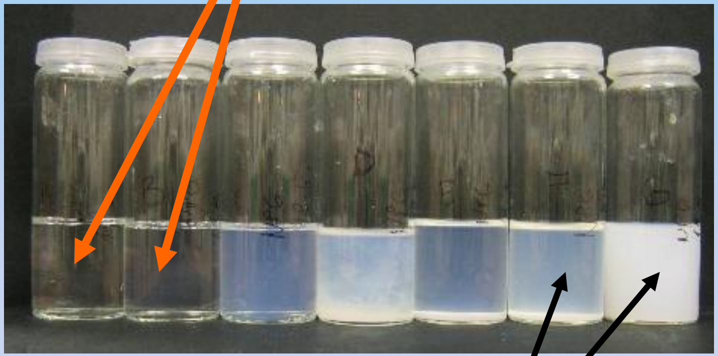

TiO_2
size ~ 5 nm

Aggregation

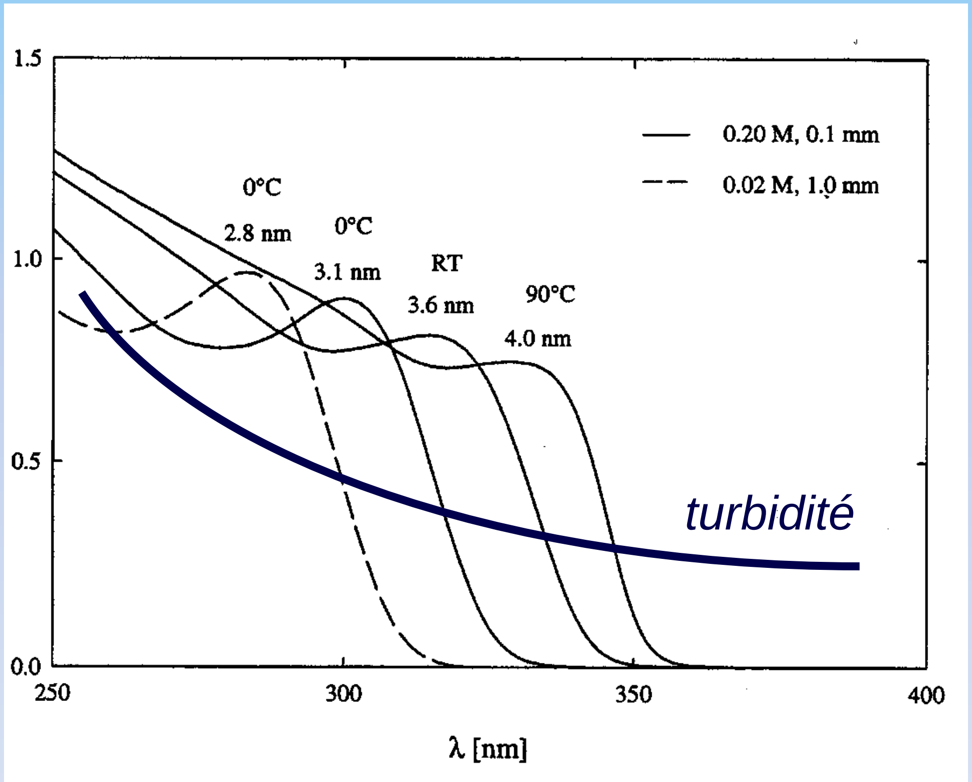

L. Spanhel

Size dependent spectral shift for R(particle) < R (exciton)
"Gap-Size" correlation function

L. Brus 1983

$$E_{nano}[eV] = E_g^{bulk}[eV] + \frac{h^2}{8\mu_{eff} R_p^2} - \frac{1.8e}{4\pi\varepsilon_r\varepsilon_0 R_p}$$

$$ZnO:$$

$$E_{nano}[eV] = 3{,}37 - \frac{1.35}{D_p} + \frac{8.47}{D_p^2}$$

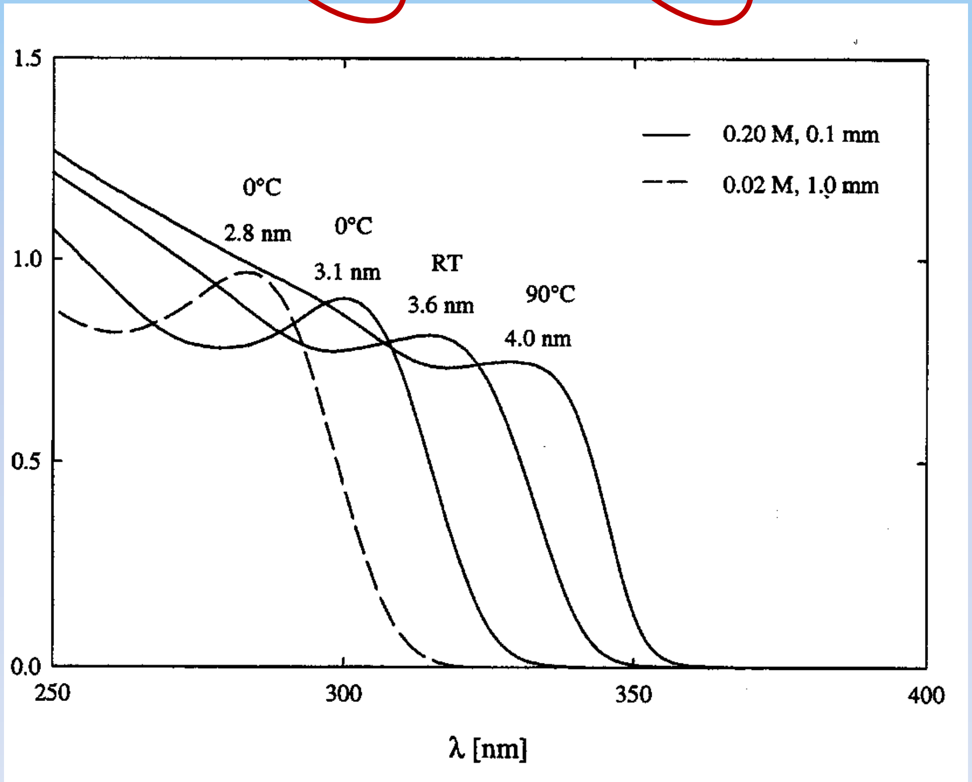

E = gap energy (eV)
μ_{eff} = effective exciton mass
ε_r = dielectric constant
ε_0 = vacuum permittivity = 8,854 10^{-12} Fm^{-1}
Dp, R_p = particle diameter , radius) (m)
e = elementary charge = 1,602 10^{-19} As
h = Planck constant = 6,626 10^{-34} J s

Now even more general

L. Spanhel

A,B,C: coefficients to be determined via linear regression

$$ZnO:$$

$$E_{nano}[eV] = A - \frac{B}{D_p} + \frac{C}{D_p^2}$$

Optical absorption spectrum

XRD/HRTEM

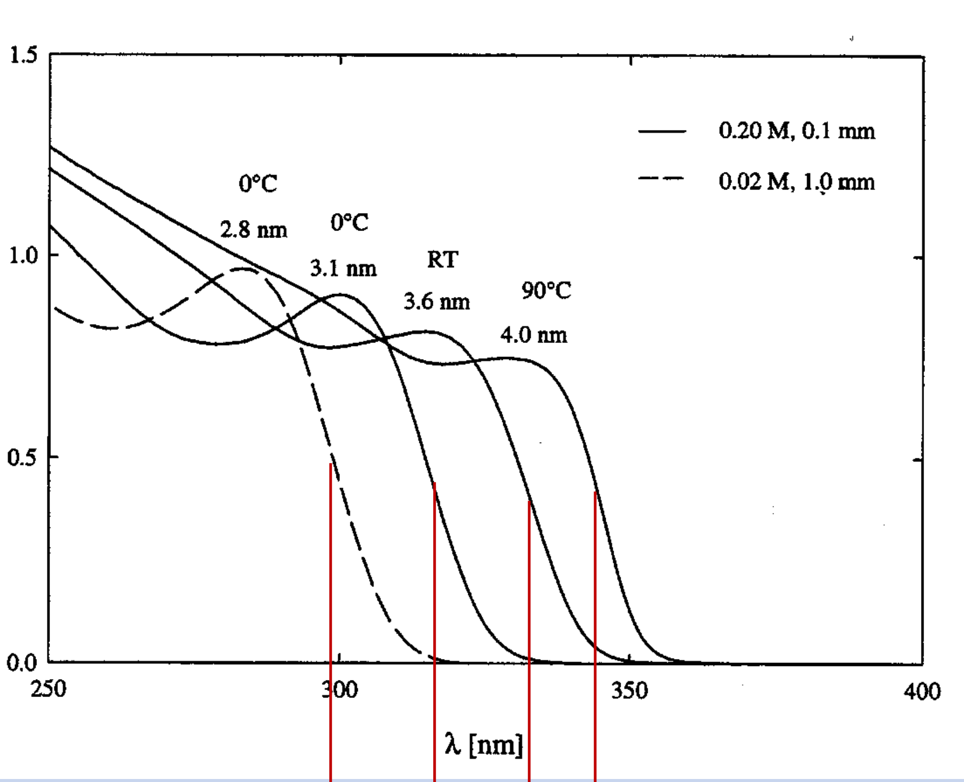

$$E_{nano}[eV] = \frac{1240}{\lambda(nm)}$$

Meulenkamp's finding, JPC B, 1998

$$ZnO:$$

1.37 8.47

$$E_{nano}[eV] = 3.3 - \frac{1.09}{D_p} + \frac{294}{D_p^2}$$

Joshua Jortner, 1991:

$$P_{nano}(N) = P_{makro} + \alpha N^{-\beta}$$

P = property
N = atomic number in cluster
α, β = empirical coefficients

Power law relationship

Number of molecules per particle

$$N_a = \frac{4\pi R_p^3 M_r N_A}{3\rho_p} = V_p \times N_A \times V_m^{-1}$$

V_p =particle volume
N_A = Avogadro number
V_m = molar volume

L. Spanhel

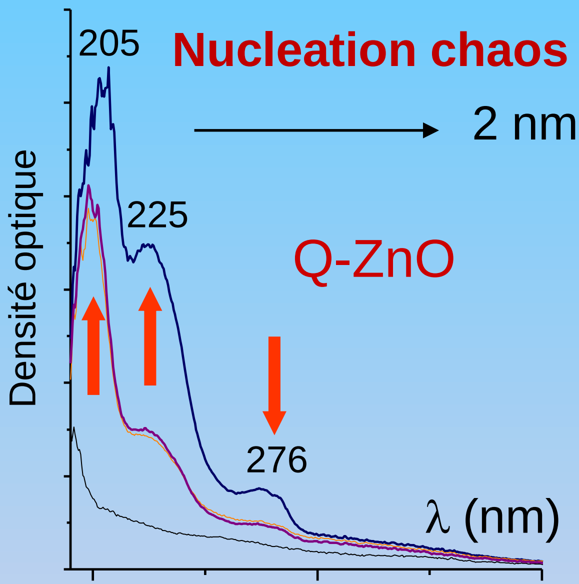
205
Nucleation chaos
2 nm
225
Q-ZnO
276
λ (nm)
Densité optique

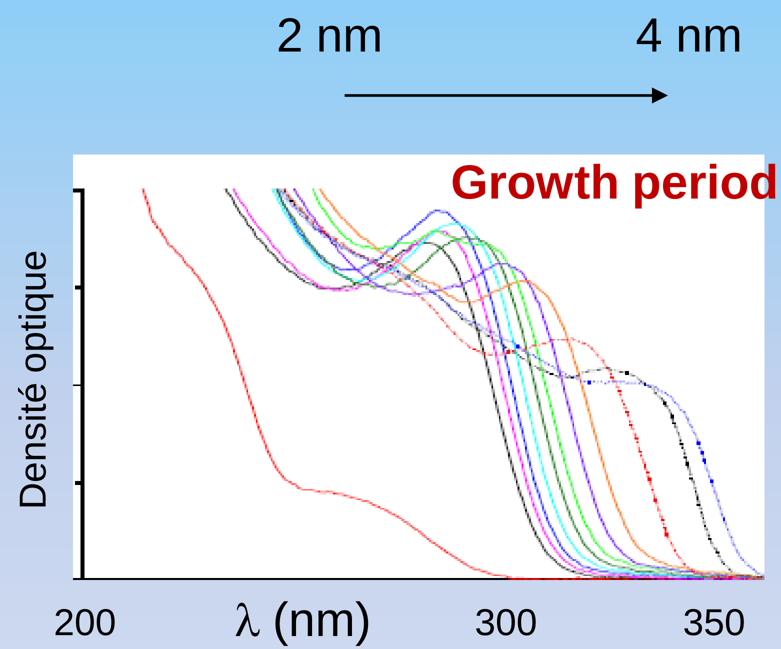
2 nm
4 nm
Growth period
Densité optique
200
λ (nm)
300
350

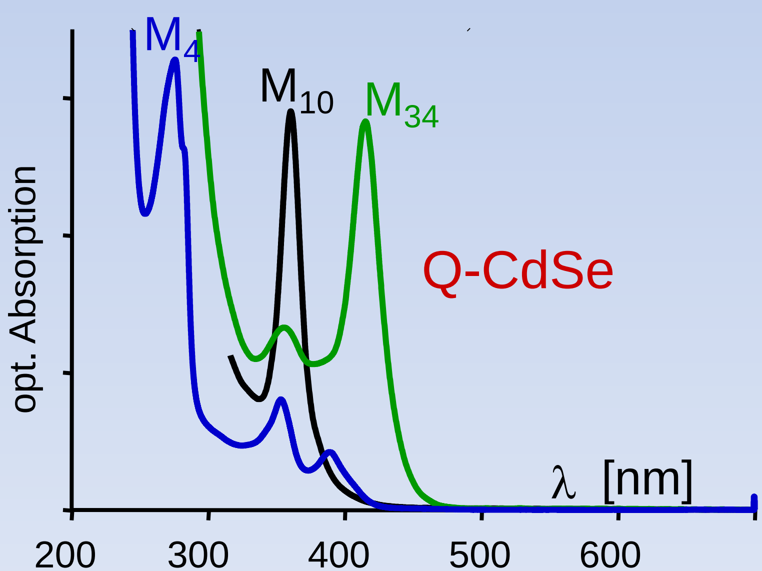
M_4
M_{10}
M_{34}
Q-CdSe
λ [nm]
opt. Absorption
200
300
400
500
600

L. Spanhel

$$\Delta E = \alpha \times N^{-\beta}$$

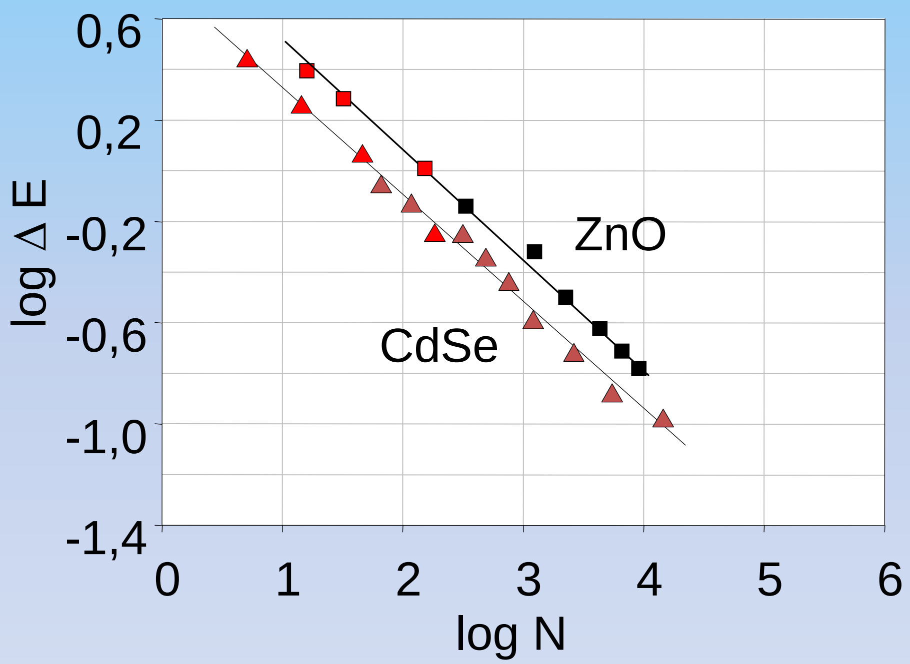

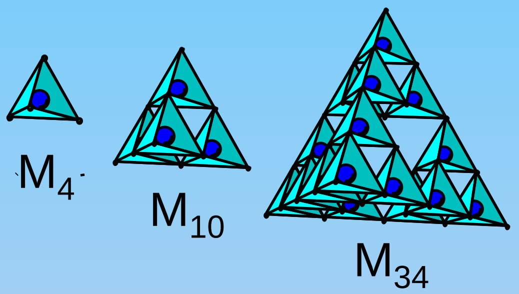

Chemical elemental analysis, MS, etc..needed to identify the clusters

α, β = ?
Physical meaning of α,β remains to be searched !!

L. Spanhel

Recall:

Absorption laws

Photophysics

$$I_T / I_0 = T = e^{-\alpha x}$$

α [cm^{-1}] = absorption coefficient

x = mean light path

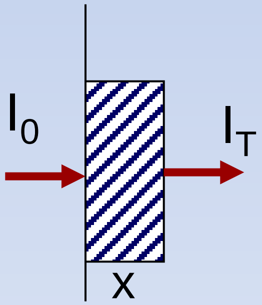

film

$$\alpha = 2{,}3\ \varepsilon / V_m$$

V_m = molar volume

Photochemistry

$$I_T / I_0 = T = 10^{-\,D.O.}$$

ε [Lmol^{-1}cm^{-1}] = molar extinction

c [molL^{-1}] = molarity

d = cell thickness

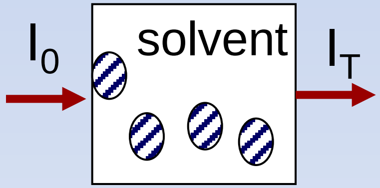

sol

L. Spanhel

Optical monitoring of the particle size distribution (PDS)

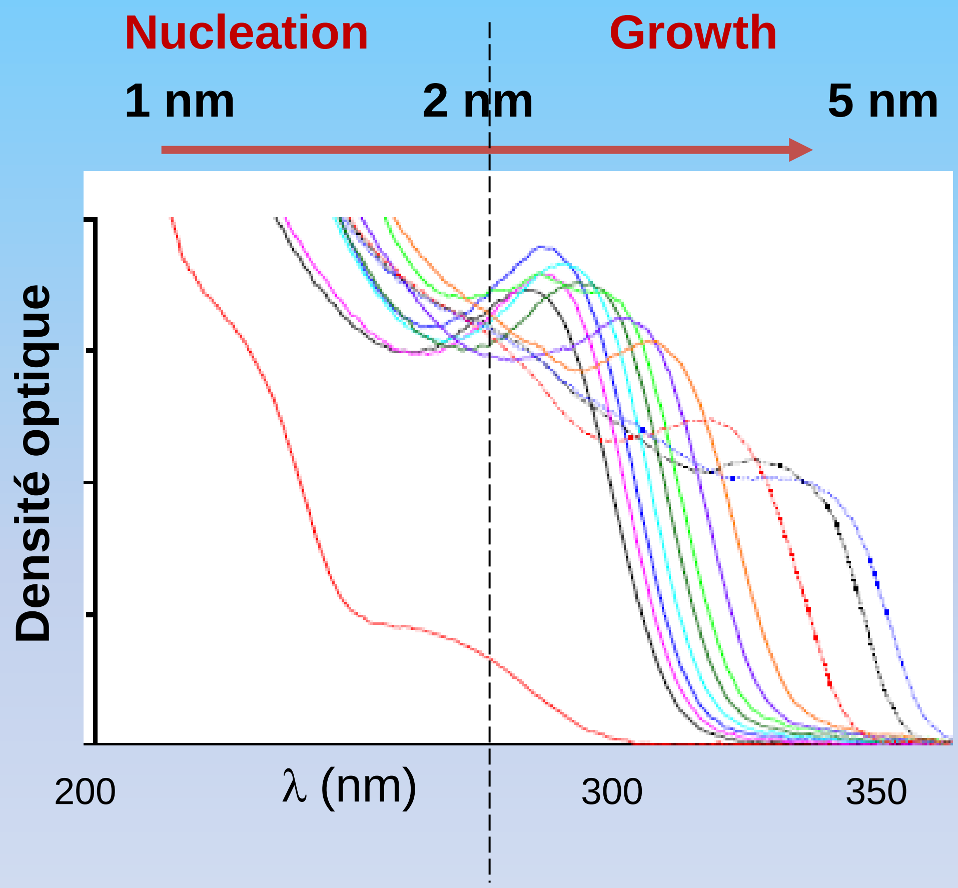

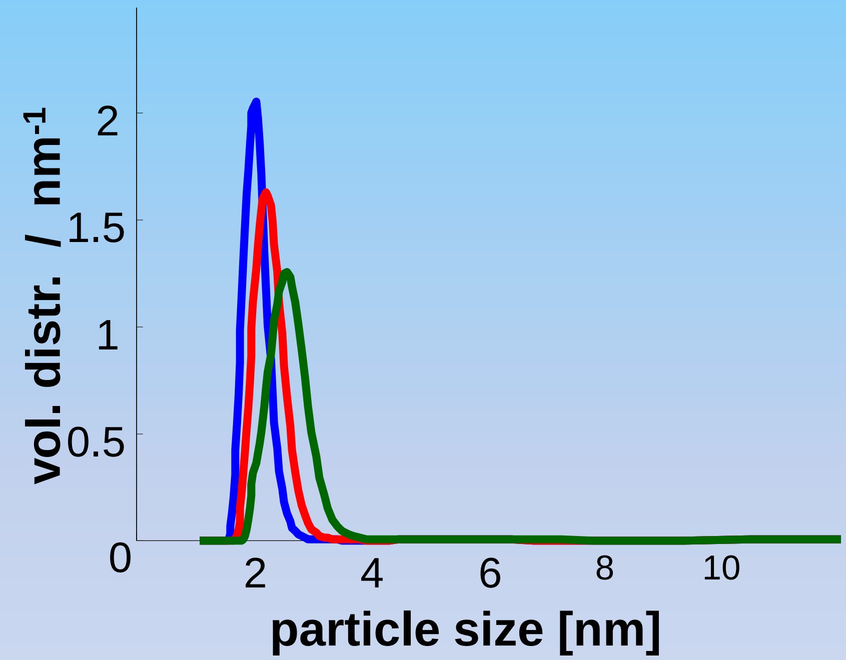

E_g (eV) = 1240 / λ(nm) ~ f(R^{-2}, R^{-1}, $R^{-\beta}$)

L. Spanhel

Structural/optical monitoring of NP's Up-scaling processes

Precursors in Y-shaped micromixer

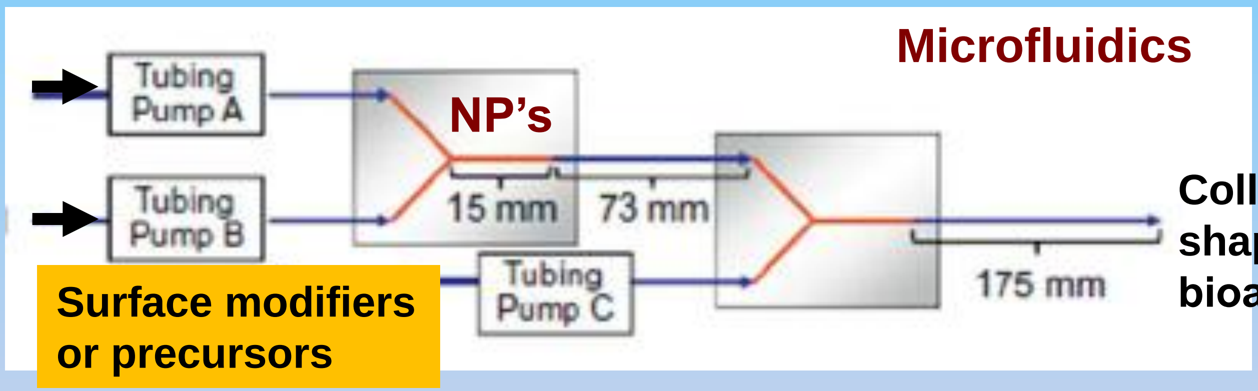

Collection of shape-tuned bioactive NP's

Precursors in T-shaped micromixer

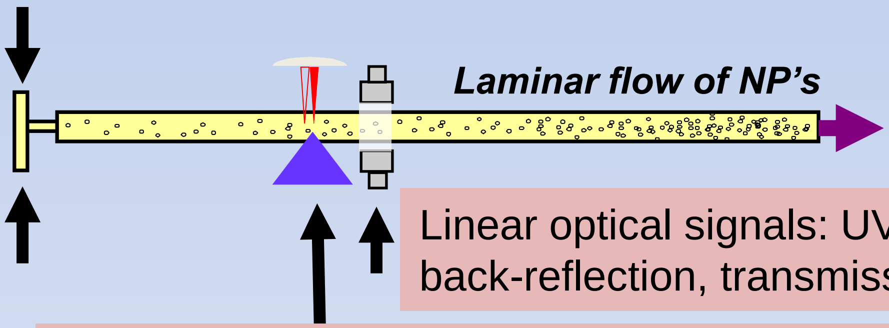

Linear optical signals: UV-vis/NIR absorption, back-reflection, transmission, fluorescence

SAXS: small angle X-ray scattering (gyration size, aggregate structures)
Raman analysis of phonons (lattice and superficial molecular vibrations,
fs-Laser induced non-linear optical signals

L. Spanhel

Spinning disc processor SDP: a way to nano-ZnO Up-scaling

LiOH, NaOH or KOH

Zn-precursor

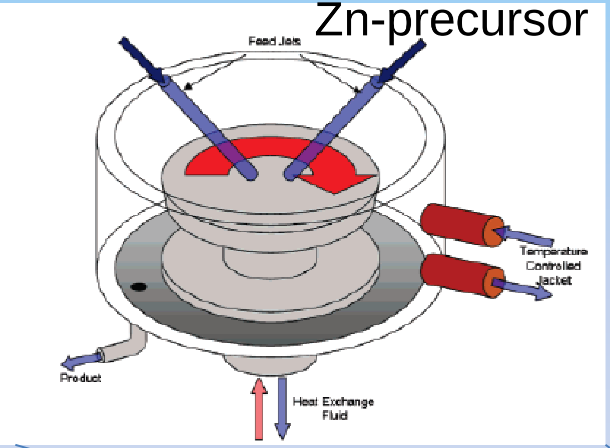

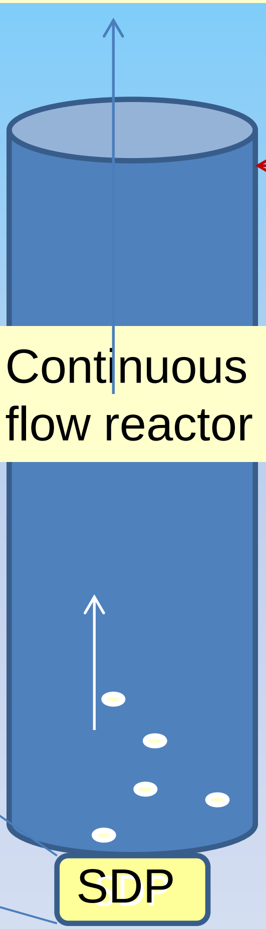

Fiber optical spectrometer

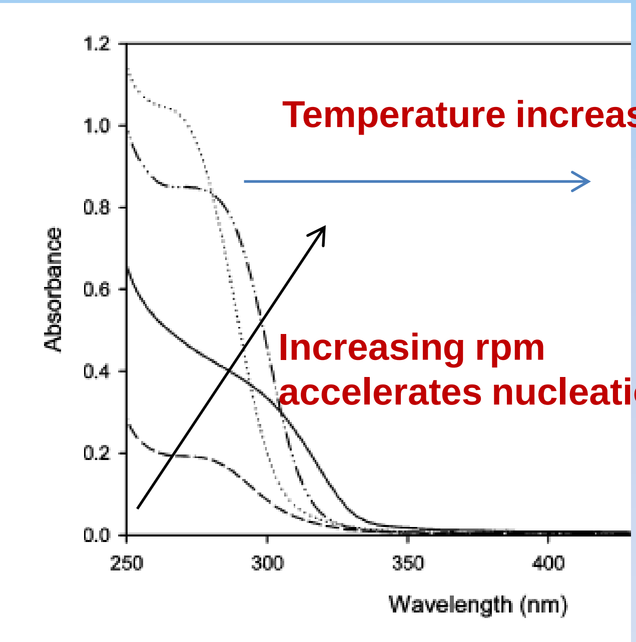

Hartlieb et al, Chem. Mater. 2007

L. Spanhel

Coupled linear UV-vis and non-linear optical (HRS) nanocolloid growth monitoring

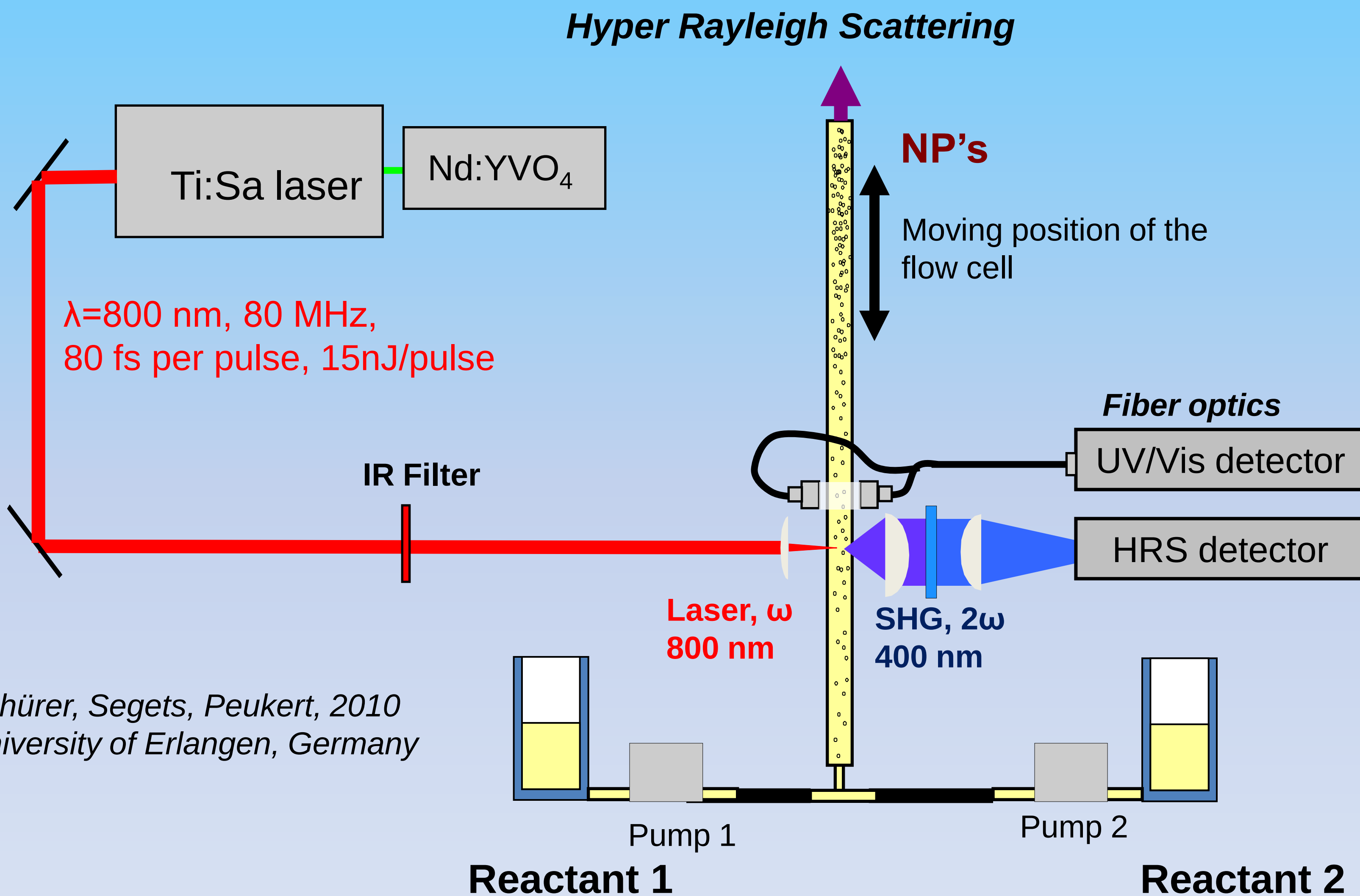

Schürer, Segets, Peukert, 2010
University of Erlangen, Germany

L. Spanhel

Essentials of non-linear optics

P [C/m²] = Polarisation

$$P = \varepsilon_0 \left(\chi^{(1)} E_{lin} + \chi^{(2)} E^2 + \chi^{(3)} E^3 + \ldots\ldots\right)$$

Linearity: n, ε = c^{te}

Non-linearity: n, $\varepsilon \neq c^{te}$

$\chi^{(1)}$ = F(n, ε_r)

= el. susceptibility

n = refractive index

ε_r= dielectric coefficient

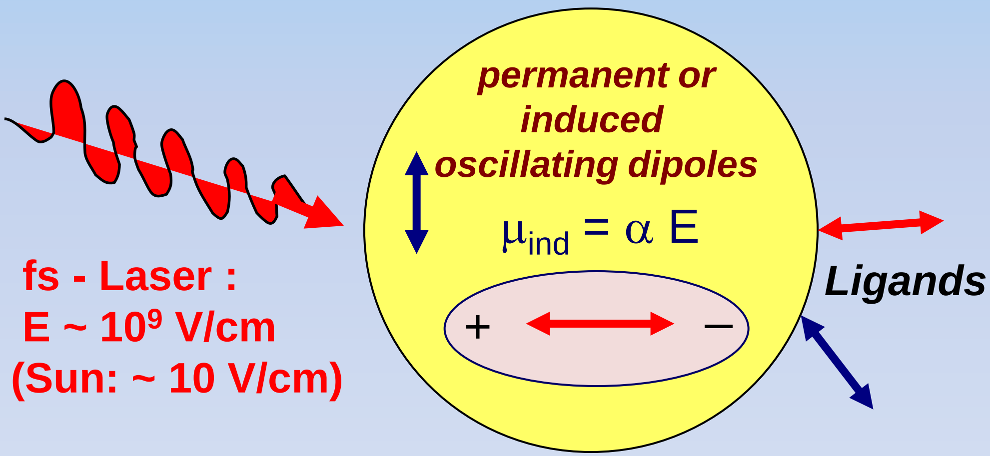

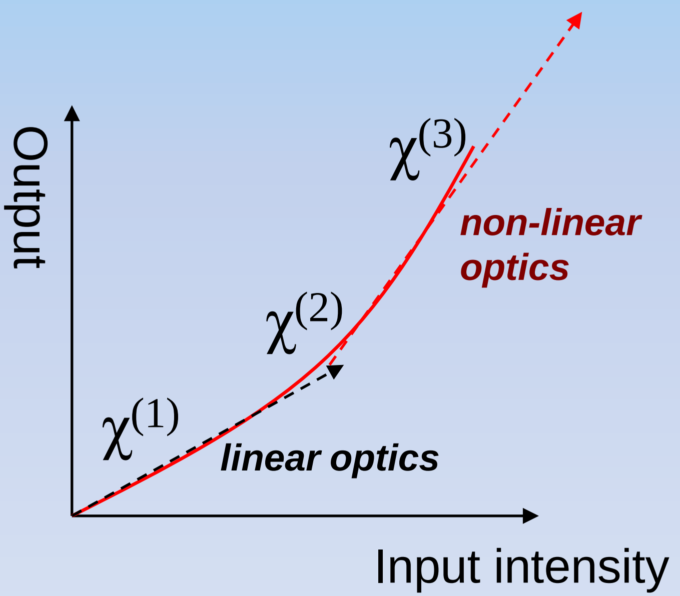

L. Spanhel

In our case:

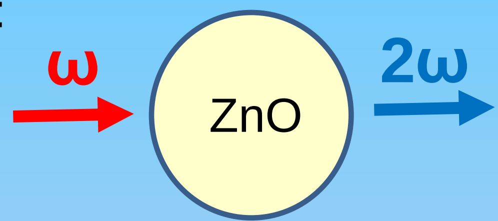

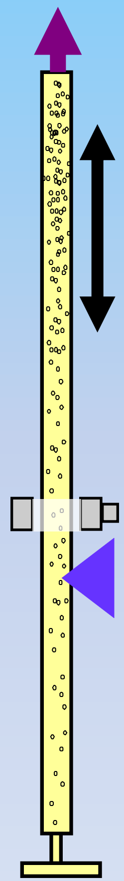

UV
HRS

LiOH + Zn-precursor

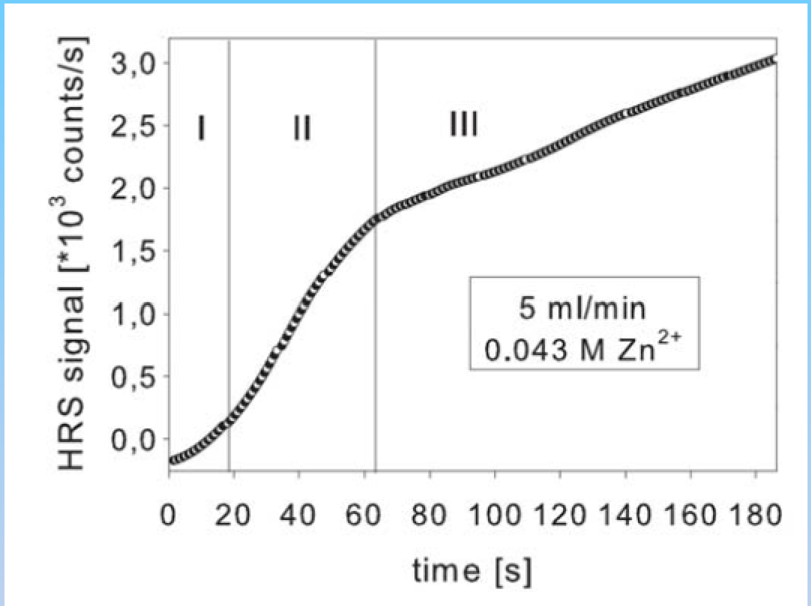

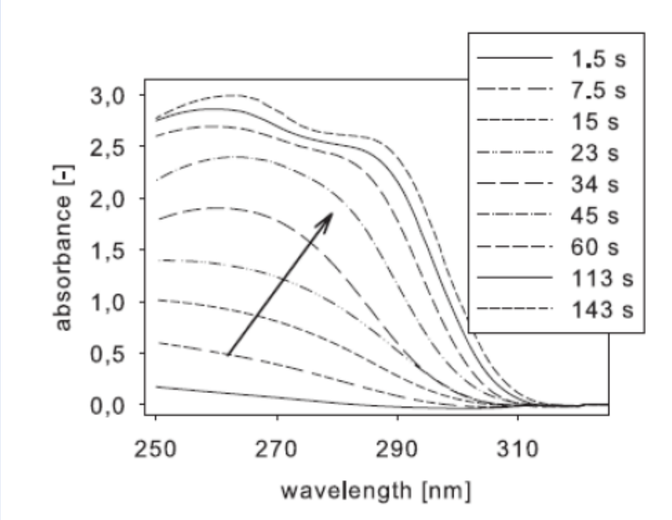

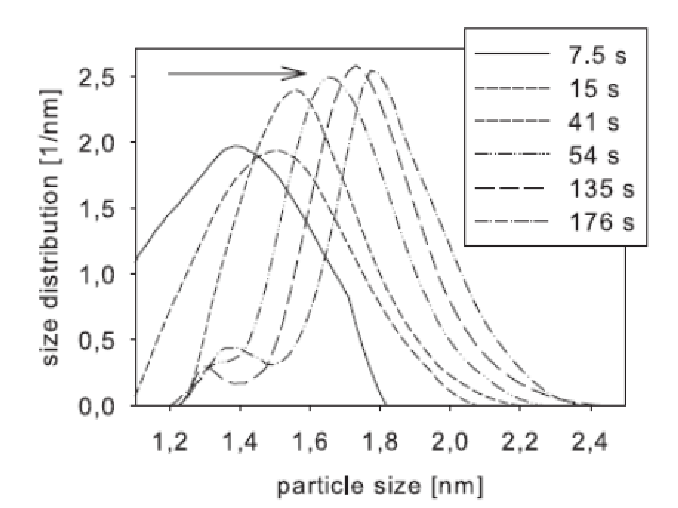

L. Spanhel

Isolation and total chemical analysis of monodispersed NP's

Goal: quantification of atoms and molecules inside and in shells
ligand exchange and addition processes
tailoring for biomedicine (theranostics) and standardizations

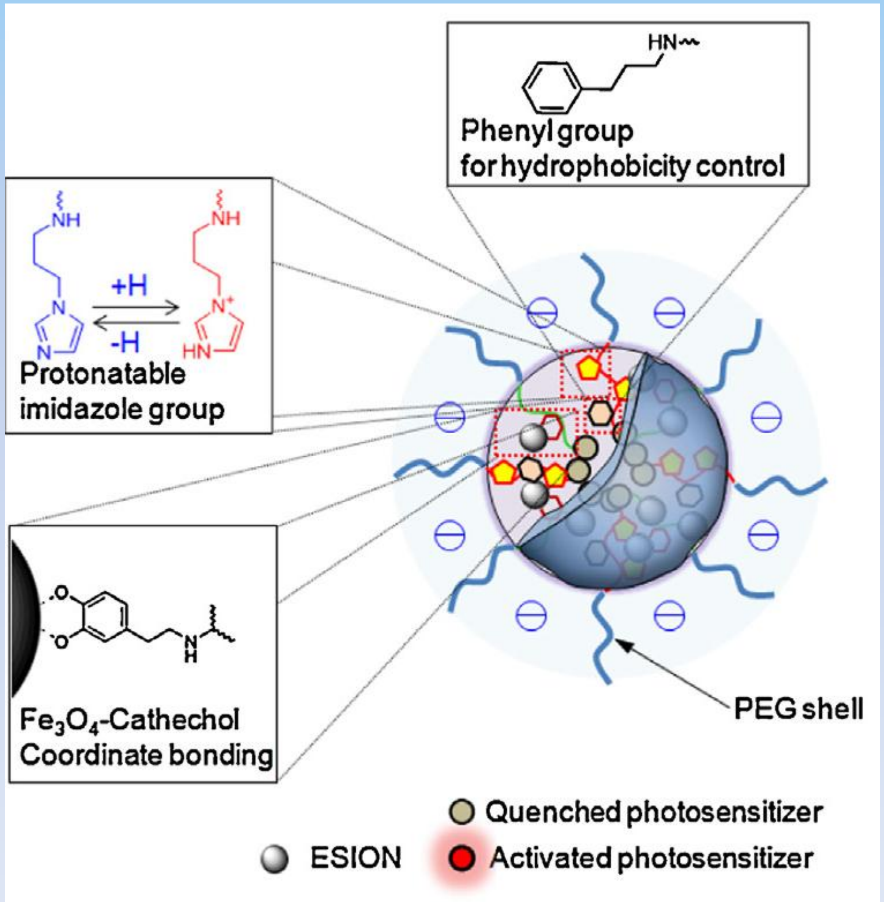

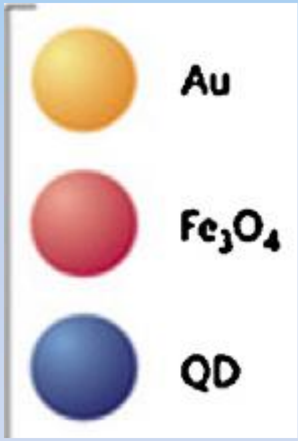

T. Hyeon et al in Nano Today 2014

L. Spanhel

Characteristic parameters of spherical nanoparticles

sample	n_A	$(n_s/n_A) \times 100$ [%]	$A = 3/R_p\rho$ [m^2/g]	$V_m = M/\rho$ [cm^3/moL]
SiO_2	92 R^3	82	1132	60,08 / 2,648
TiO_2	99 R^3	81,7	750	101,96 / 4,00
Al_2O_3	126 R^3	78	709	79,86 / 4,23
ZnO	174 R^3	74	535	81,4 / 5,6
Ag	245 R^3	68	285	107,86 / 10,49
Pt	277 R^3	67	139	195,08 / 21,45

R_p = 1 nm

R_p = radius
M_r = molar mass
ρ_p = density
A = spec. surface area
V_m = molar volume

"agglomeration number" molecules per particle

$$n_A = \frac{4\pi R_p^3 M_r N_L}{3\rho_p}$$

Number of surface molecules

$$n_s \approx (n_A)^{2/3}$$

L. Spanhel

FFF Forced Field Fractionation

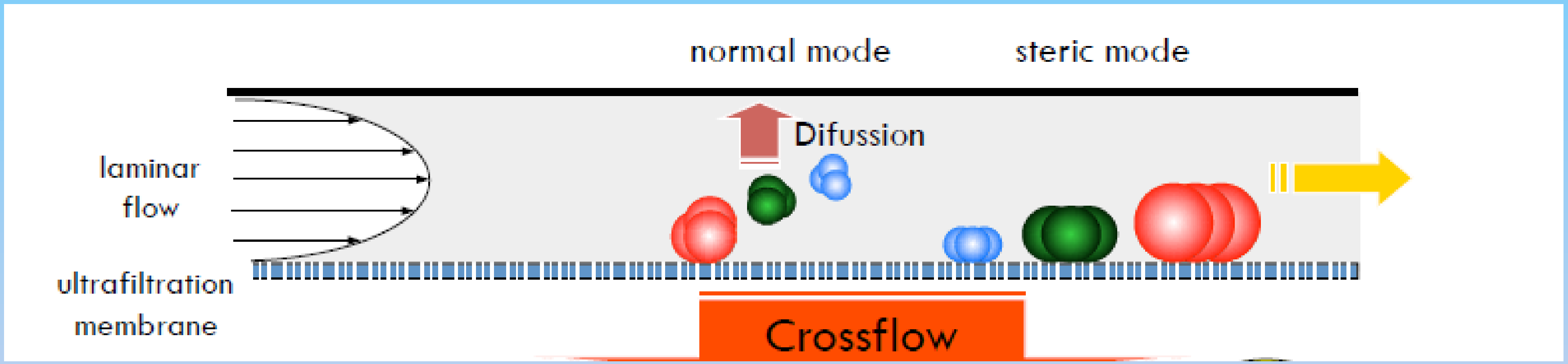

ppb-range!

L. Spanhel

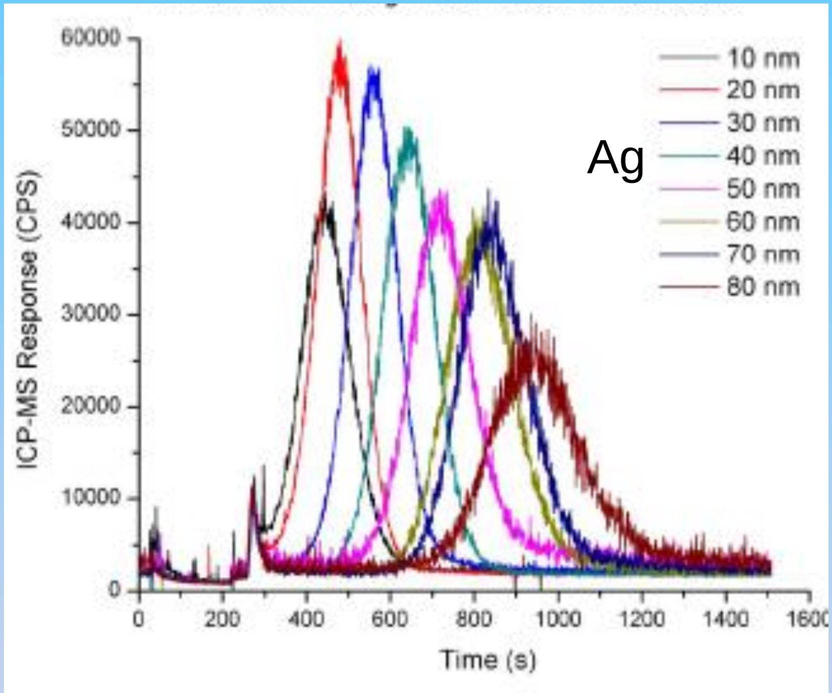

FFF-ICP-MS in comparison with HRTEM and DLS

Note!:
FFF-ICP-MS : ~ µg/L
HRTEM-DLS : ~ mg/L

Nominal	10nm	20nm	30nm	40nm	50nm	60nm	70nm	80nm
TEM	9±1	20±1	32±4	42±4	55±5	67±4	72±3	84±5
DLS	22 (11 - 84)	29 (13 - 90)	41 (15 - 124)	51 (35 - 113)	54 (14 - 121)	67 (32 - 133)	74 (64 - 104)	86 (58 - 142)
FFF-ICP-MS	26	31	40	52	61	75	76	86

Chapter 2 solar sector

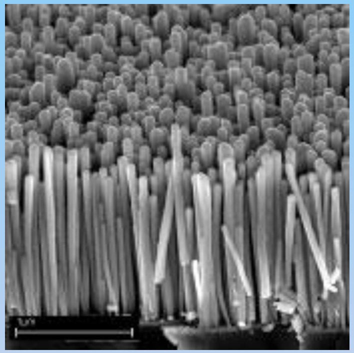

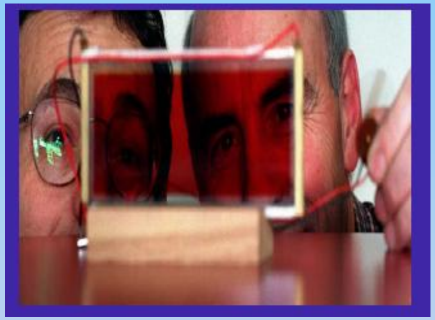


Inorganic nanostructures and Solartech

Introduction to renewable energy resources
Theory and applications of nanoscaled photocatalysts
Classical photovoltaics and future solar cells on the nanoscale

L. Spanhel

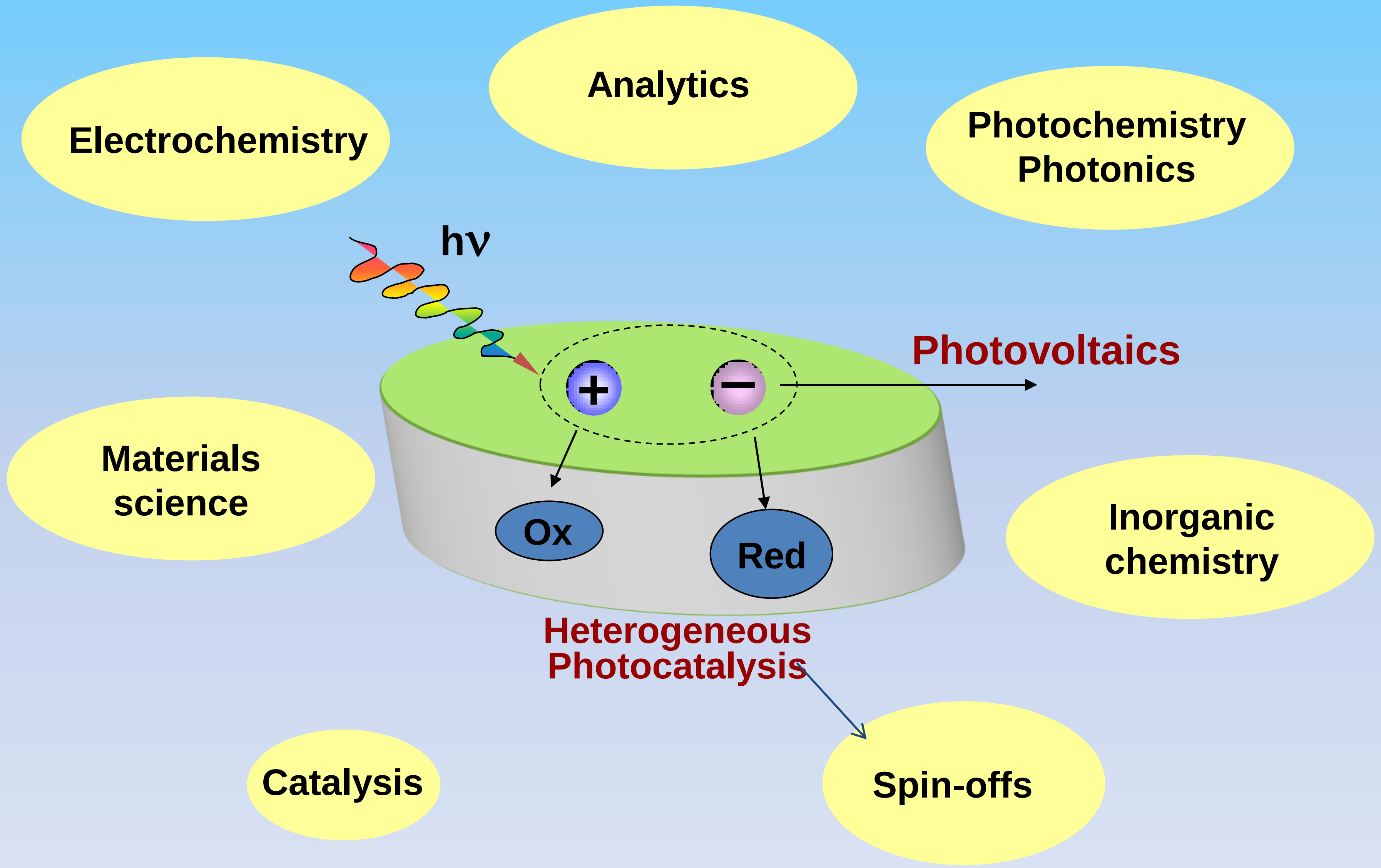
Analytics
Electrochemistry
Photochemistry
Photonics
hν
Photovoltaics
Ox
Red
Materials
science
Inorganic
chemistry
Heterogeneous
Photocatalysis
Catalysis
Spin-offs

L. Spanhel

Energy resources of 21 century

Cosmic neutrino field

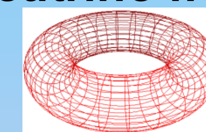

Photovoltaics

Photocatalysis

decentralized energy

CO_2/H_2 storage
CH_4/CH_3OH storage

light
heat
transport

Nuclear power

Green synthetic chemistry
UV protection
Detox of ecosystems

L. Spanhel

Veselovskii & Shub 1952

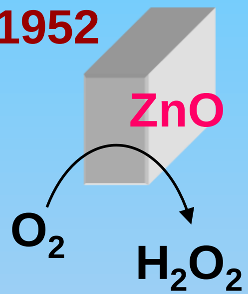

Fujishima & Honda 1972

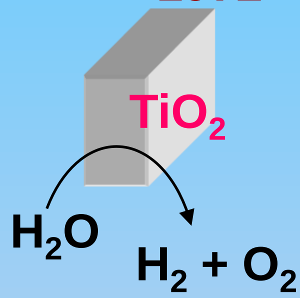

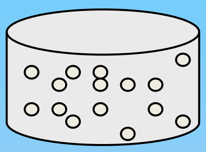

preparative org. synthesis

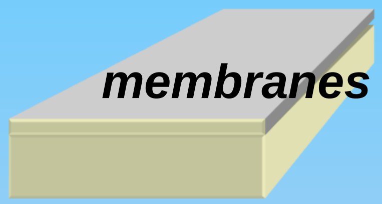

environmental applications

TiO_2, ZnO, Fe_2O_3, CdS, ZnS, …

1839 1954 1980 nanotechnology 2010

History of solar technology

Photoelectric effect

A. Becquerel

PV 1. generation → mono-Si

Chapin, Fuller, Pearson

PV 2. generation → a-Si, CdTe, $CuInSe_2$

PV 3. generation → nanostructures, metamaterials

L. Spanhel

Semiconductor (SC) nanoelectrodes in solar sector

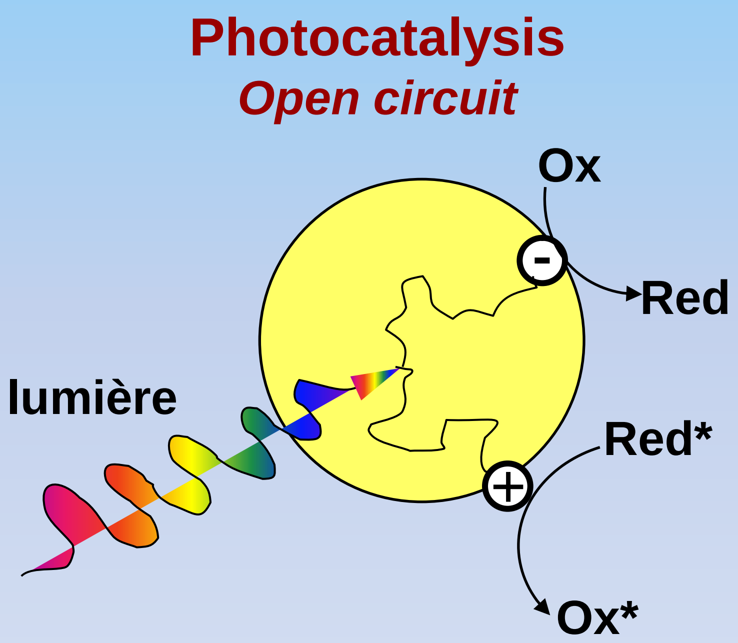

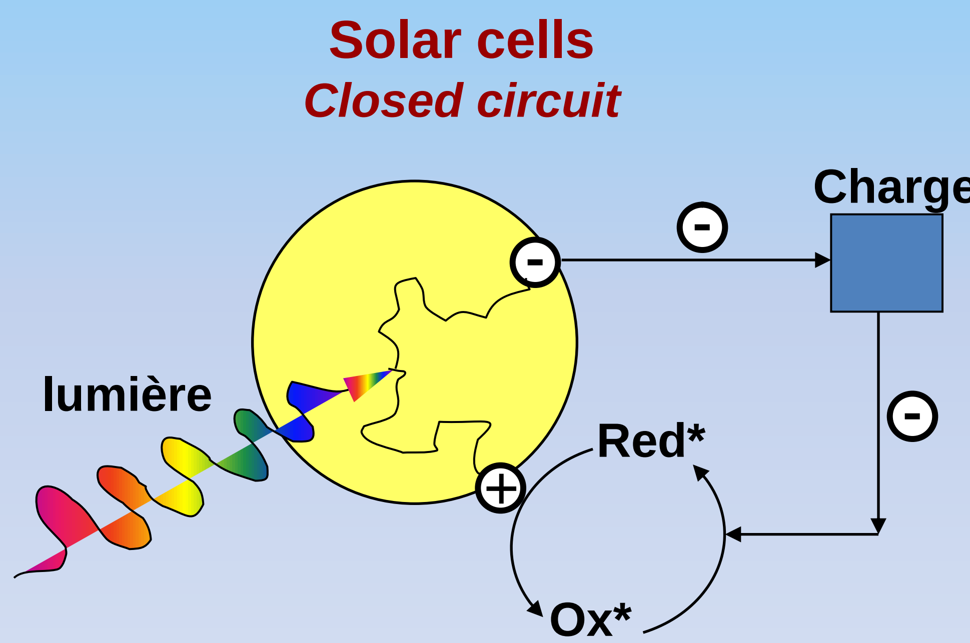

L. Spanhel

Emission spectrum of our sun

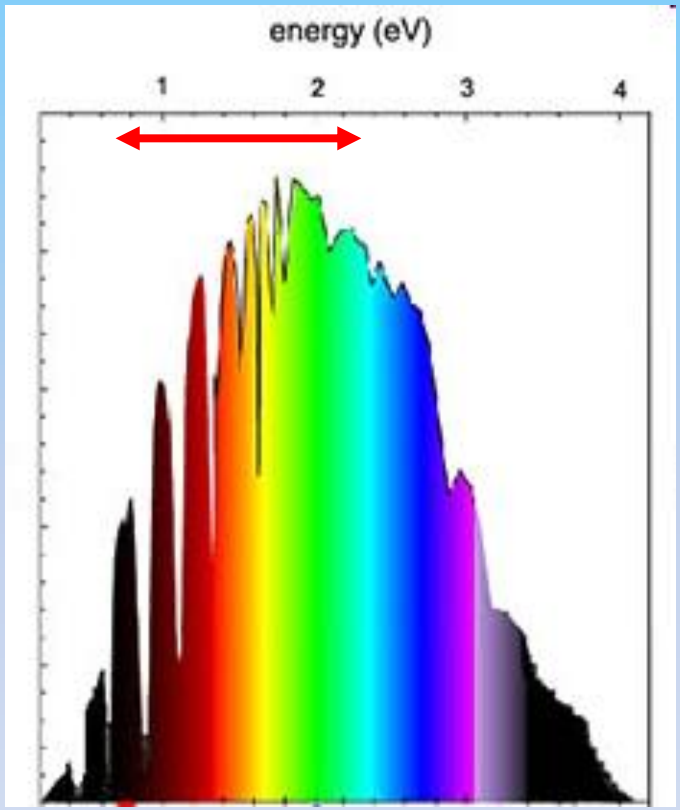

Sun spectrum

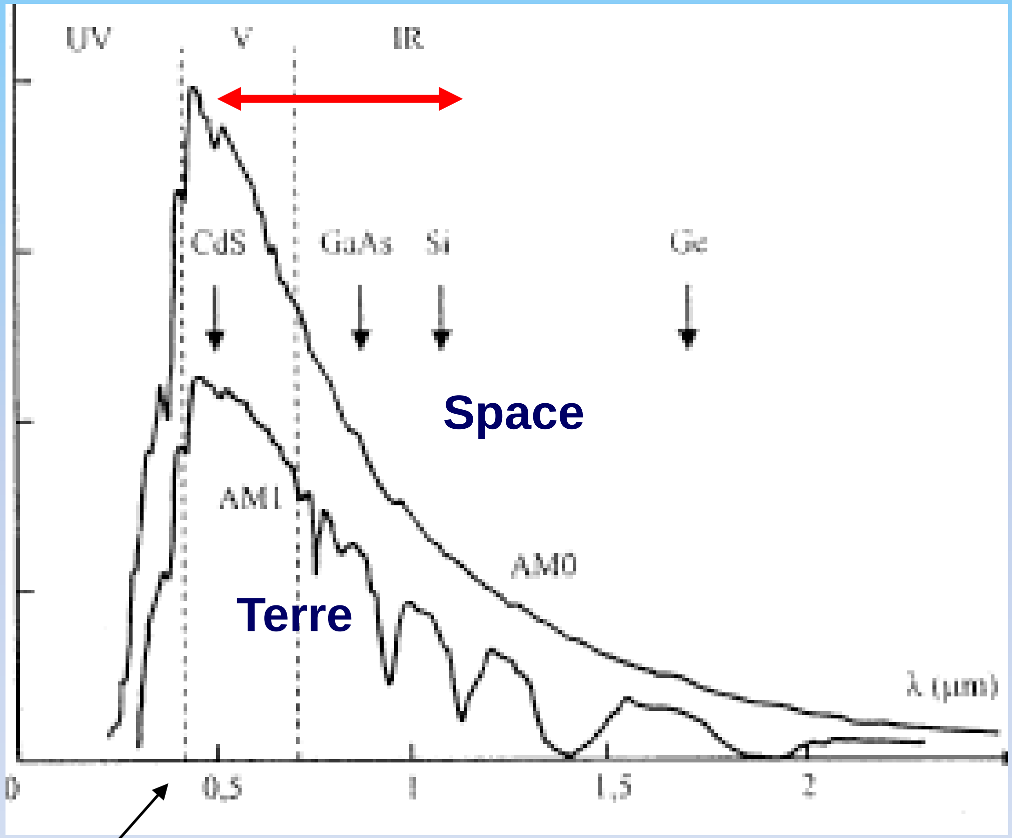

E = hc/λ

SC - Electrochemistry: from micro to nano scale

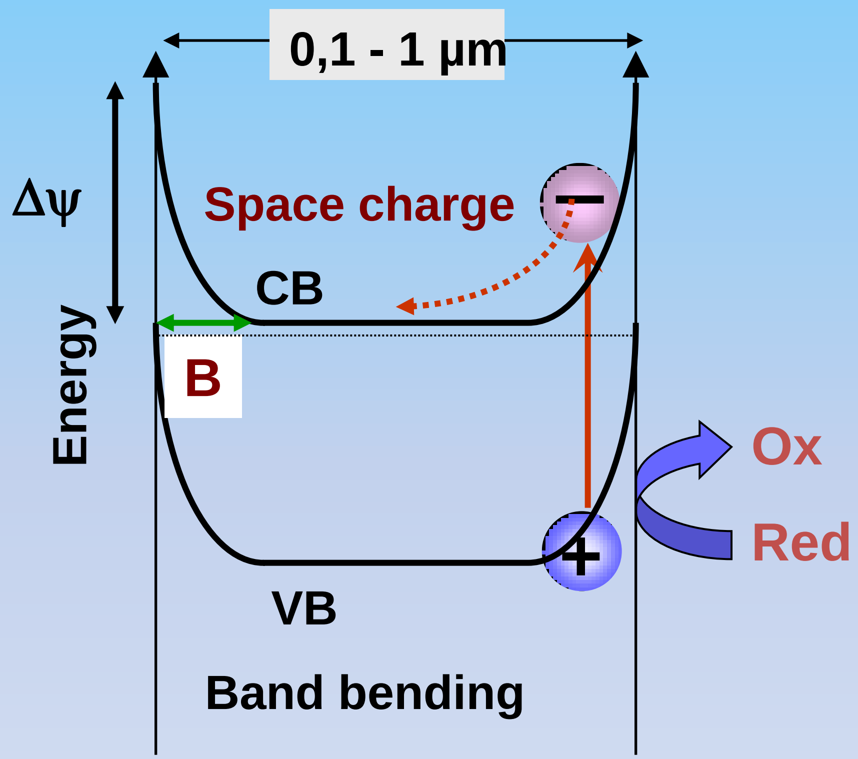

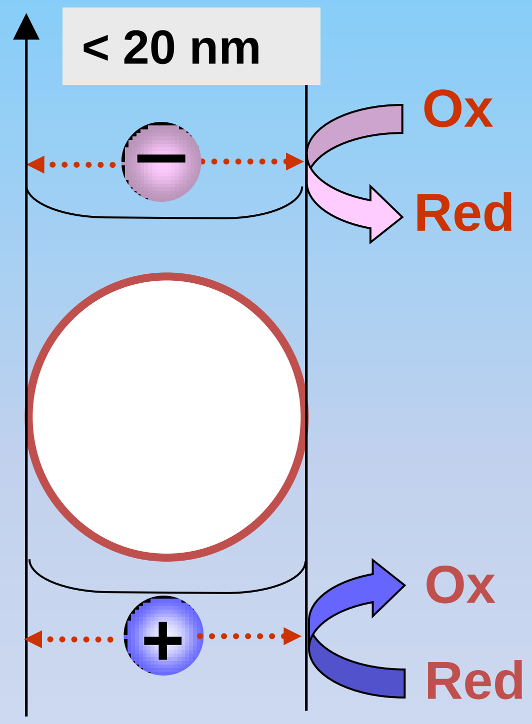

$$\Delta\psi = \frac{kT}{2e}\cdot\left(\frac{B}{1/\kappa}\right)^2$$

$$\Delta\psi = \frac{kT}{6e}\cdot\left(\frac{R_p}{1/\kappa}\right)^2$$

Thermodynamics and kinetics of semiconductor photocatalysis

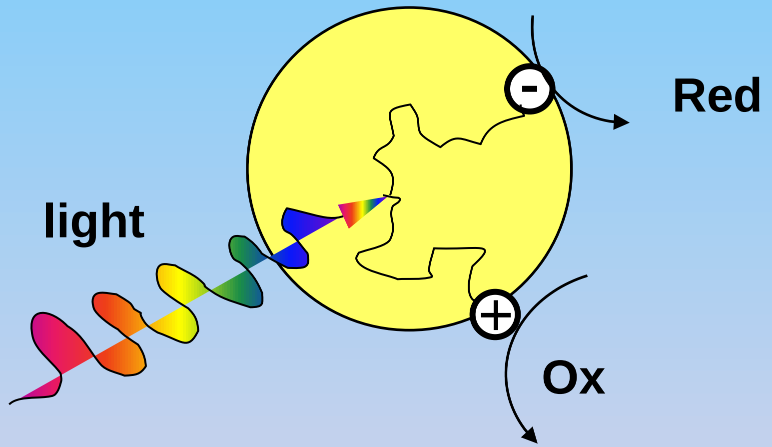

1. Driving force of interfacial red ox processes
   $E_{CB,VB}$, E° (red ox)

2. Elementary processes in photoexcited nanoparticles:
   diffusion, recombination, transfer, reaction

L. Spanhel

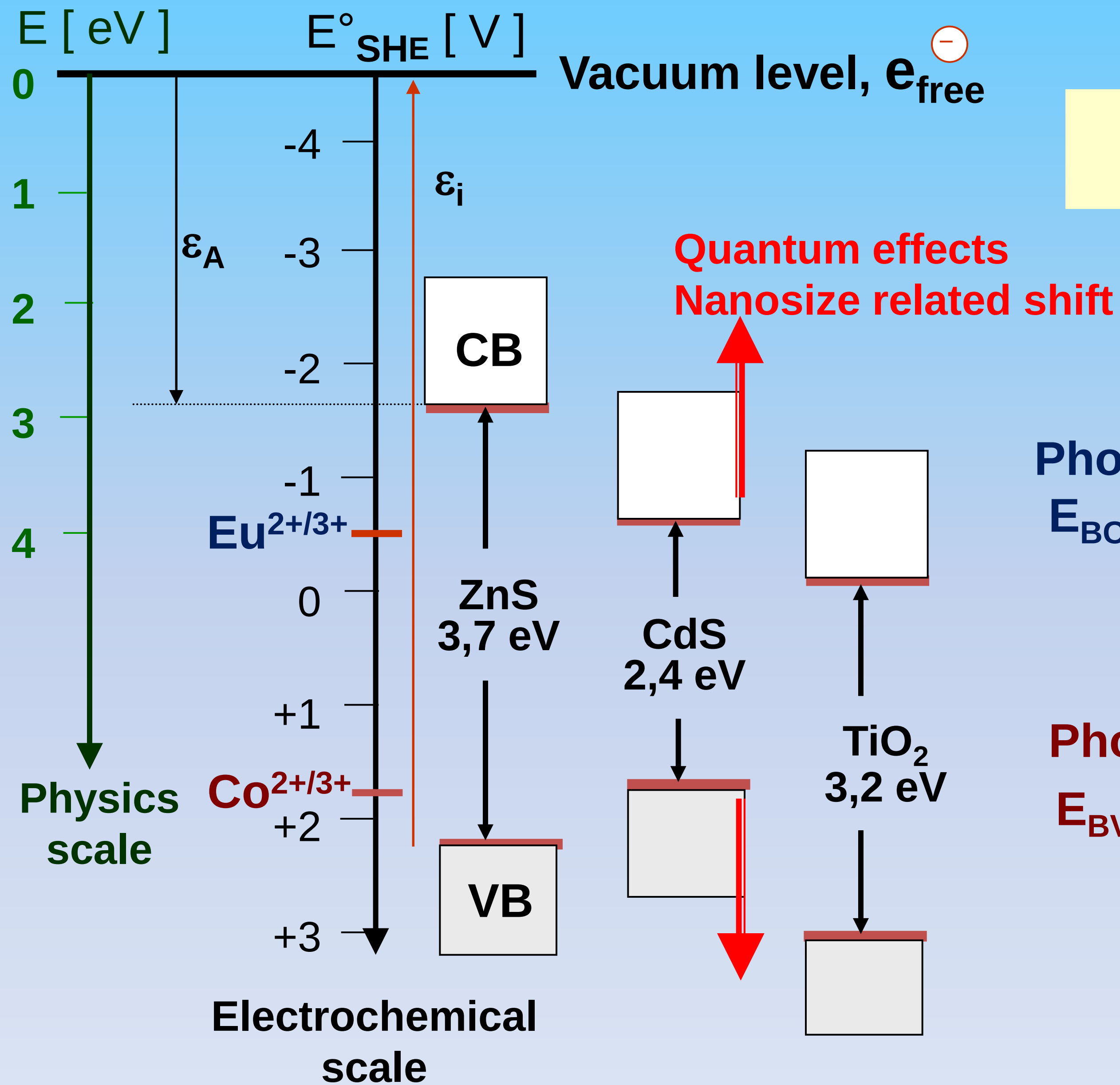

Note:
$E_{BC} = E° + 0{,}059\ pH$

Photoreduction:
$E_{BC} < E°(A/A^{-})$!

Photooxidation:
$E_{BV} > E°(D/D^{+})$!

L. Spanhel

Kinetics and photocatalysis

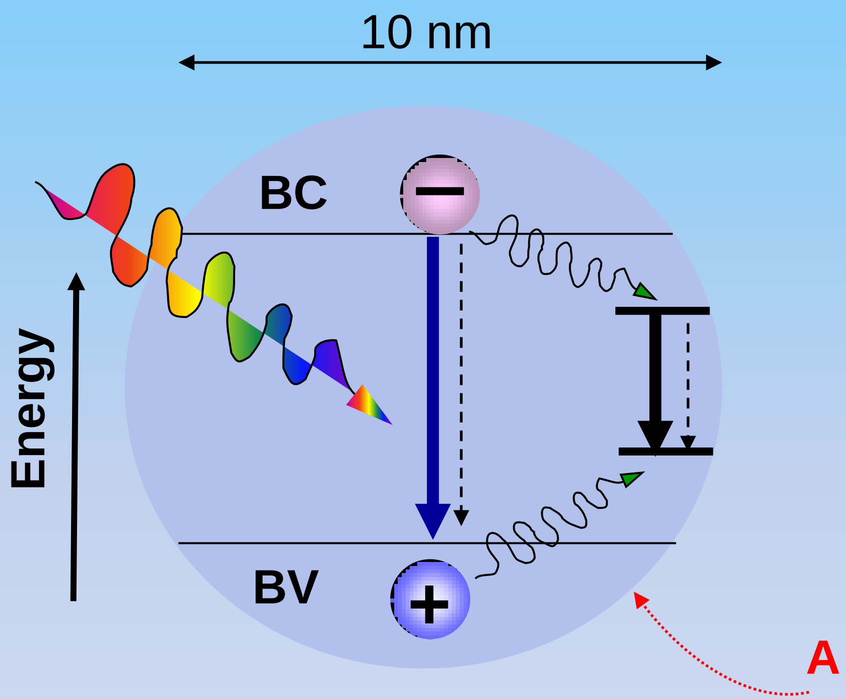

$$\tau_D = \frac{R_p^2}{\pi^2 \cdot D_{e,h}}$$

$D_{e,h} \sim 10^{-5}\ m^2/s$:

$$\langle x^2 \rangle = 2\,D\,t$$

$D_{10nm} = 10^{-9}\ m^2/s$

$D_A = 10^{-7}\ m^2/s$

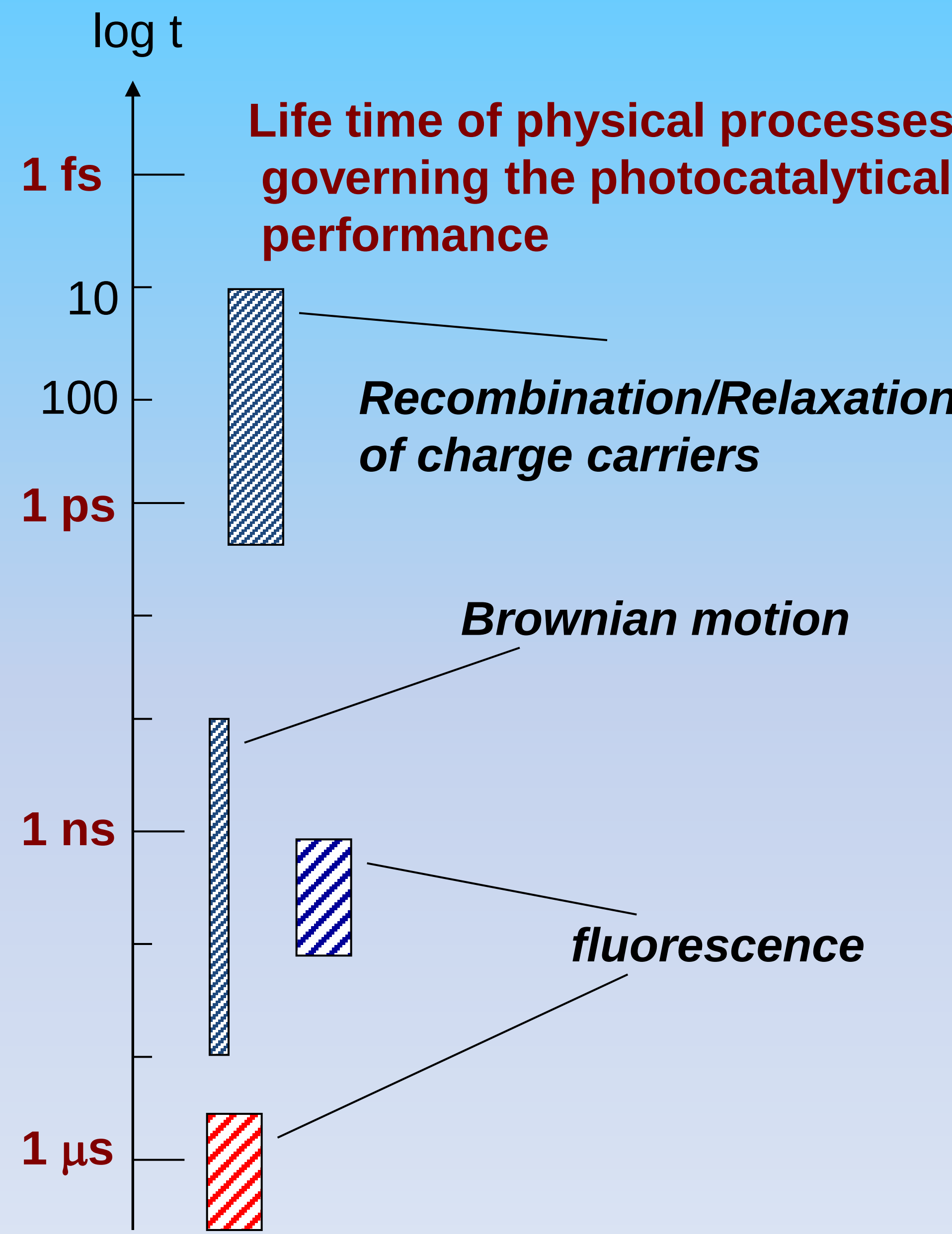

L. Spanhel

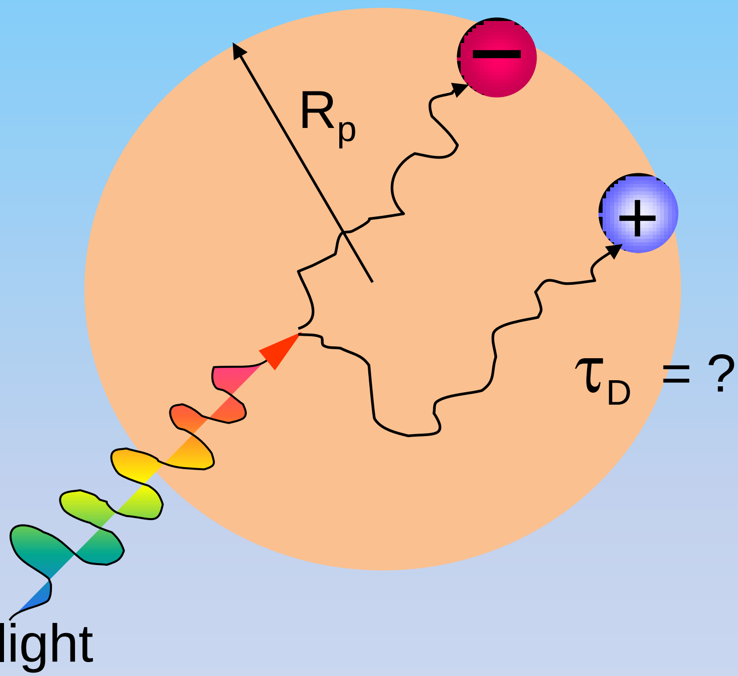

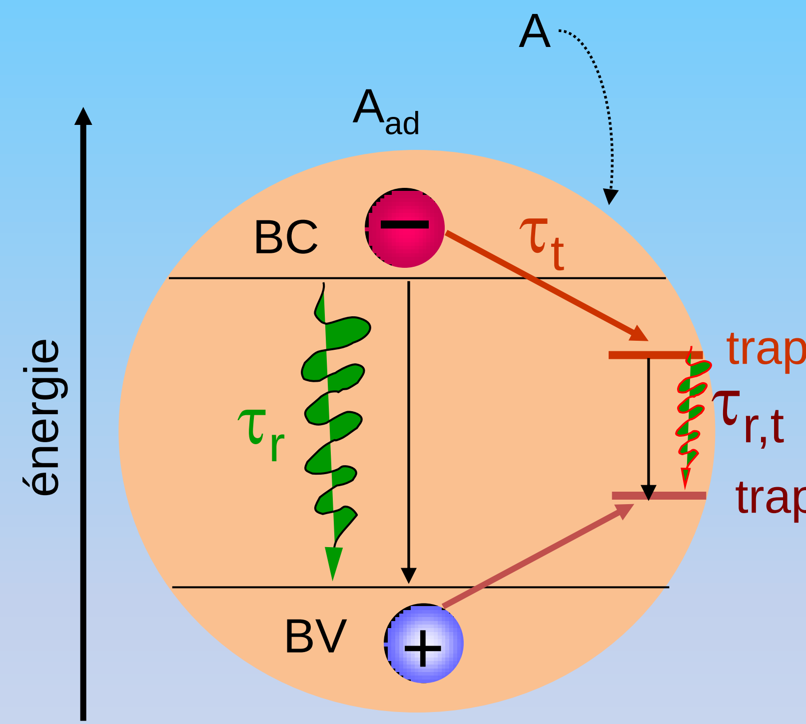

$$\tau_D = \frac{R_p^2}{\pi^2 \cdot D_{e,h}}$$

$D \sim 10^{-5}\ m^2/s$:

R_p:	τ_D:
5 nm	250 fs
20 nm	4 ps

$\tau_t \sim \tau_D \sim \tau_{nr}$

$\tau_{r,t} > \tau_r > \tau_{nr}$

L. Spanhel

Nanophotocatalyst optimization strategies

► **spectral profile**
visible light active nano's are needed (400 – 600 nm)

► **longe distance charge separation**
heterostructures, dopings and surface modifications

► **morphology of immobilized nanostructures**
particle shapes, aggregate architectures and mesoporosity

► **integration into photoreactor prototypes on various scales**
nanocolloids, powders, thin coatings, photoreactor design

Photocatalysts of choice

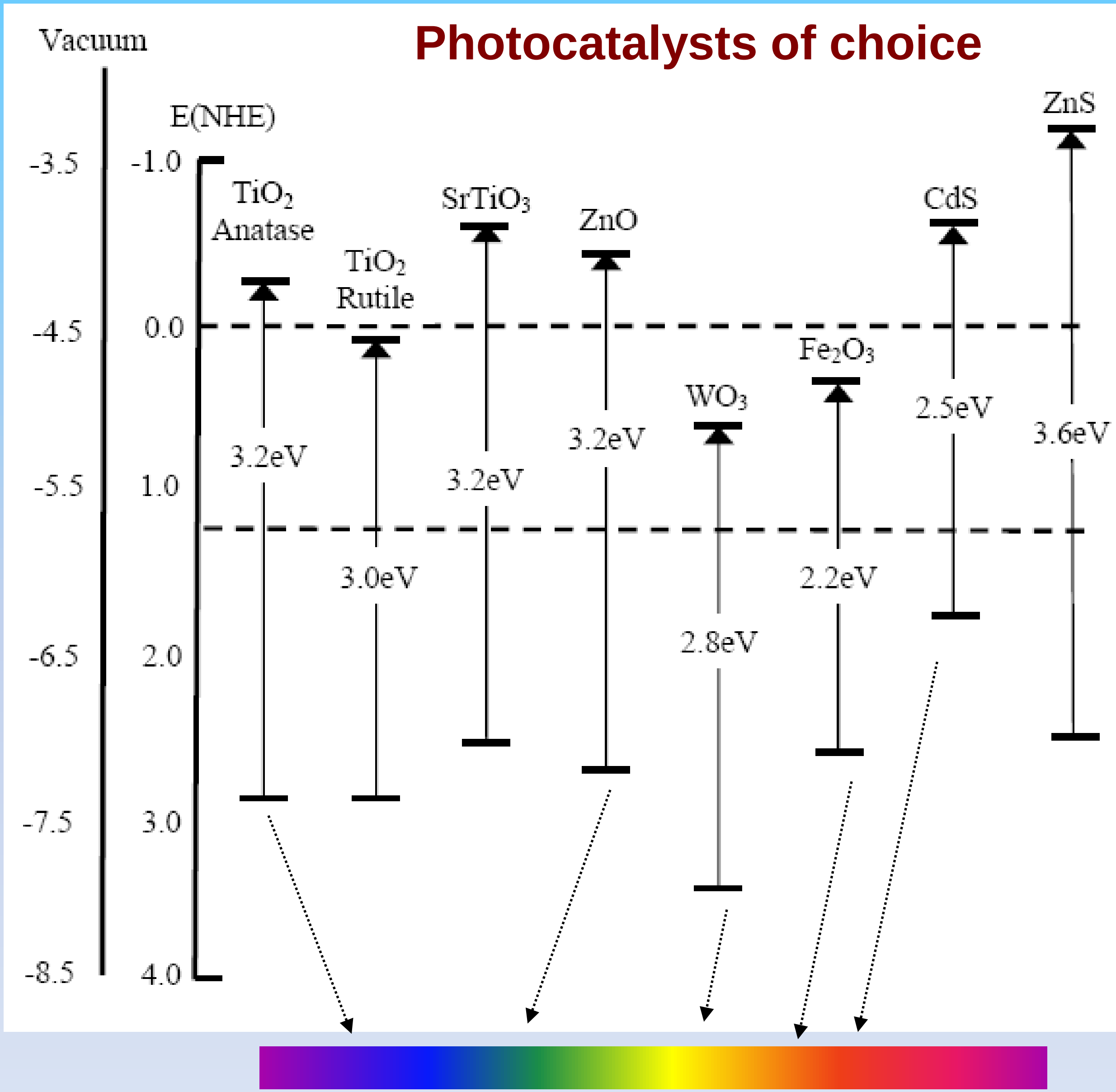

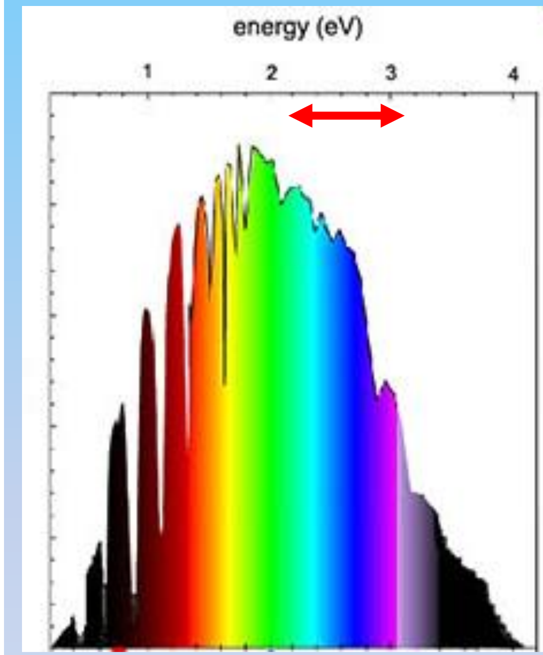

Note:

Avoid photo-corrosions

CdS, ZnS, Fe_2O_3

Doping delivers better charge separation
relevant oxides: TiO_2, ZnO, $ZnTiO_3$

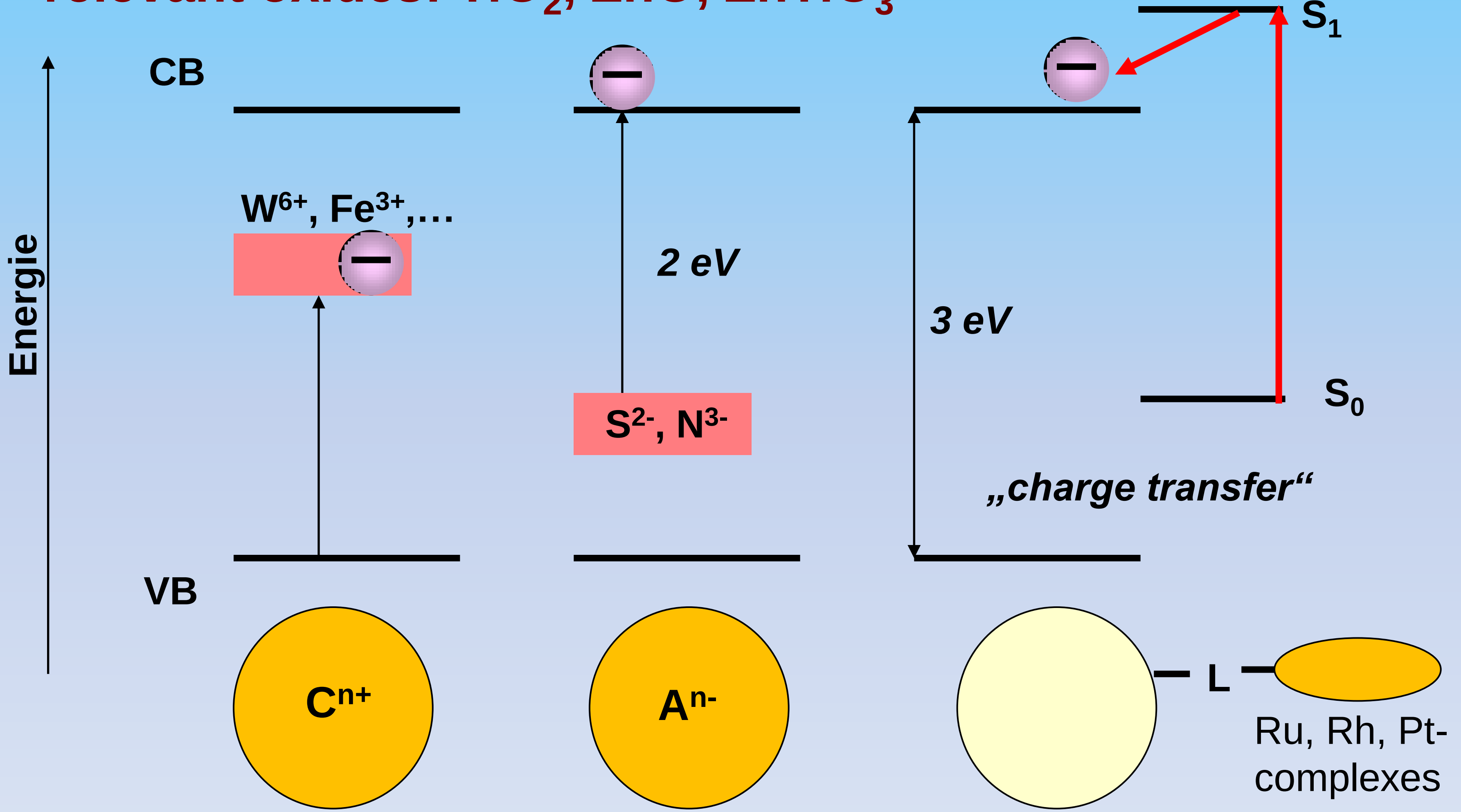

L. Spanhel

Rapid separation of electron-hole pairs blocks their thermal deactivation (nr, e-h recombination)

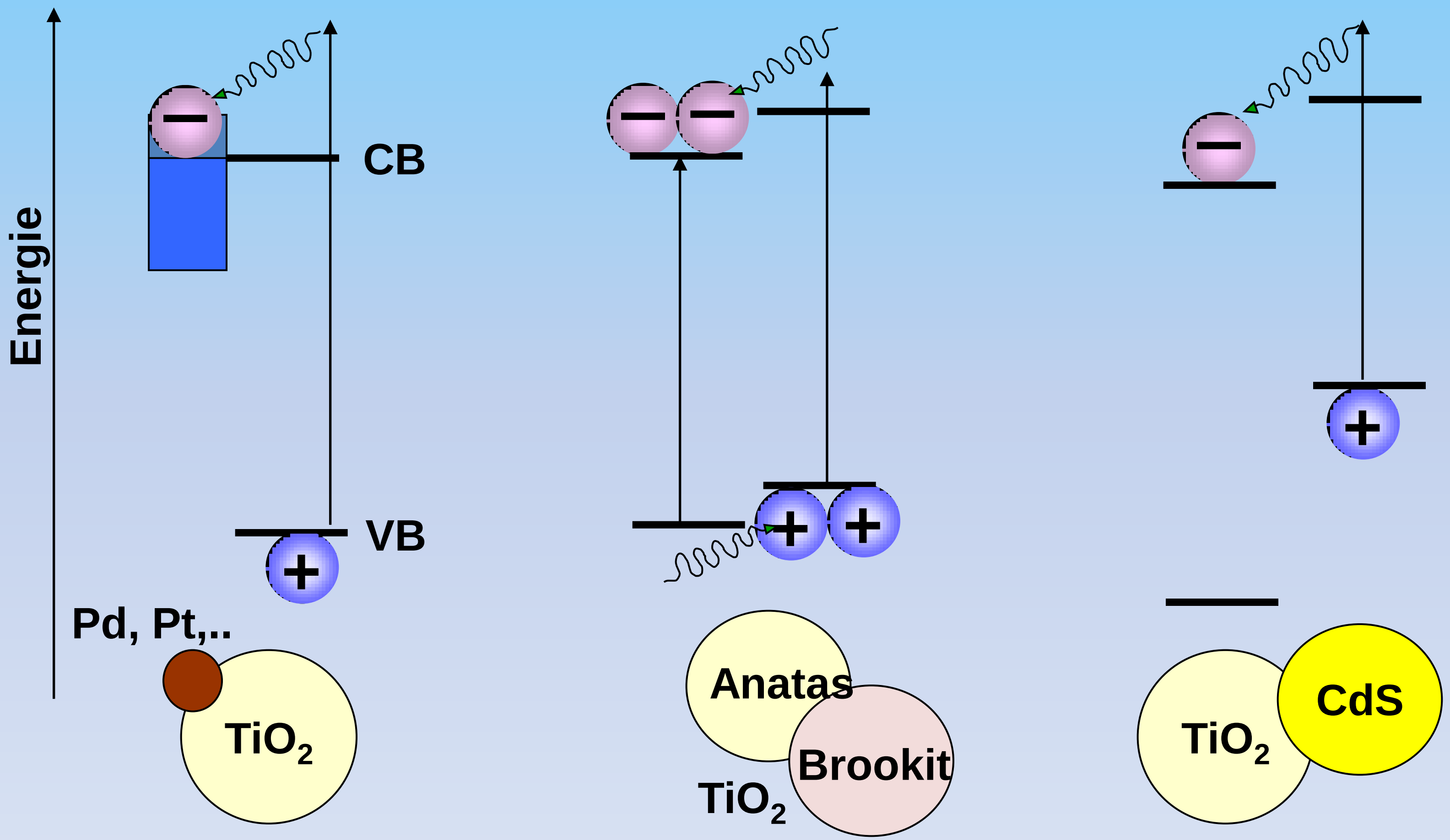

L. Spanhel

Photocatalysis applications

1. Organic preparative synthesis
2. Environmental detoxification
3. Self-cleaning windows
4. Solar water splitting (solar fuels, hydrogen technology)
5. Carbon dioxide transformations
6. Biosystems in photocatalysis

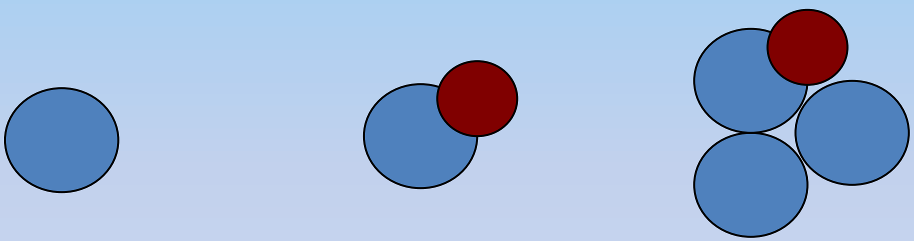

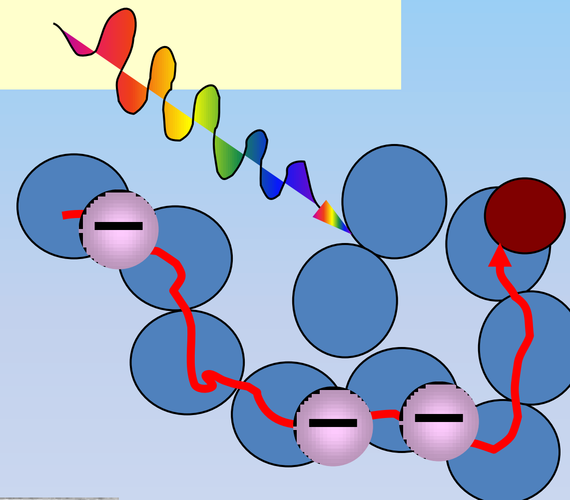

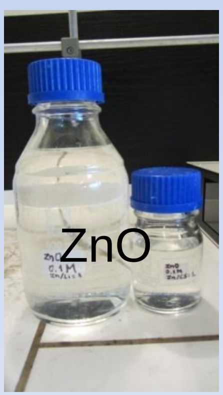

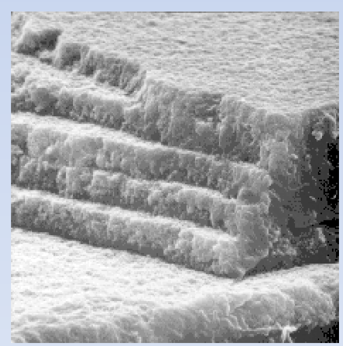

L. Spanhel

Photomineralisation of organic pollutants

$$C_xH_yCl_z + \left[x + \frac{y - z}{4}\right] O_2 \xrightarrow[TiO_2]{h\nu} xCO_2 + zHCl + \left[\frac{y - z}{4}\right] H_2O$$

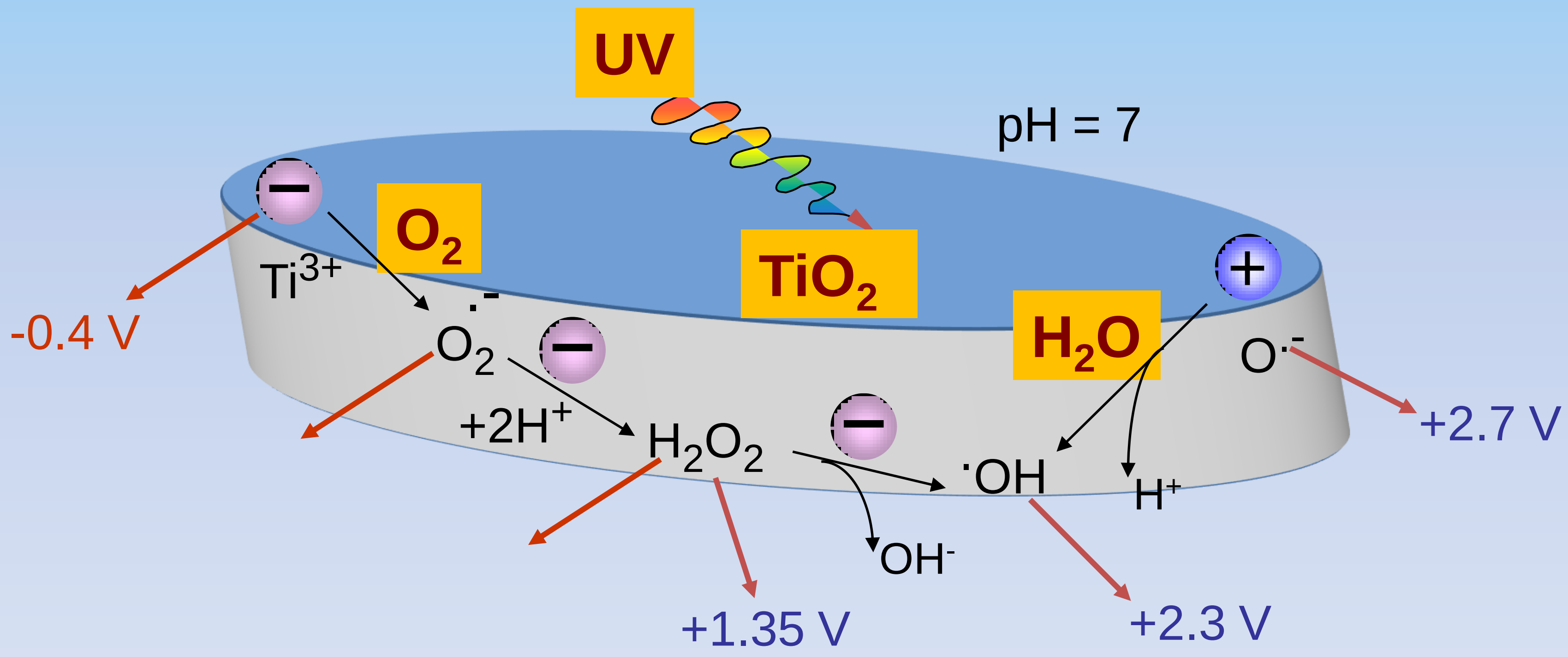

L. Spanhel

Solar decontamination of industrial waters in the VW company in Taubate (Brasil) since 1999

Total surface: 50 m^2

Turnover : 1 m^3/jour

CATA: Hombikat-TiO_2 (Anatase)

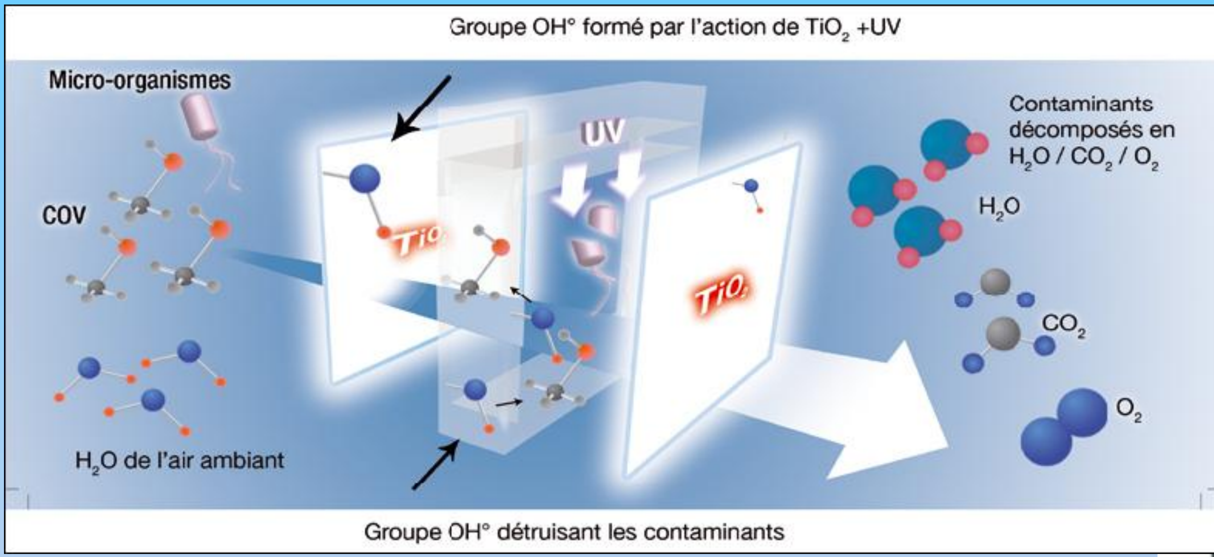

photoclean® QUARTZ

de l'air propre à l'air pur

Florence Benoit, Toulouse

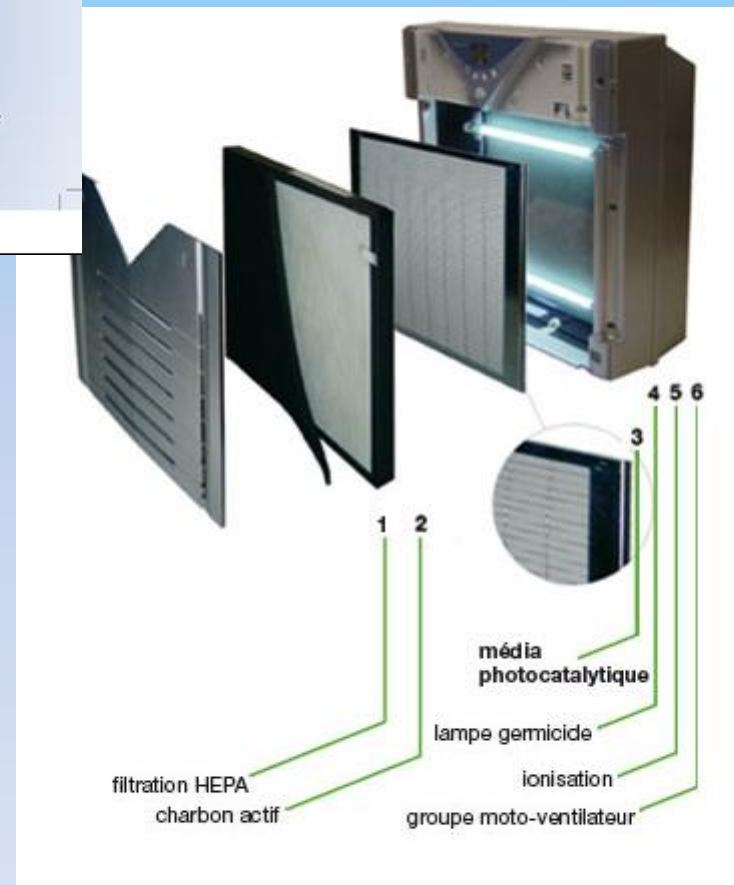

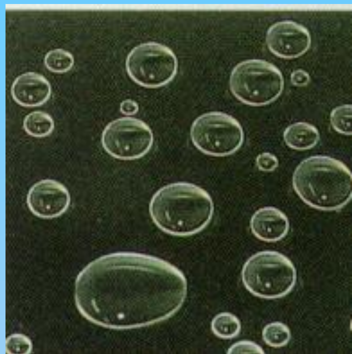

Super-Hydrophilicity via photocatalysis

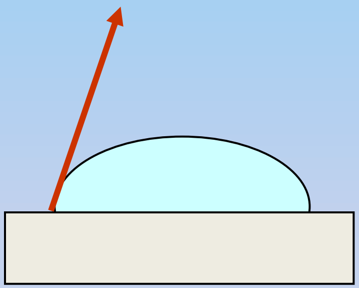

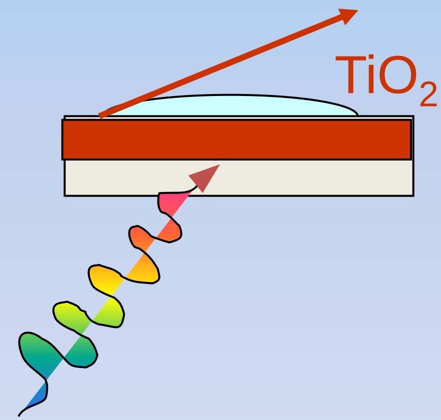

Asahi
Pilkington
St. Gobain
PPG

L. Spanhel

Mechanistic view of the formation of Super-Hydrophilicity

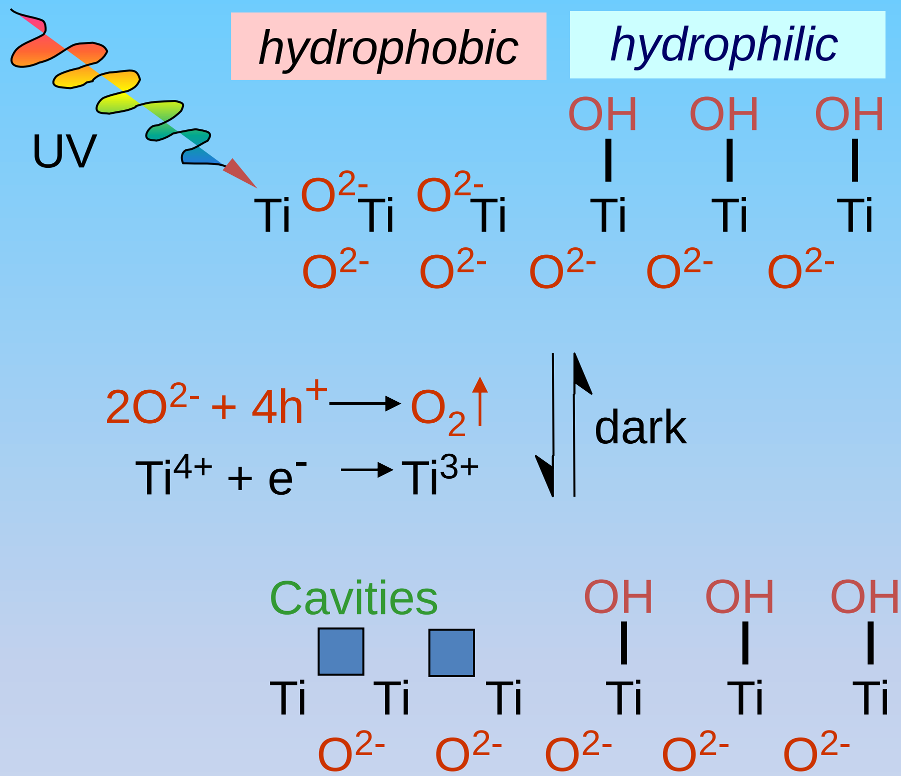

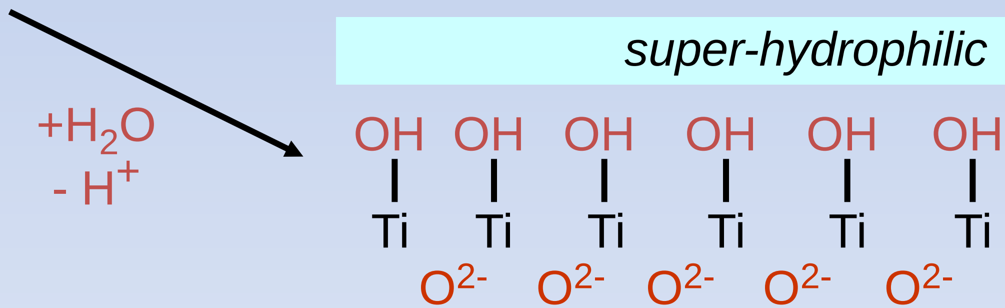

L. Spanhel

Super-Hydrophilicity in the car industry

Bacteria killing

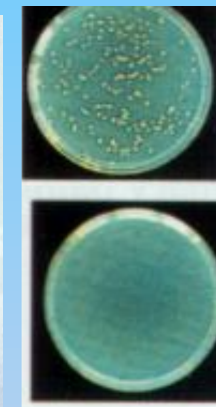

Super-Hydrophilicity in building constructions

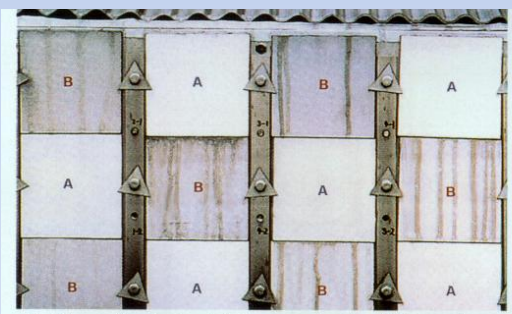

Self-cleaning and sterilisation of textiles

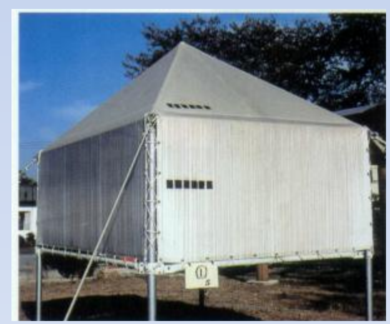

L. Spanhel

$Zn_xTi_yO_z$ Spinel-Nanostructures

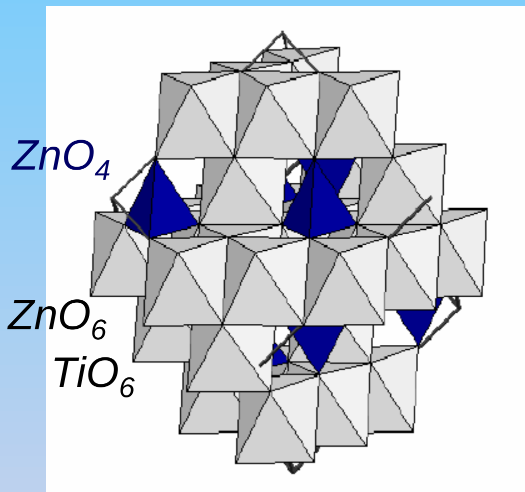

Fd3m
a = 840 - 844 pm

Cubic inverse spinels

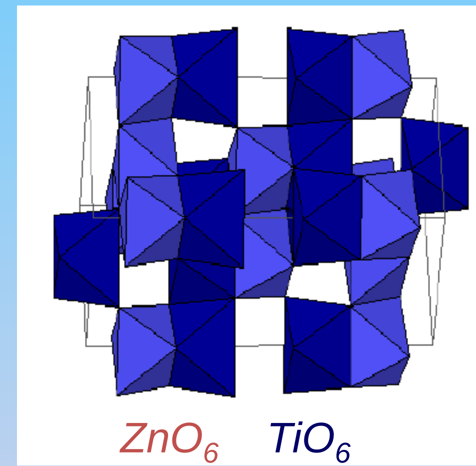

Ilmenite
h-$ZnTiO_3$

R3
a = 549 pm

$Zn_2TiO_4 = Zn_8{}^T(Zn_8\ Ti_8)^O O_{32}$

$ZnTiO_3 = Zn_8{}^T(Zn_{8/3}\ Ti_{32/3}\square_3)^O O_{32}$

$Zn_2Ti_3O_8 = Zn_8{}^T(Ti_{12}\square_4)^O O_{32}$

Recall normal spinel:
$AB_2O_4 = A_8{}^T B_{16}{}^O O_{32}$

L. Spanhel

Synthesis of 2 M “polymeric” $Zn_xTi_yO_z$ Sols

$$4\ Zn(Ac)_2 \cdot 2(H_2O) \longrightarrow 2\ HAc + 7\ H_2O + [Zn_4O](Ac)_6$$

Complexation

Esterification

Hydrolysis
Condensation

„Ti-O-Ti“
„Ti-O-Zn-O-Zn“

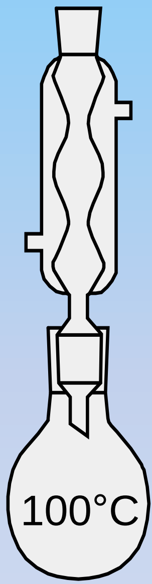

$Zn(Ac)_2\ 2H_2O$
$Ti(OBut)_4$
EtOH

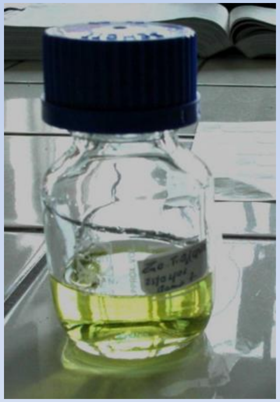

Z. Phys. Chem. 2007
G. Starukh et al.
Adv. Mater. 2006
F. Grasset et al.

L. Spanhel

Thermal growth of $Zn_xTi_yO_z$ nanocrystals > 350°C

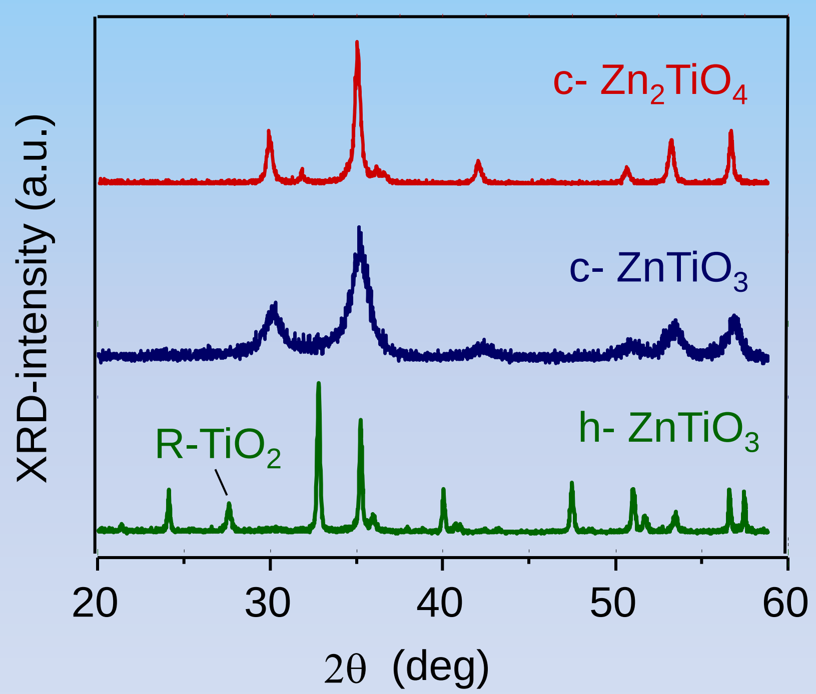

Zn/Ti = 2

Zn/Ti = 1

Zn/Ti = 2/3, 3/5

L. Spanhel

h-$ZnTiO_3$/r-TiO_2 films in Photocatalysis

Photodegradation of Fetty Acids, Xe-lamp, air, rel. humidity: 80%

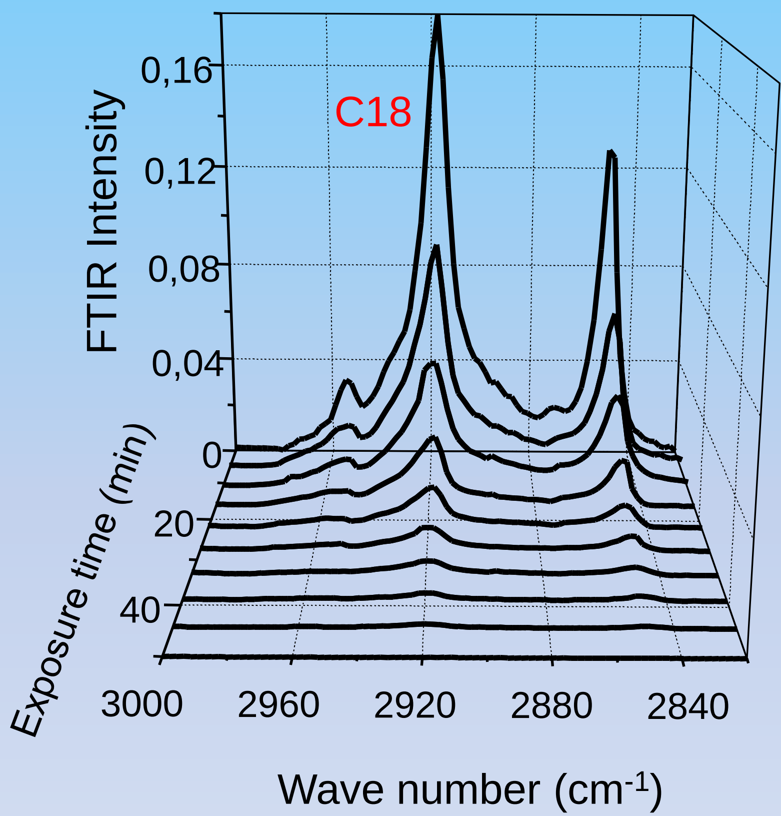

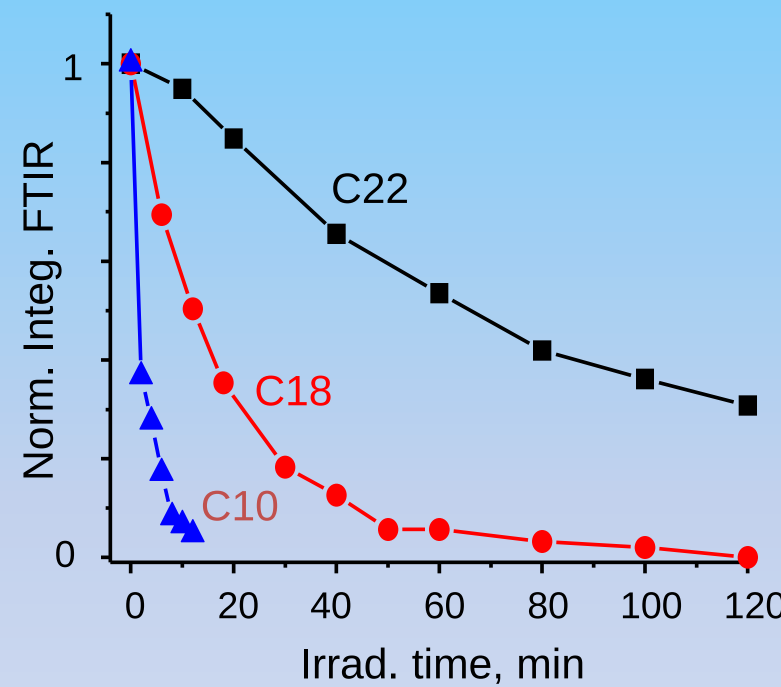

Phys. Chem. Chem. Phys. 2010
Krylova et al.

L. Spanhel

Methylene Blue photodegradation on “ZnTiON”-Spinel layers
(λ_{ex} > 430 nm, Xe – Lamp, humid air)

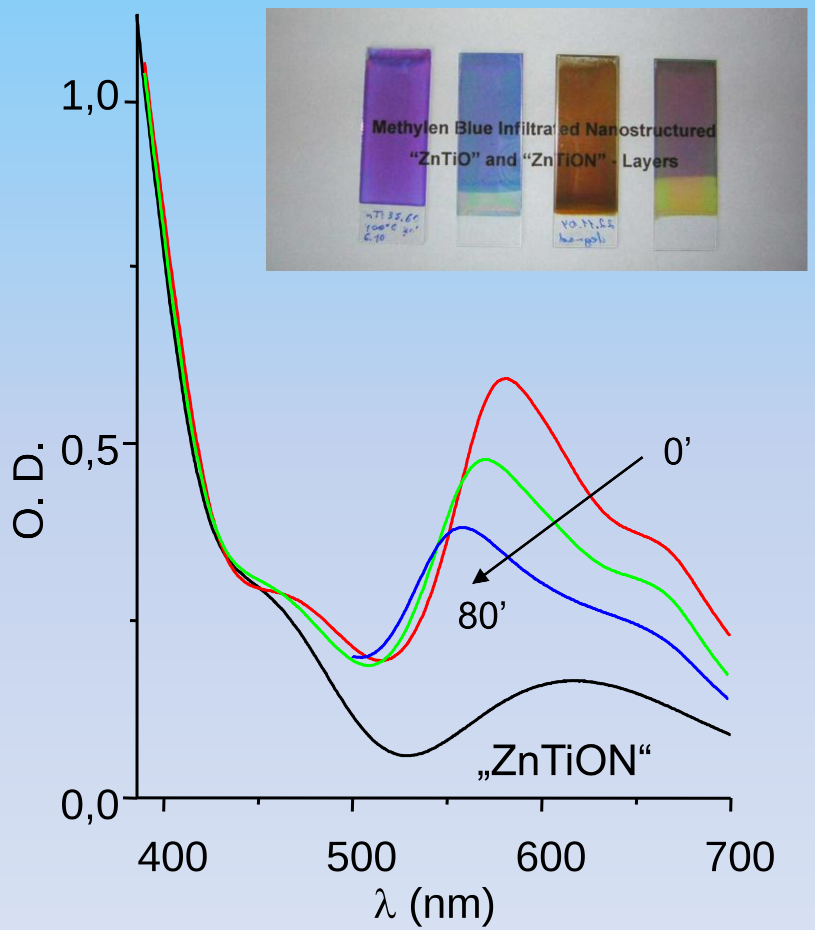

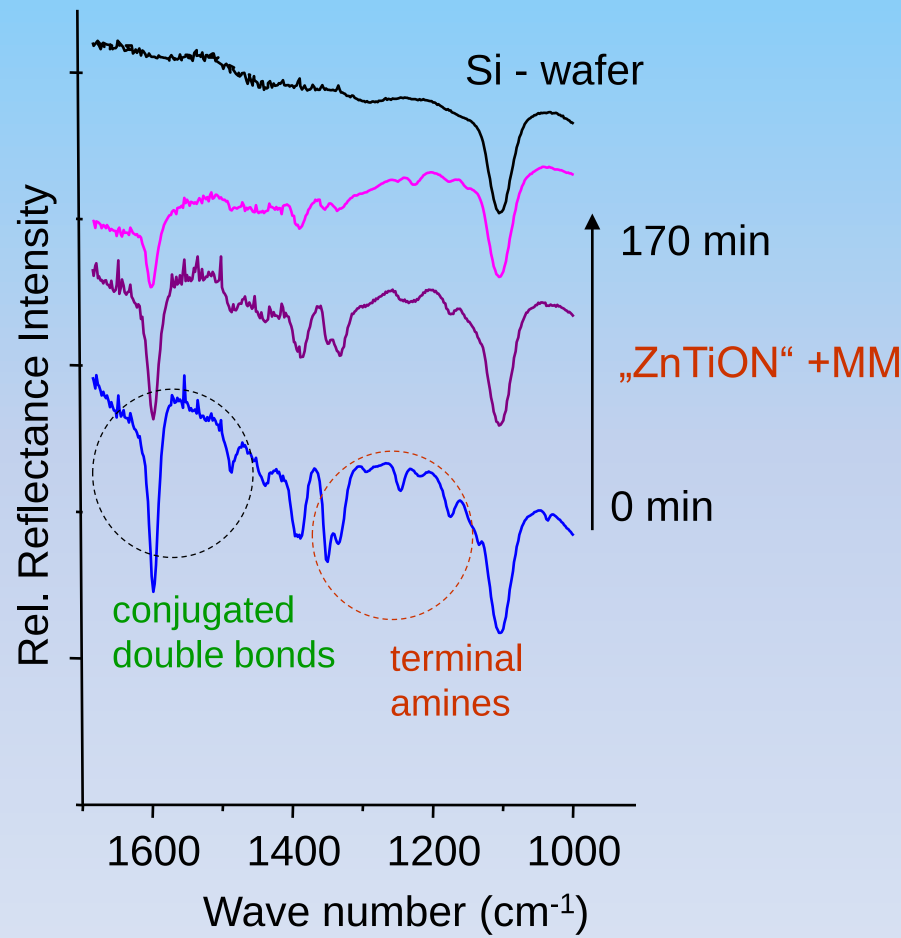

L. Spanhel

« Nanotechnology for hydrogen industries »

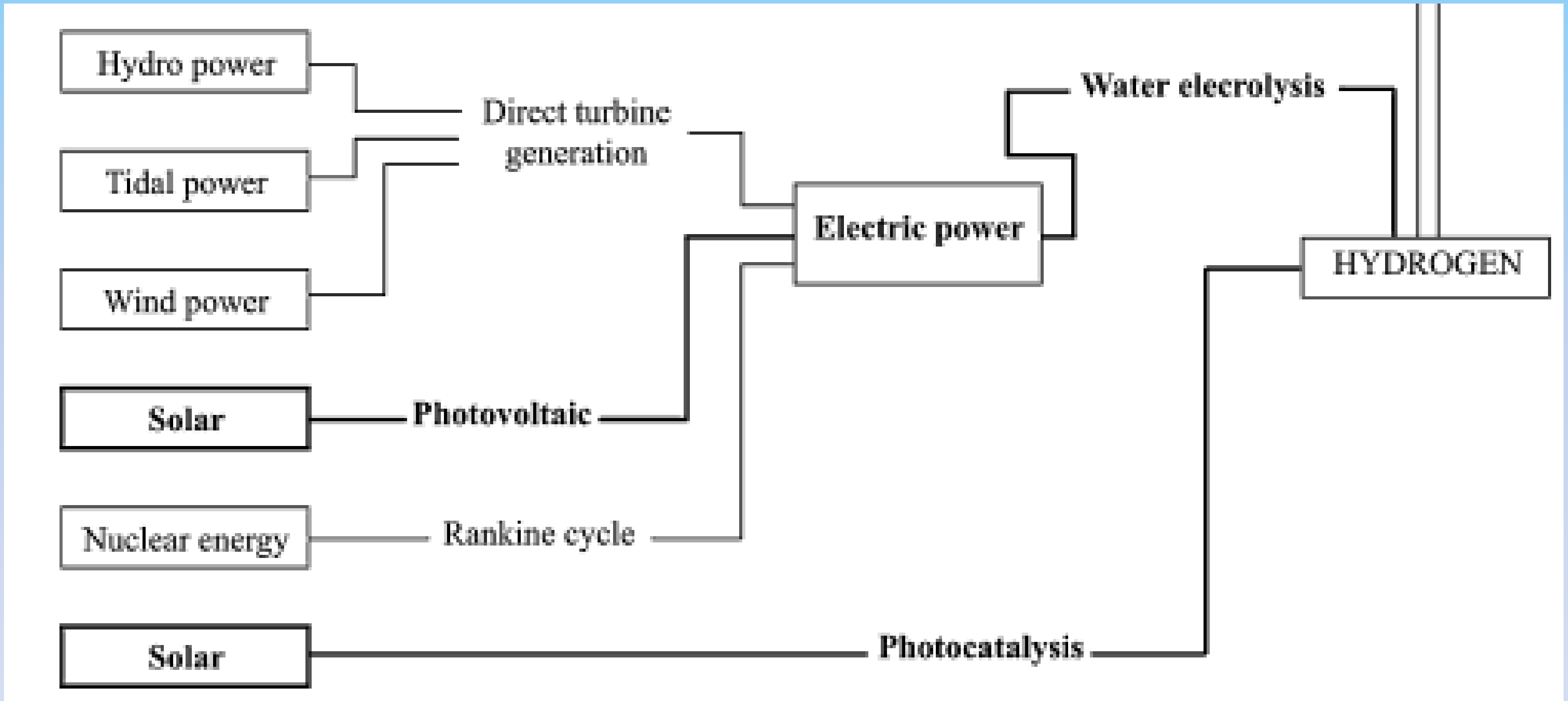

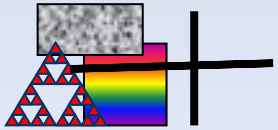

L. Spanhel

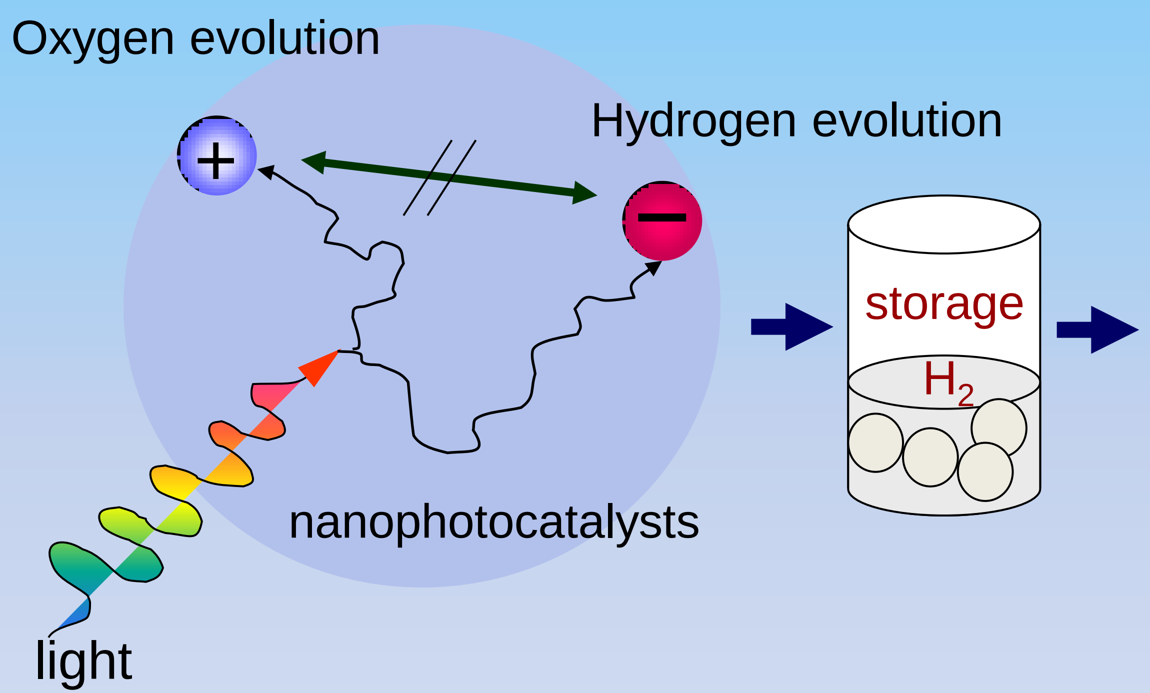

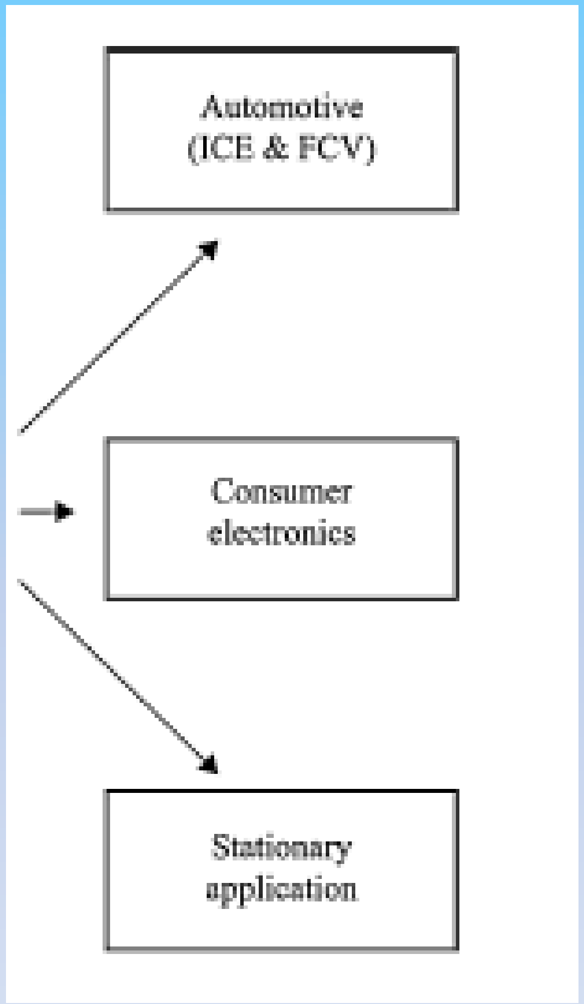

Required photocatalytic efficiency: 10%

L. Spanhel

Hydrogen storage

In the car industry:
5-13 kg, ~ 500 km

1. Metal hydrides (chemisorption)

$$Mg + H_2 (g) \underset{T\uparrow,\ p\downarrow}{\rightleftharpoons} MgH_2 \qquad \Delta_{ad}H < 0$$

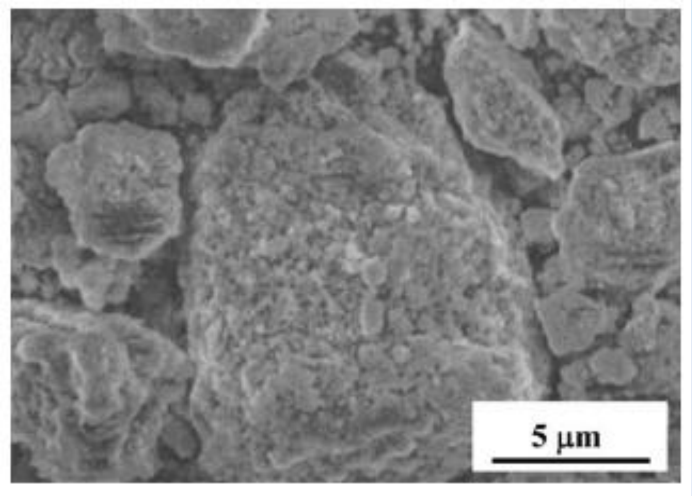

Capacity: 0,076 kg/kg (0,101 kg/L) with nano-Pd

2. Physisorption on MOF
metal organic frameworks

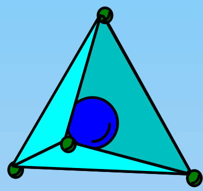

$[M_4O](OOCR)_6$ M: Mg, Zn, Be

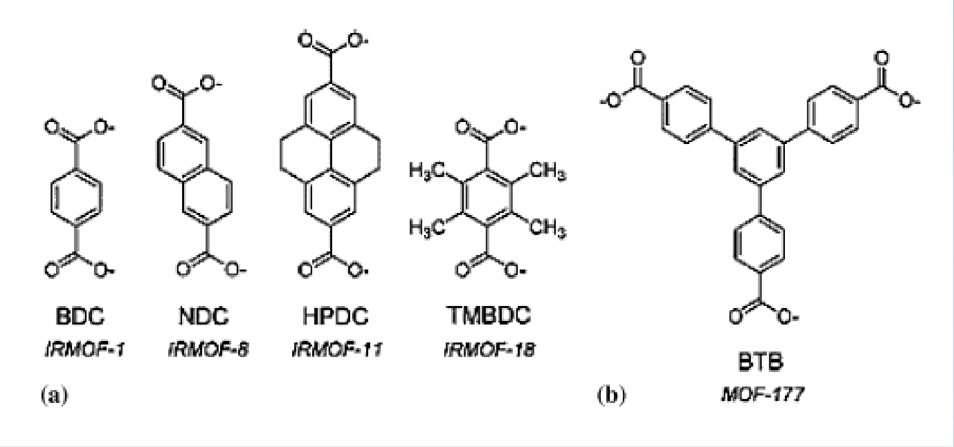

Capacity: 5-10 % w.

L. Spanhel

Best result on solar water splitting so far (ϕ ~ 5%)

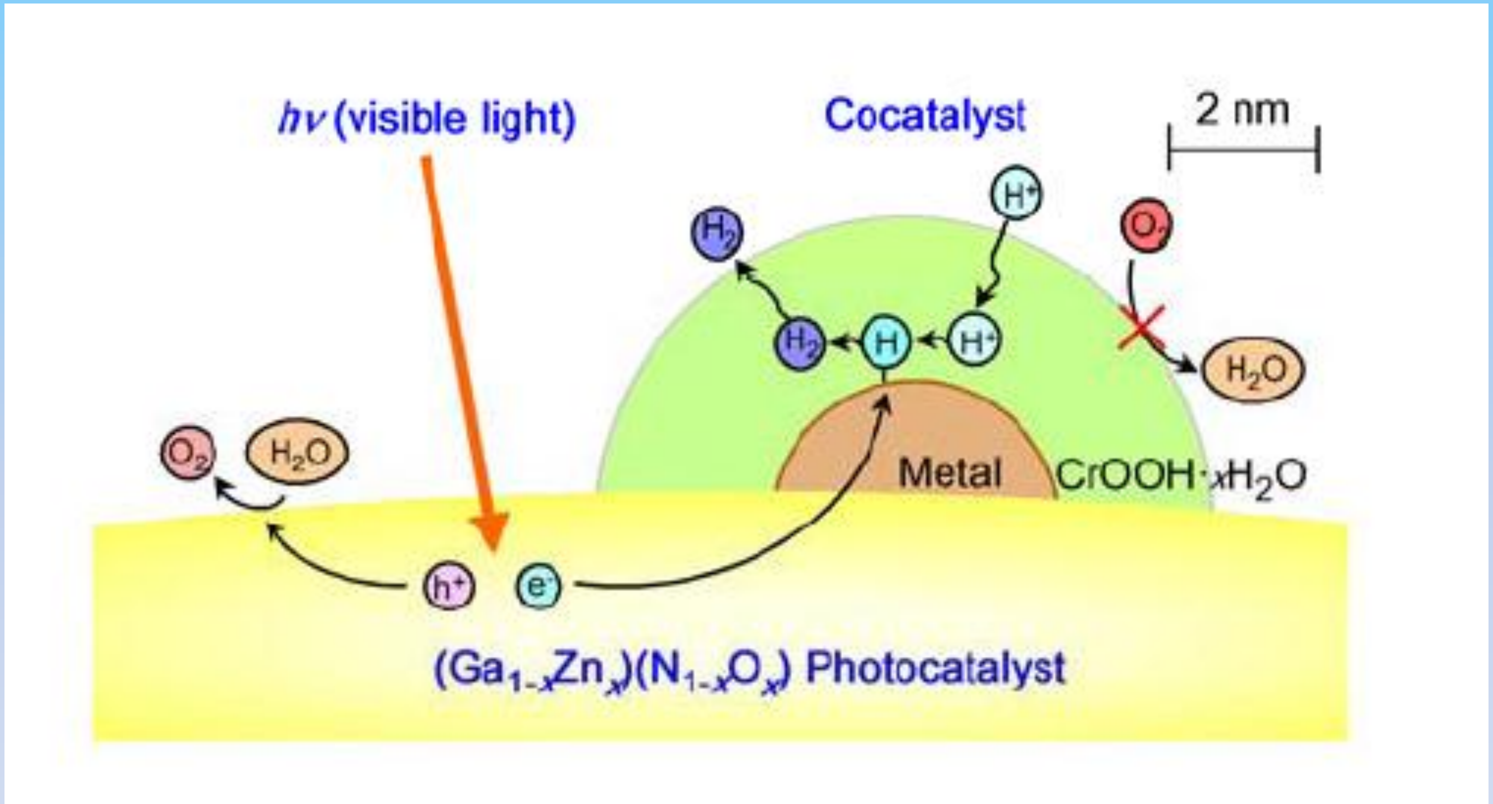

K. Maeda et al, Nature 2006

L. Spanhel

Other Photoreduction processes on combined SC-M hereterojunctions

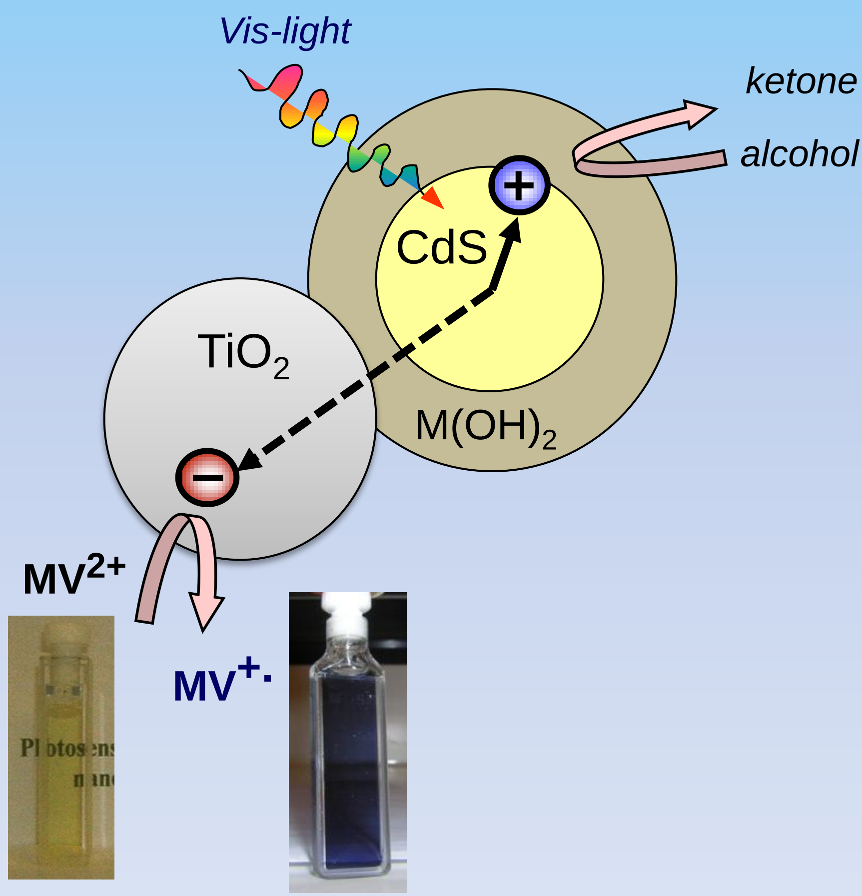

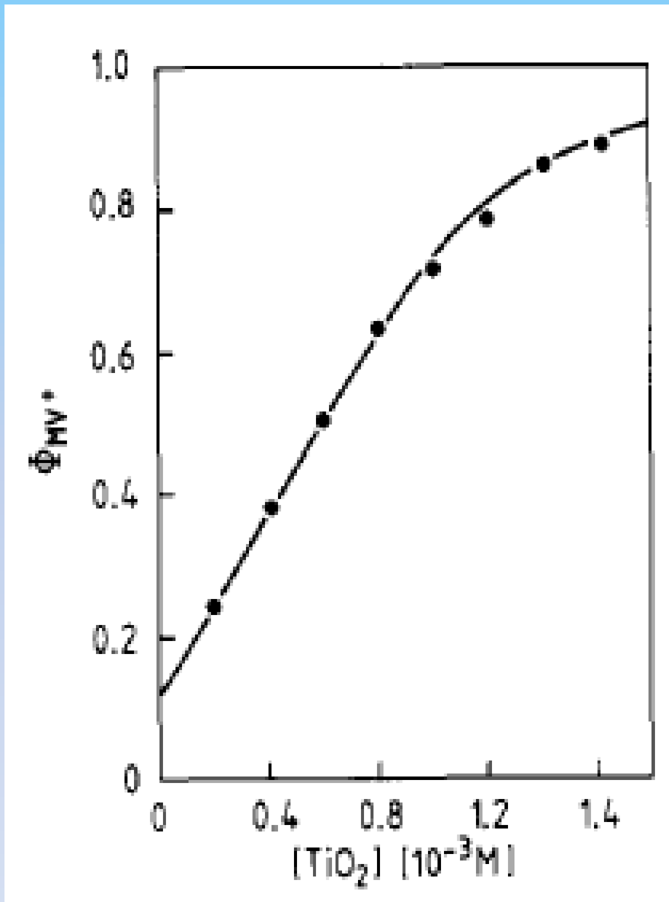

CO_2 photo-transformations via surface plasmons

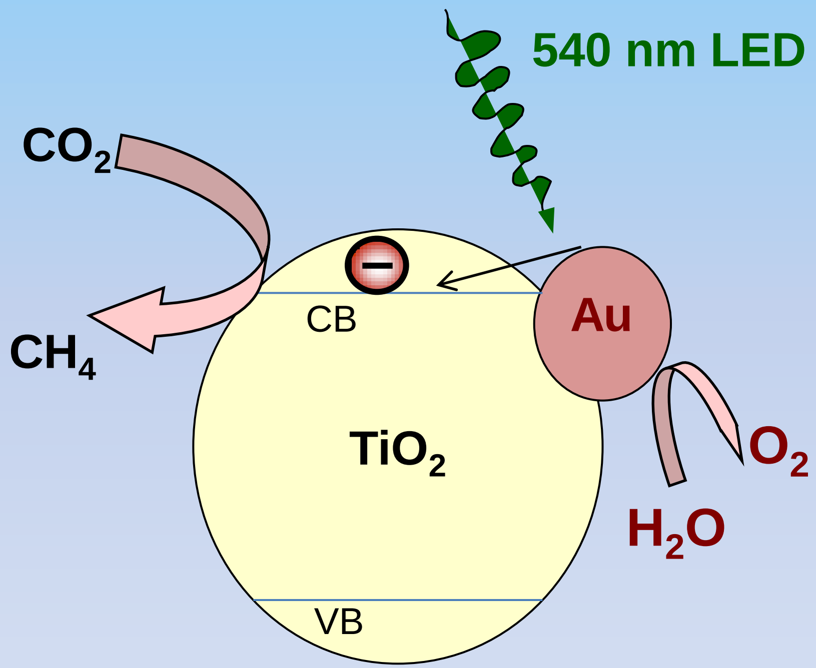

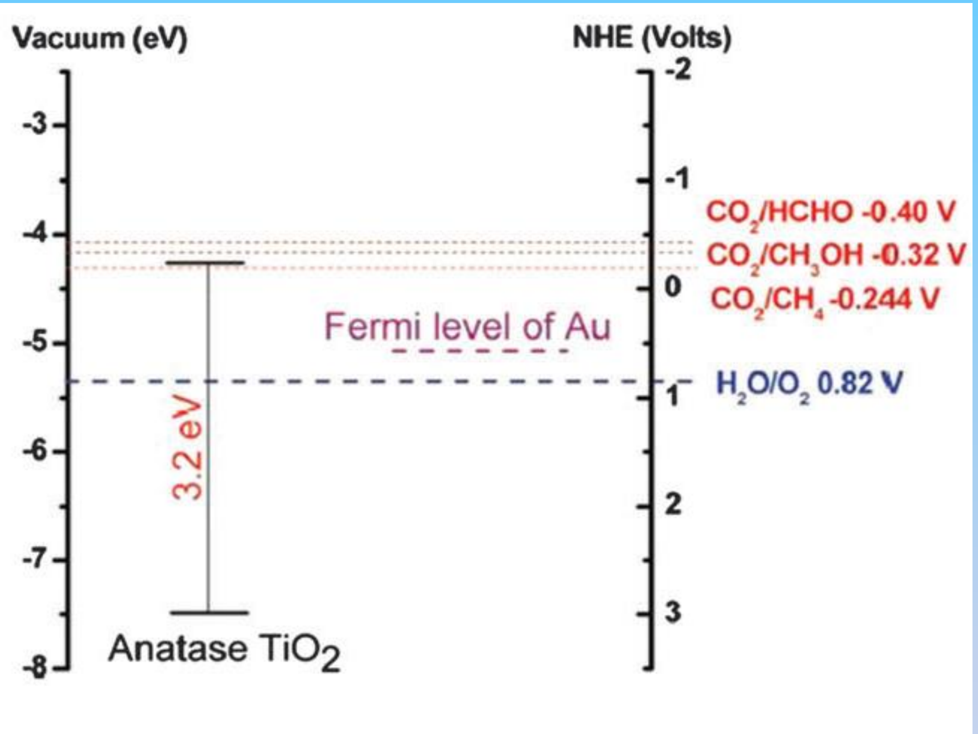

reaction	$E°$ (V) vs SCE at pH = 7
$CO_2 + 2H^+ + 2e^- \rightarrow CO + H_2O$	−0.77
$CO_2 + 2H^+ + 2e^- \rightarrow HCOOH$	−0.85
$CO_2 + 4H^+ + 4e^- \rightarrow HCHO$	−0.72
$CO_2 + 6H^+ + 6e^- \rightarrow CH_3OH$	−0.62
$CO_2 + 8H^+ + 8e^- \rightarrow CH_4$	−0.48

D. Astruc, Univ. Bordeaux
RSC-Chem. Soc. Rev. 2014, 43, 7188

L. Spanhel

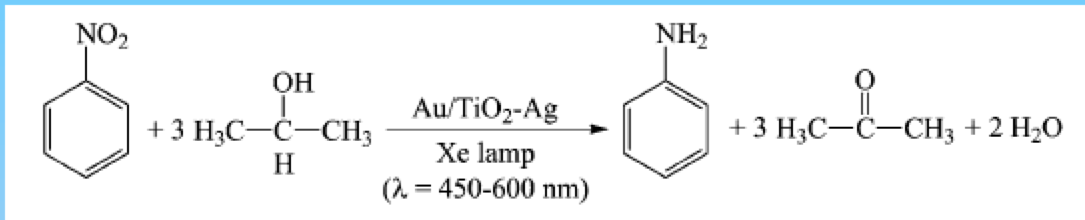

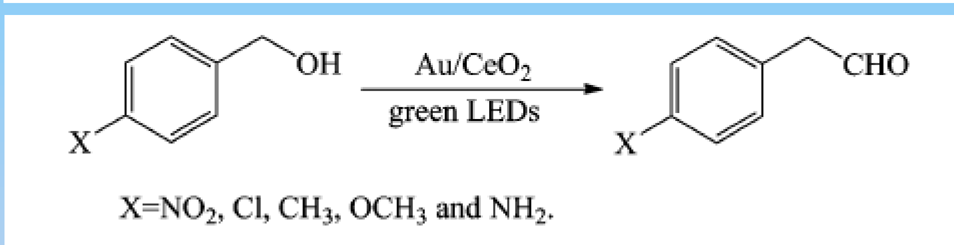

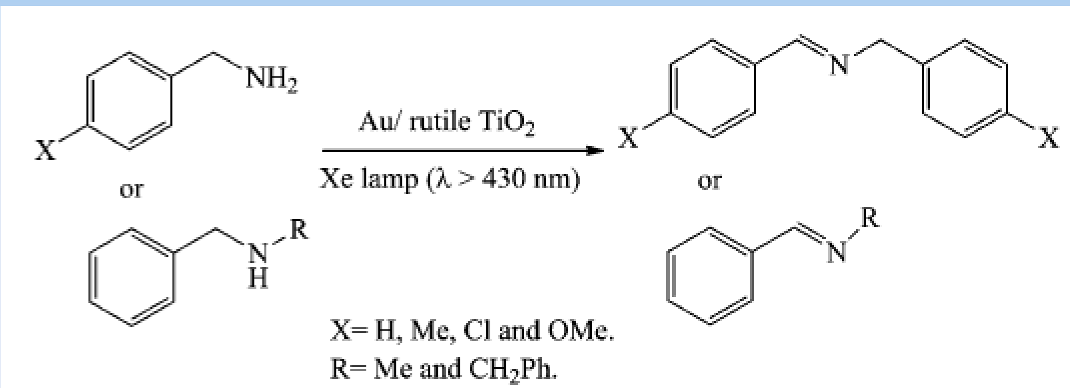

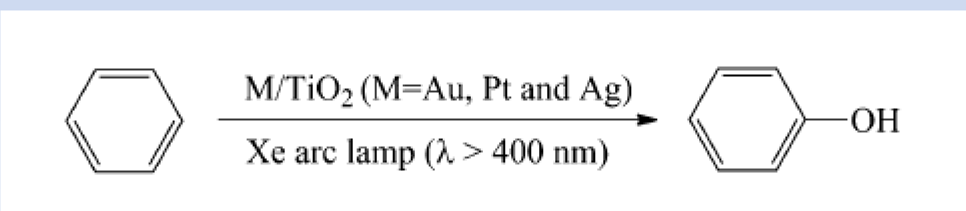

In most cases:
Yield > 50%
Selectivity > 90%

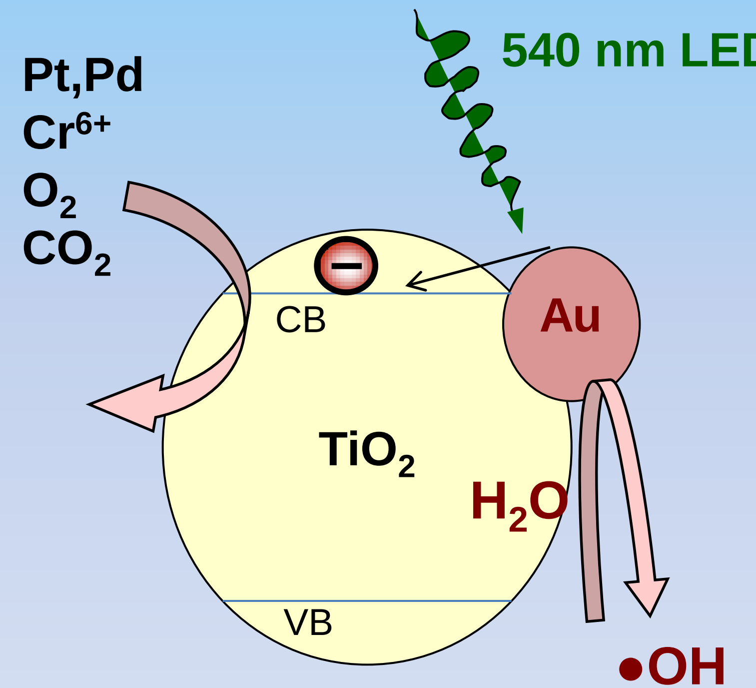

D. Astruc, Univ. Bordeaux
RSC-Chem. Soc. Rev. 2014, 43, 7188

L. Spanhel

Theory of Solar Cells of the 1. and 2. generation

Diode

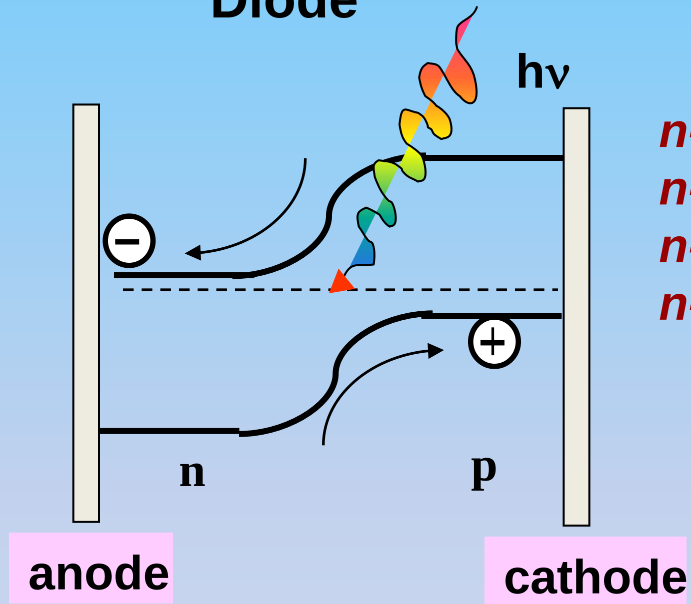

n-Si/p-Si
n-GaAs/p-GaAs (InP)
n-CdS/p-CdTe
n-CdS/p-CuInSe$_2$

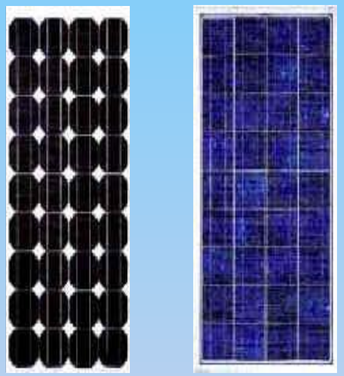

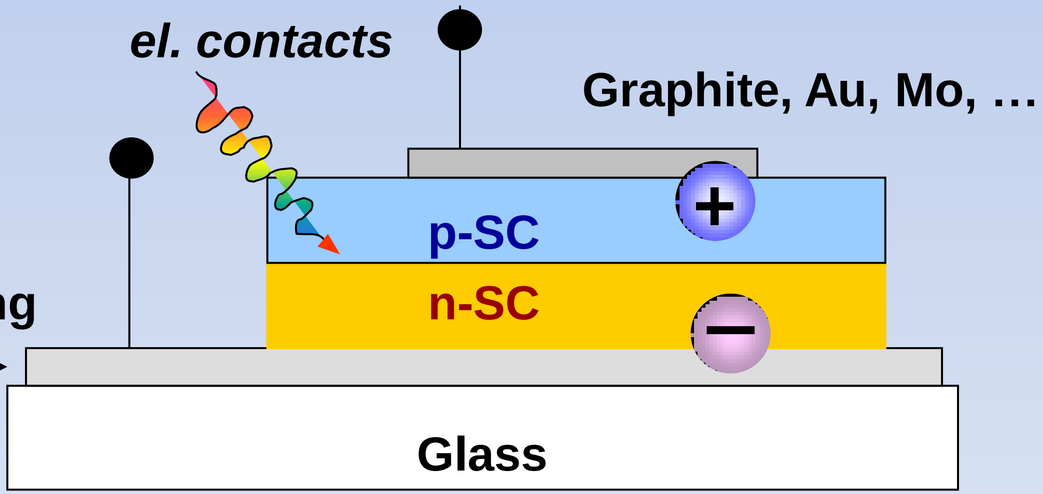

Transparent conducting electrode
Al@ZnO, F@SnO$_2$

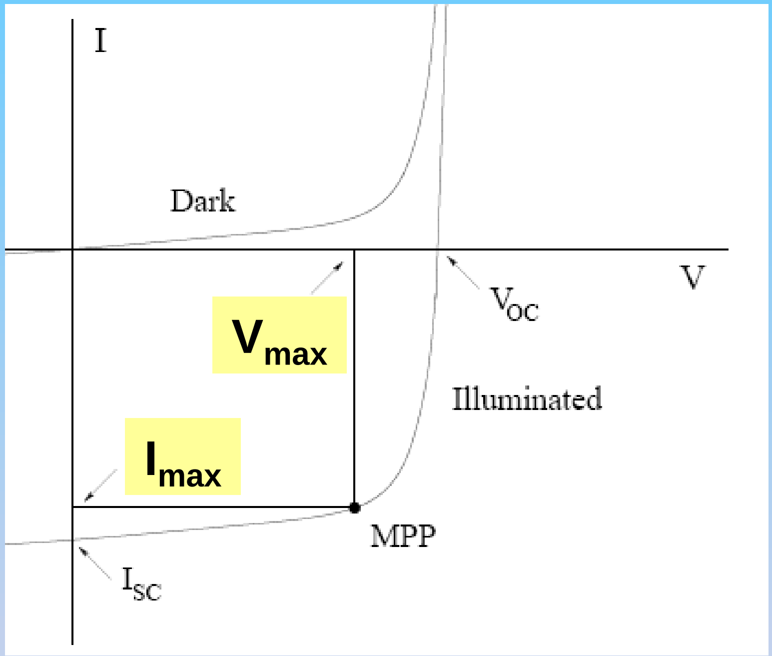

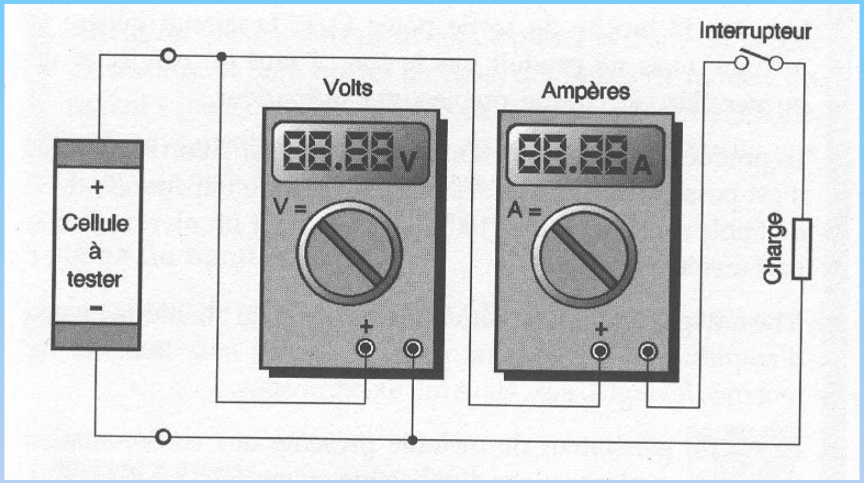

$$\eta = FF\,\frac{V_{oc} I_{sc}}{P_{in}} = \frac{V_{max} I_{max}}{P_{in}}$$

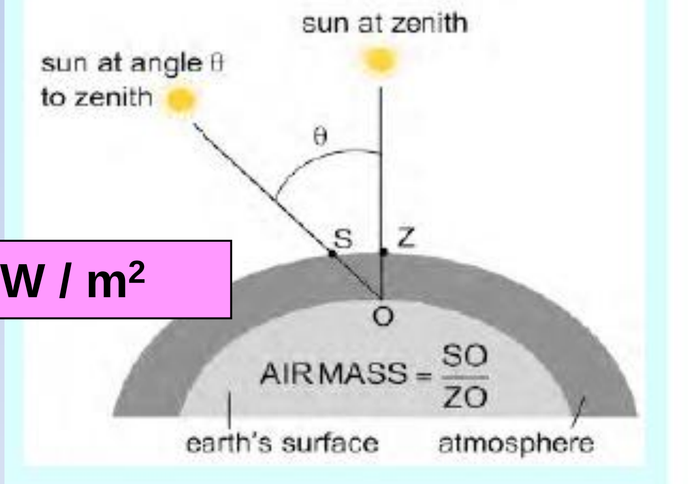

P_{in} = 1 kW / m^2

η = conversion efficiency (0 - 1)
FF = fill factor
V_{OC} = open circuit voltage (V)
I_{SC} = short circuit current (A/m^2)
P_{in} = solar input power (W/m^2)

L. Spanhel

Polycrystalline Thin Film Cells

Cell Type	η (%)	Area cm^2	V_{OC} mV	J_{SC} mA/cm^2	FF %	Lab / Company	Date
CdTe (cell) 3.5 mm CSS	16	1.0	840	26.1	73.1	Matsushita	1997
CIGS submodule	14.2	51.7	6808	3.1	68.3	Showa Shell	1996
GaInP/GaAs monolithic	30.3	4.0	2488	14.22	85.6	Japan Energy	1996
Si (large thin film)	16	95.8	589	35.6	76.3	Mitsubishi (77µm on SiO_2)	1997
a-Si (submodule) non stabilised	12	100	1250	1.3	73.5	Sanyo	1992

$$\eta = FF\frac{V_{oc}I_{sc}}{P_{in}} = \frac{V_{max}I_{max}}{P_{in}}$$

Origin of losses in solar cells

1. Dissipation de la lumière limitée
2. Relaxation thermique
3. Perte lors de la séparation de charges
4. Contacts électriques non-idéales
5. Désactivation thermique (recombinaison)

losses

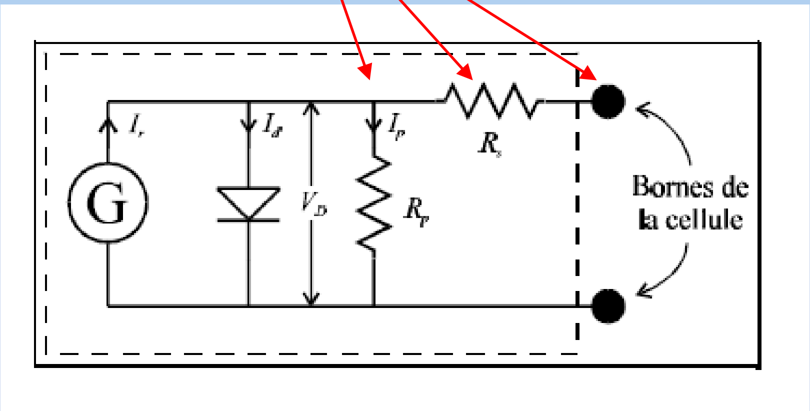

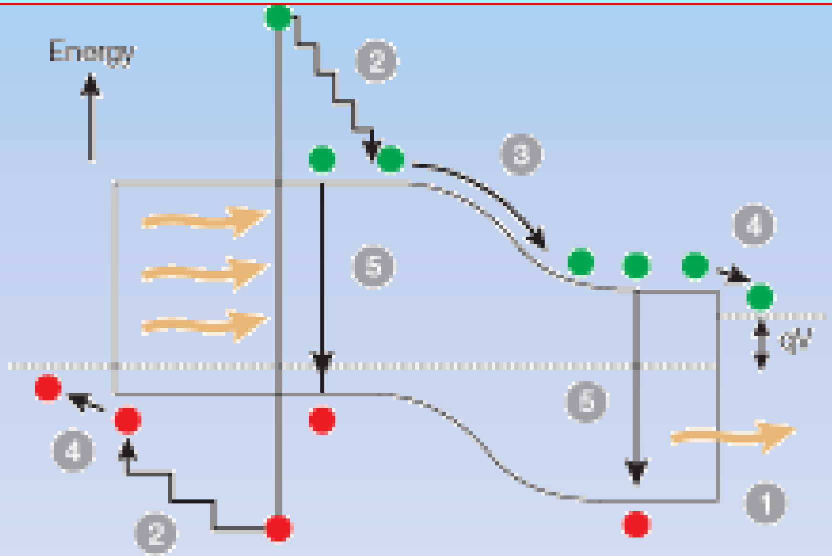

L. Spanhel

Cellules à base de Si



Mono-Si 12-16%   poly-Si 11-13%   amorphe Si 6-10%

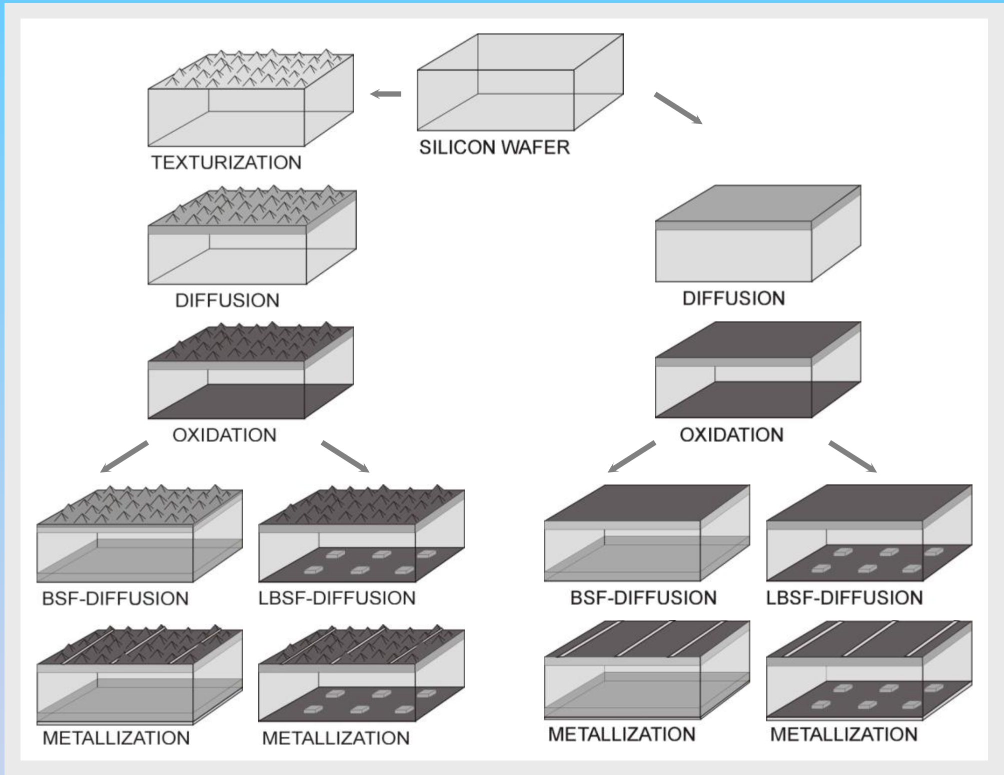

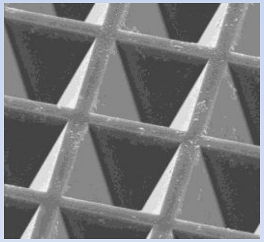
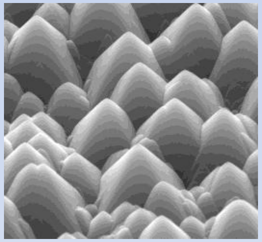

L. Spanhel

p-CdTe/n-CdS heterojunction

Conversion efficiency > 21%

Au, Ti, Ag-graphite

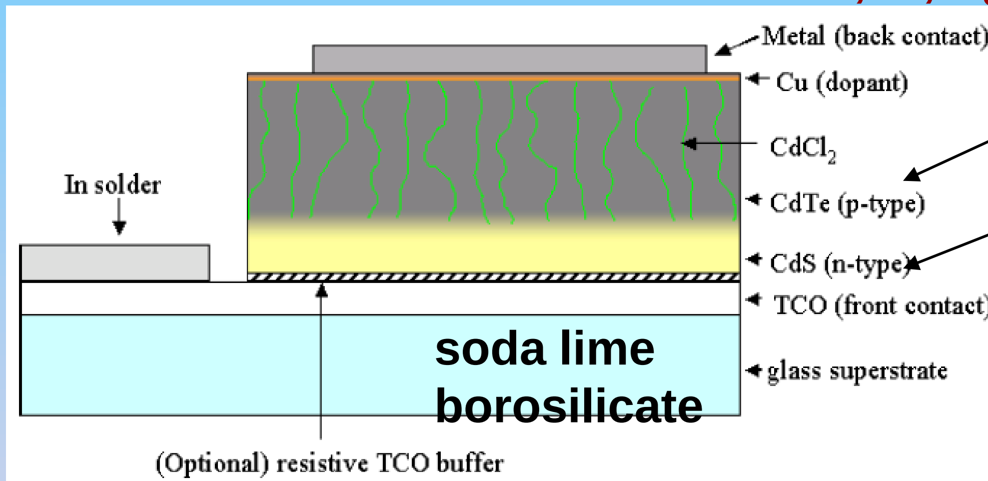

1-8 µm, Eg=1,5 eV

80-300 nm, Eg=2,4 eV

ZnO:Al SnO2:F

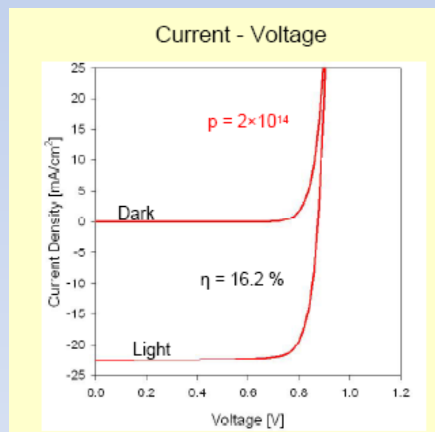

CdTe module

L. Spanhel

Solar Cells of the 3. generation

Nanostructured solar cells – 3. generation cells

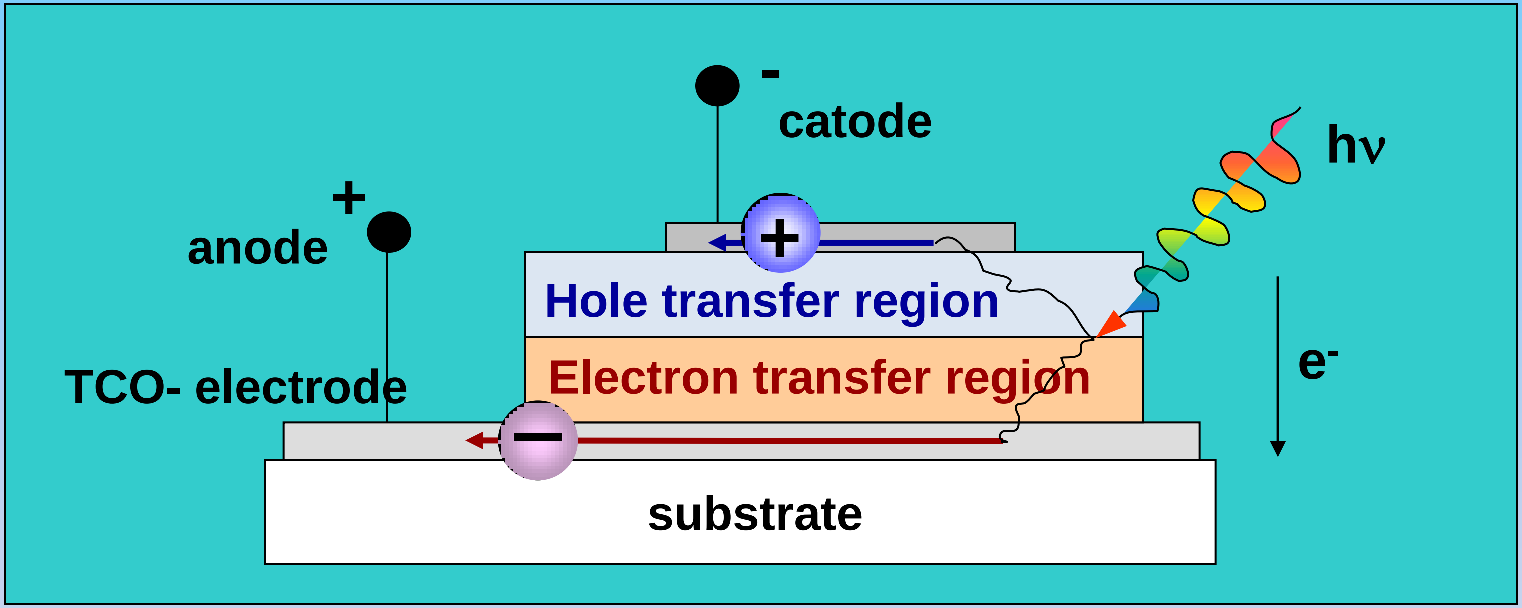

solar nano-antenna design

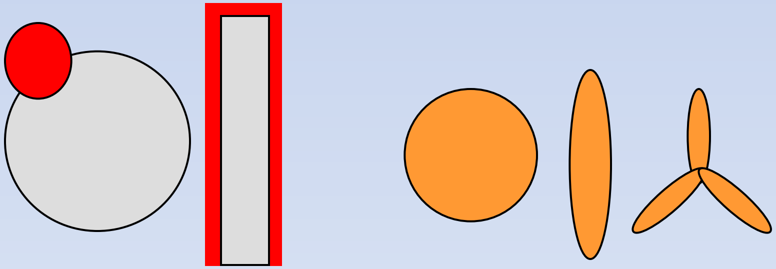

Oxides, M-Chal., fulerenes, dyes

org. polymers
PPV, PEDOT-PSS

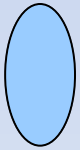

nano-composites

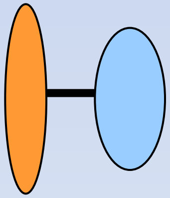

L. Spanhel

„Man-made“ micro-électrodes selon le principe de la nature

Same approach to nanostructured solar cell and photocatalysts

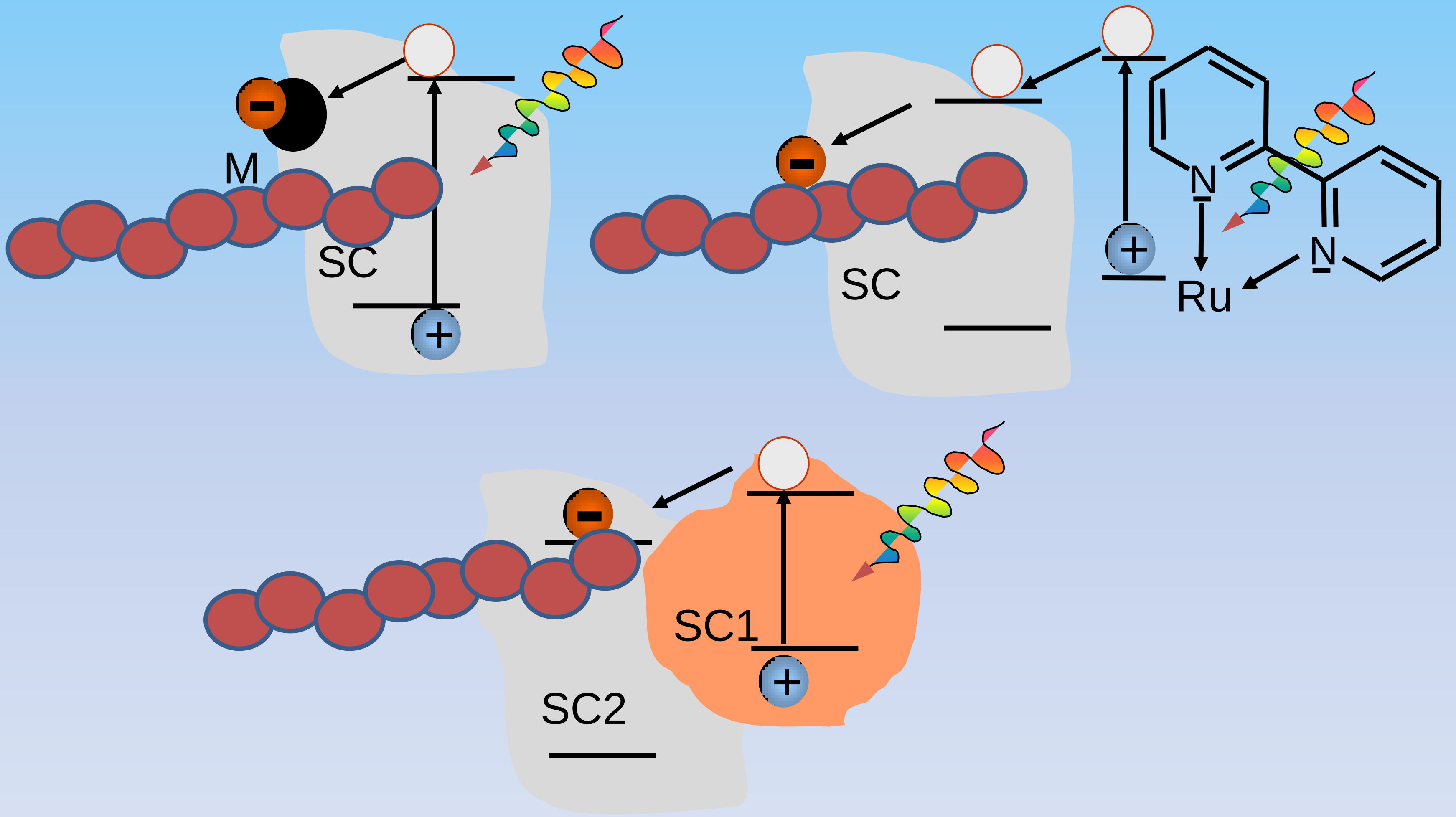

L. Spanhel

1. Jonction SC-métal

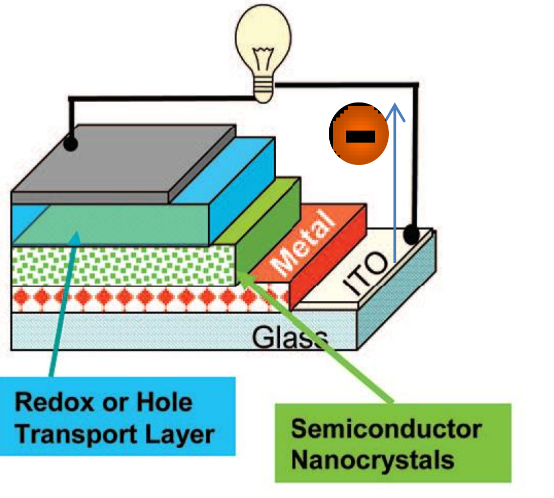

2. SC-polymère org.

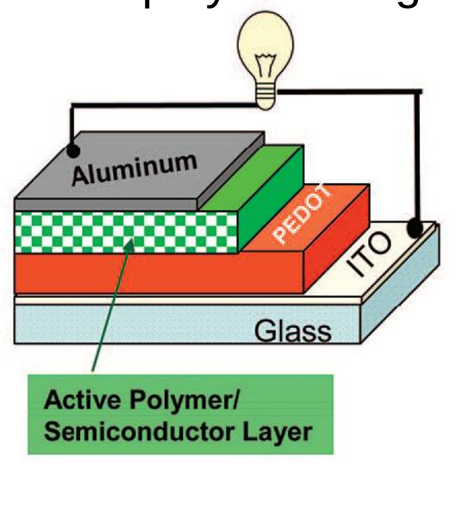

3. SC-SC

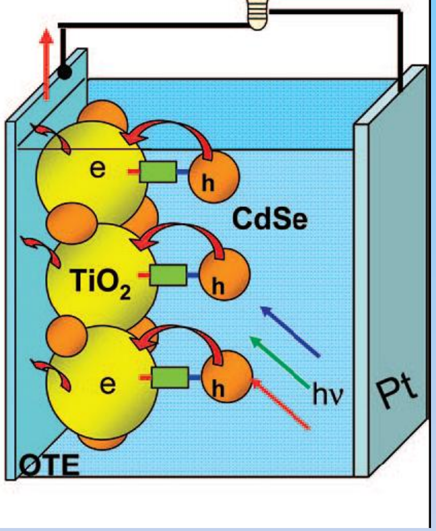

4. Cellule de Grätzel

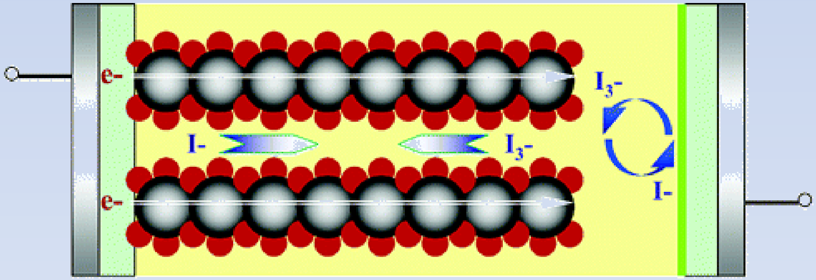

Adopted from P. Kamat et al
ND National Lab, USA

L. Spanhel

1. Jonction SC-métal

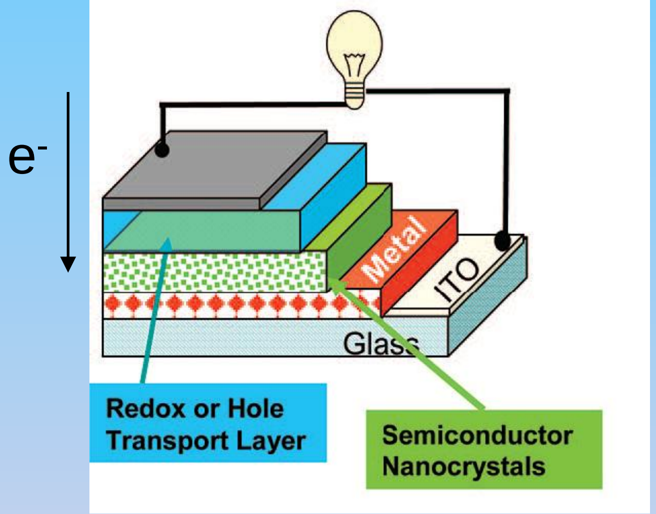

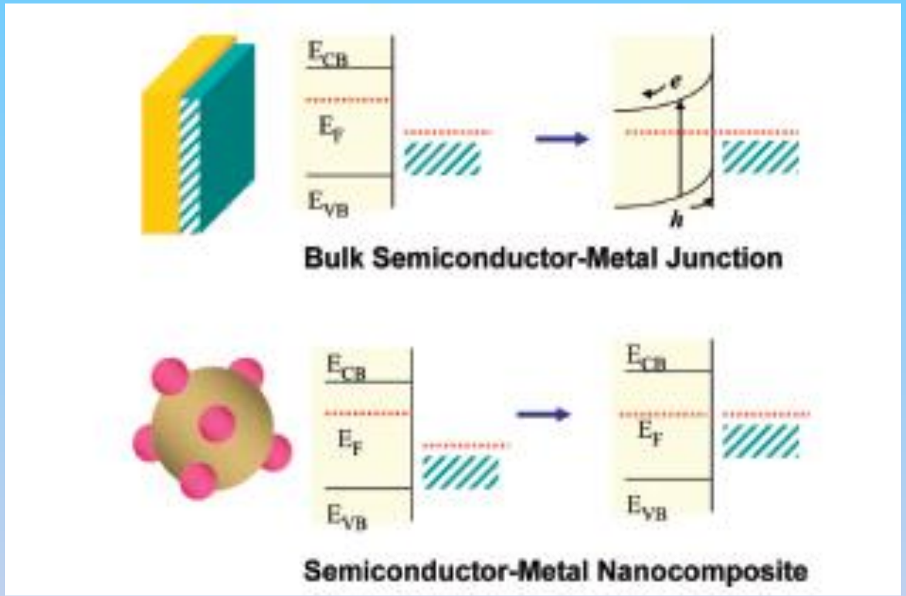

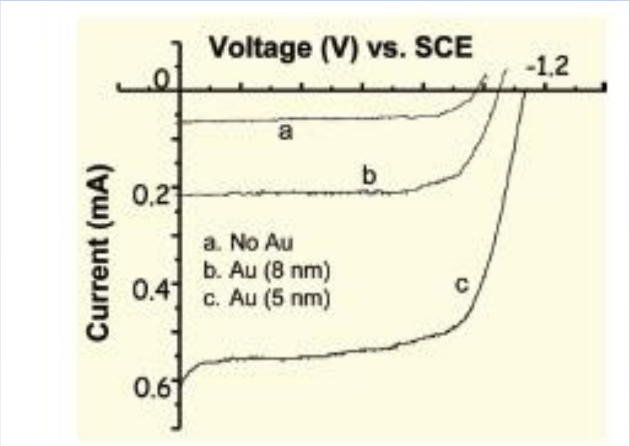

Rendement : 1 - 4%

Kamat et al,
Notre Dame National Lab

Nanocomposites based on Q-CdSe, CdTe (antenna) and organic Poly(3-hexylthiophene) (hole conductor)

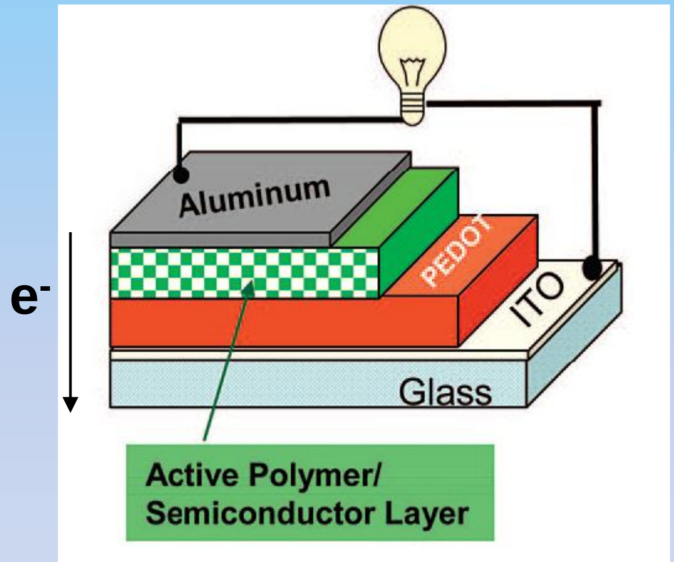

$\eta \sim 5\%$

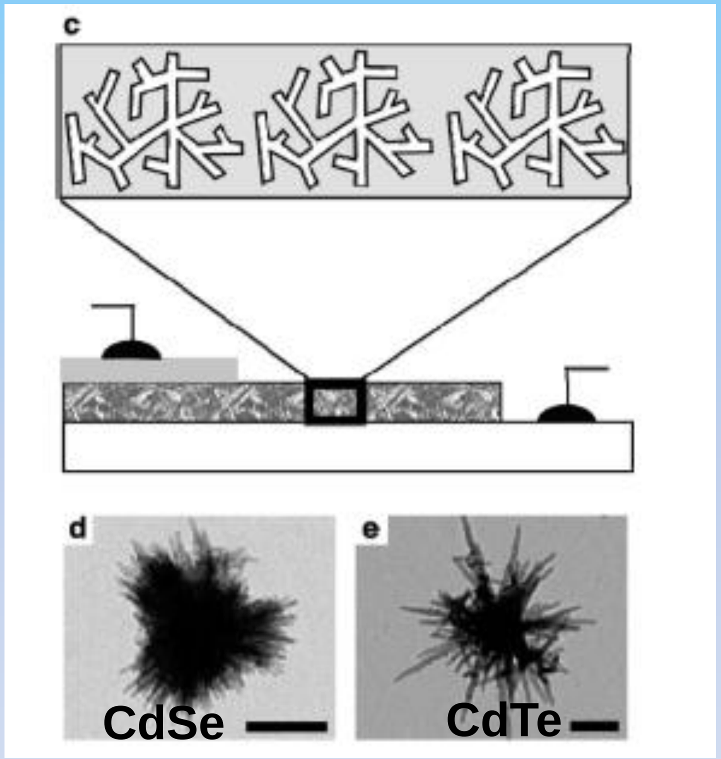

Alivisatos et al, Berkeley

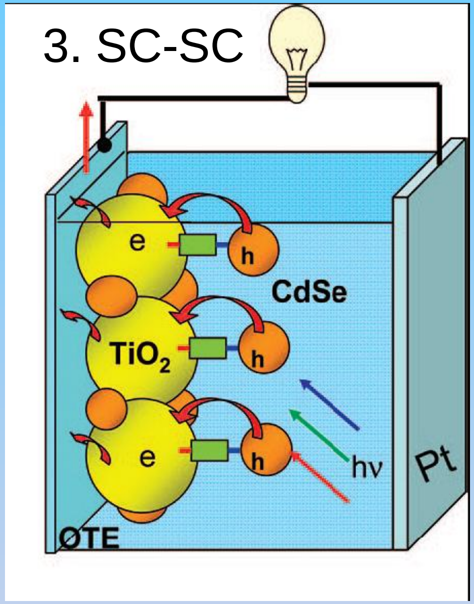
3. SC-SC
e
h
CdSe
TiO2
e
h
hν
Pt
OTE

Rendement ~ 8 %

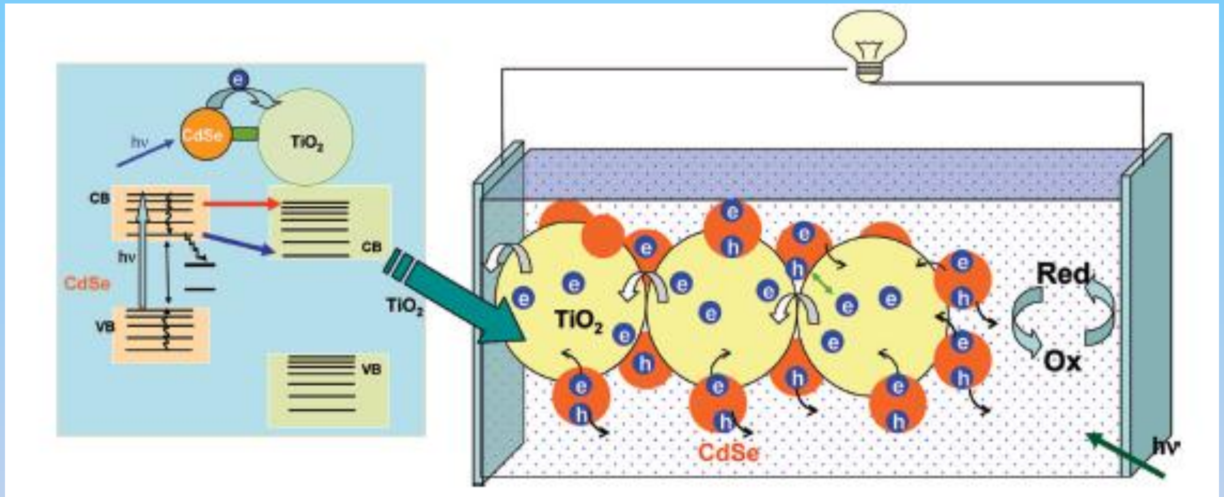
e
hν
CdSe
TiO2
CB
hν
CdSe
VB
CB
TiO2
VB
TiO2
Red
Ox
CdSe
hν

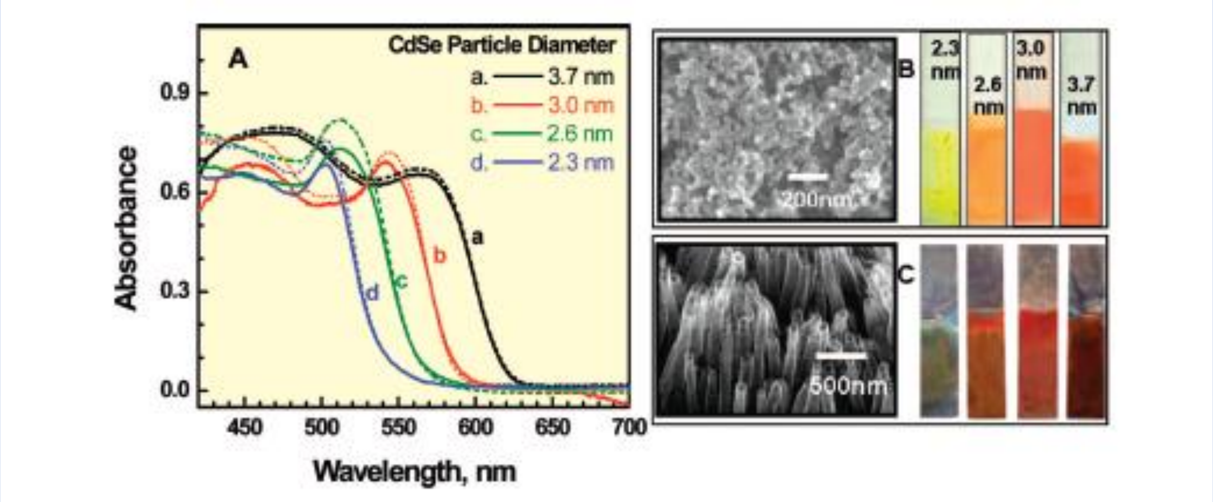
A
CdSe Particle Diameter
a. 3.7 nm
b. 3.0 nm
c. 2.6 nm
d. 2.3 nm
Absorbance
Wavelength, nm
B
200nm
2.3 nm
2.6 nm
3.0 nm
3.7 nm
C
500nm

Cellule de Grätzel (1988)

η ~ 10-12 %

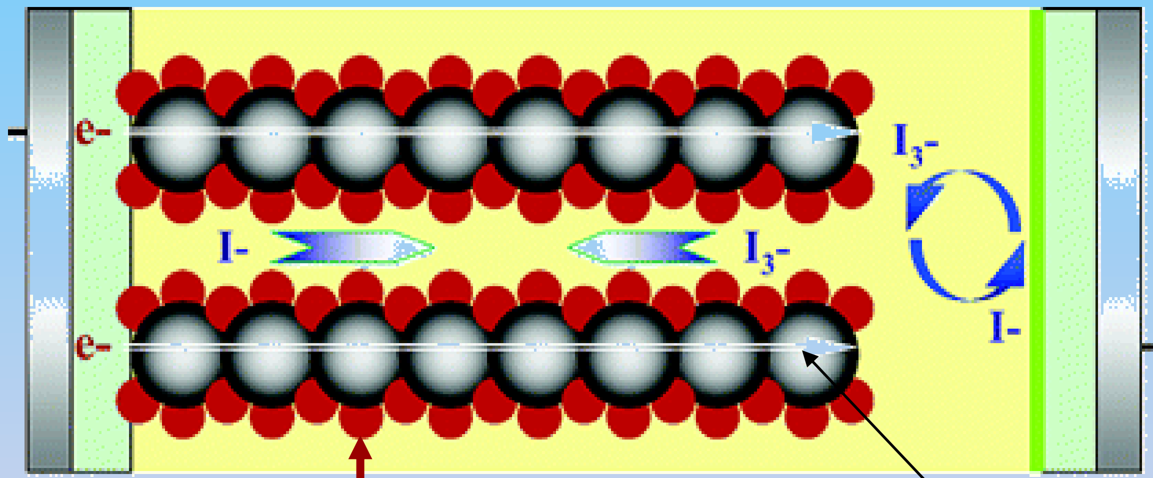

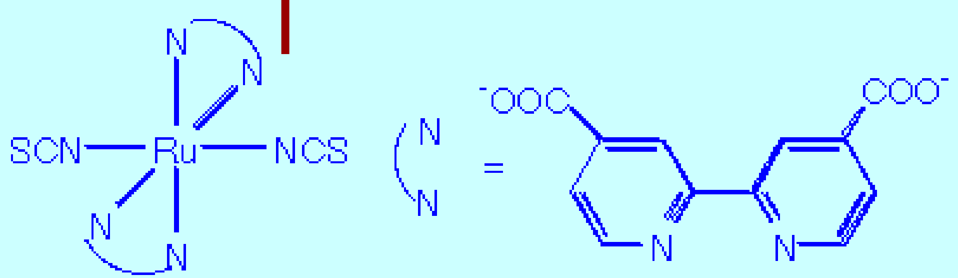

[Ru(dcbpy)$_2$(SCN)$_2$]

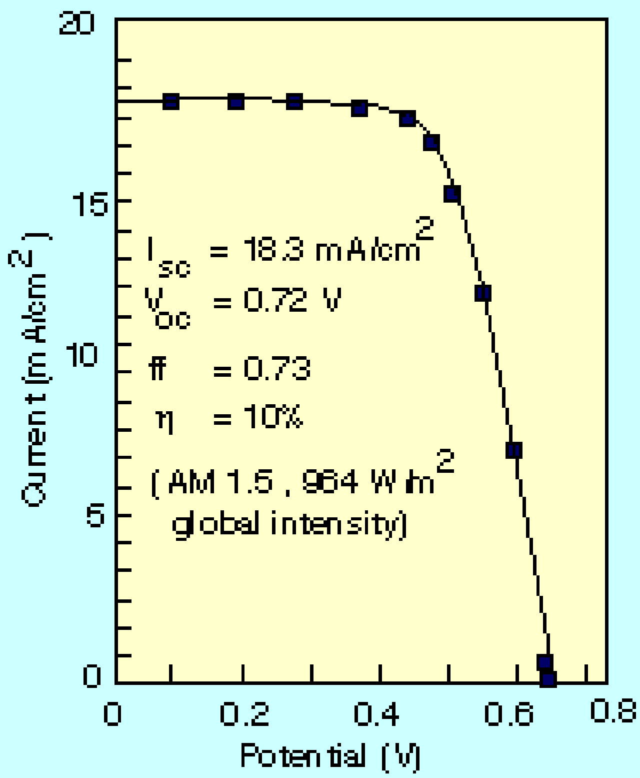

L. Spanhel

Why and how actually is Grätzel cell functioning?

1. Morphology !

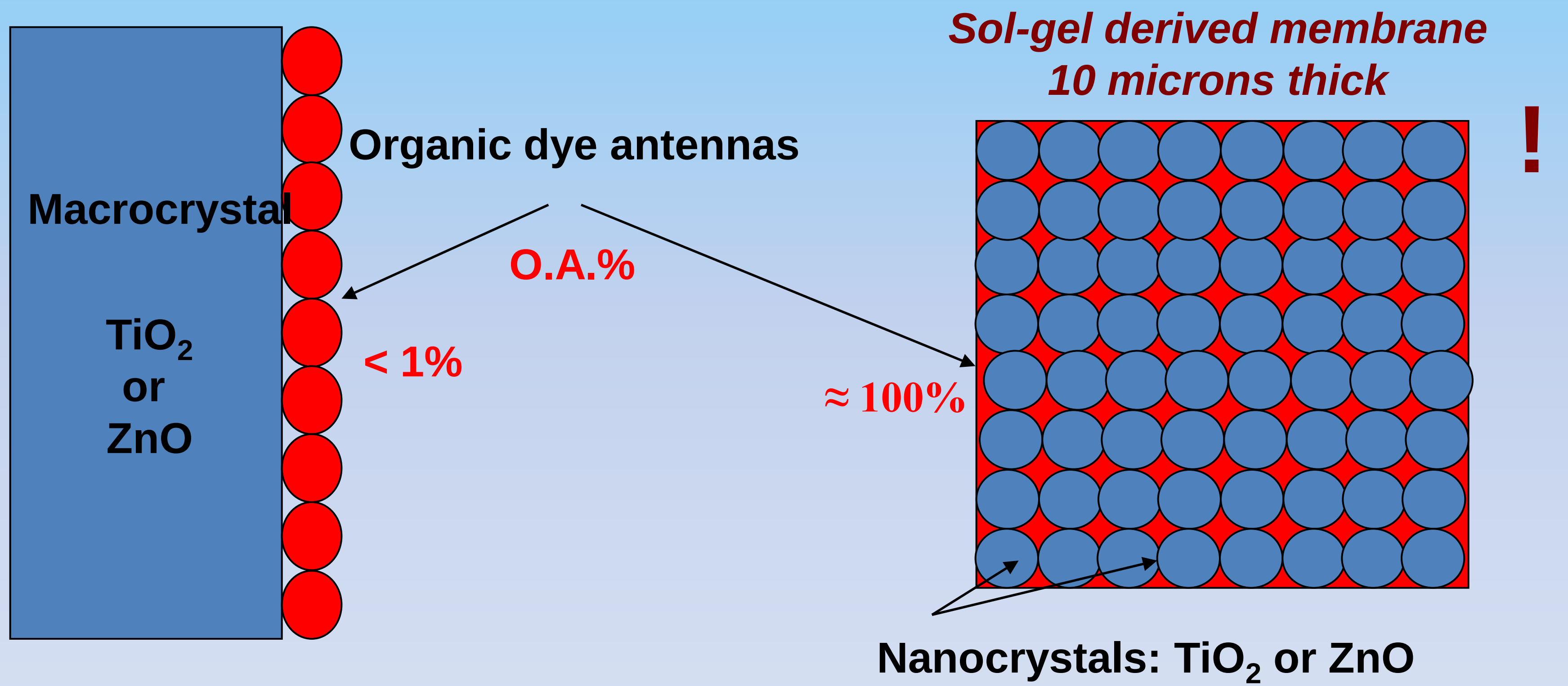

L. Spanhel

ZnO

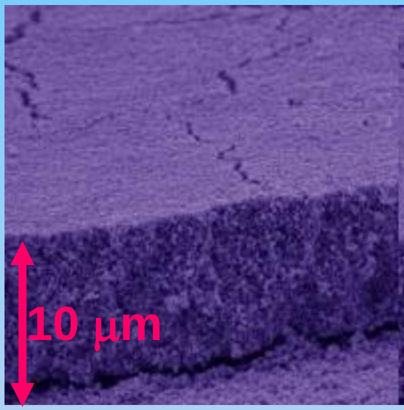

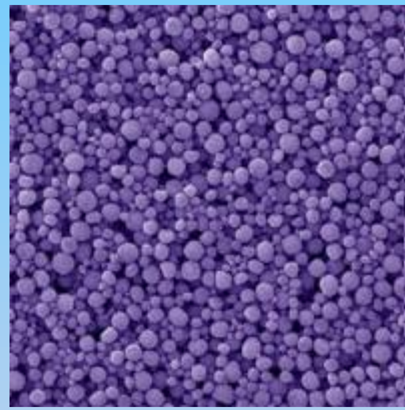

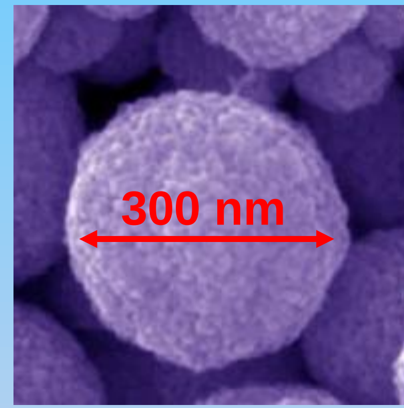

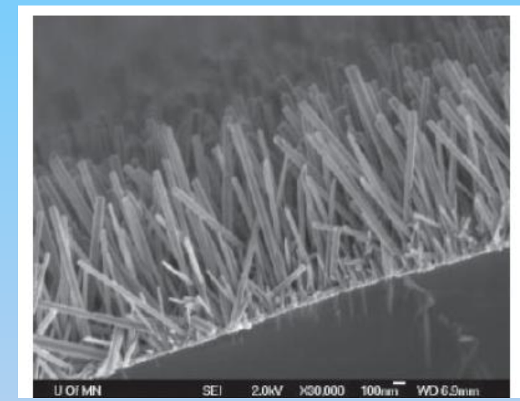

TiO_2

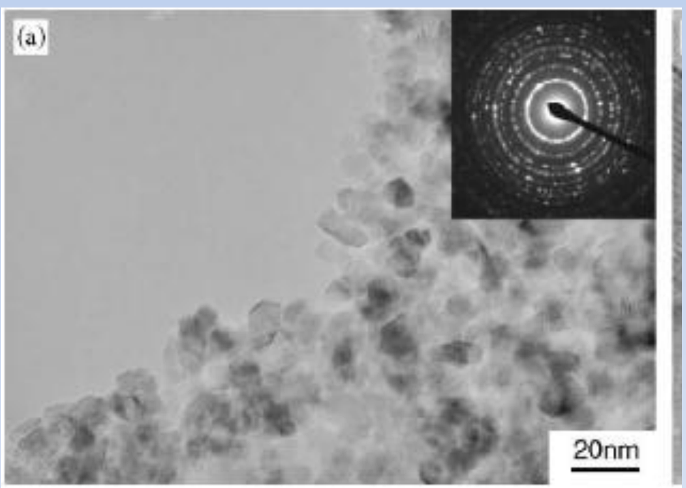

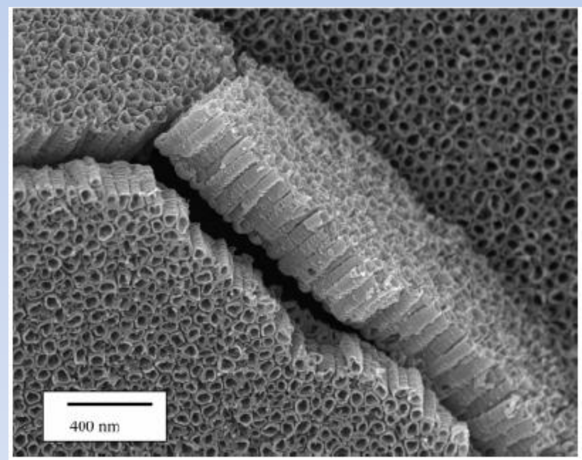

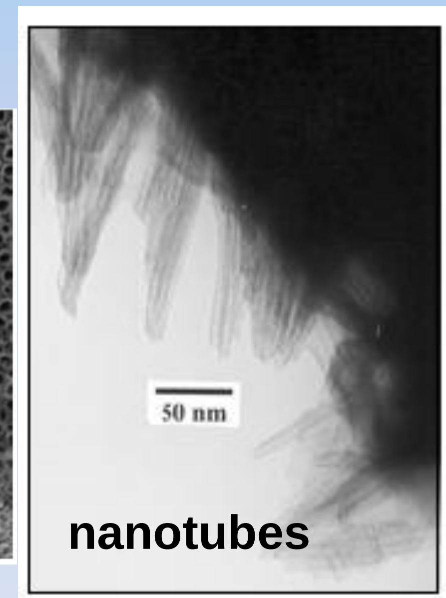

2. Antenna !

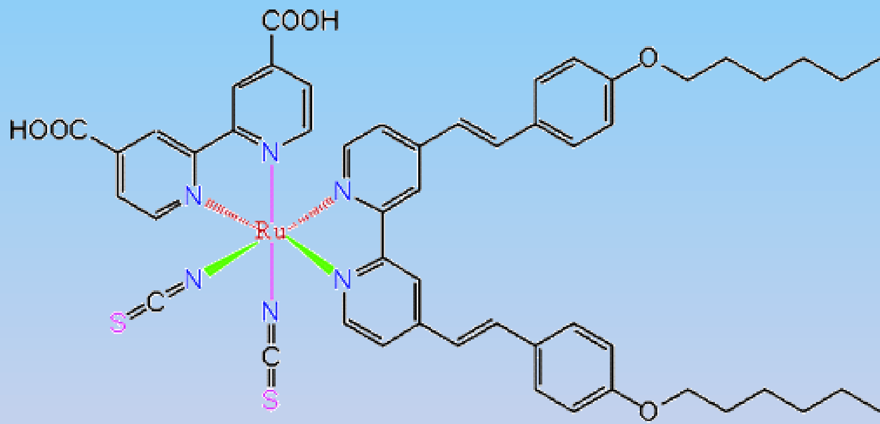

K-19

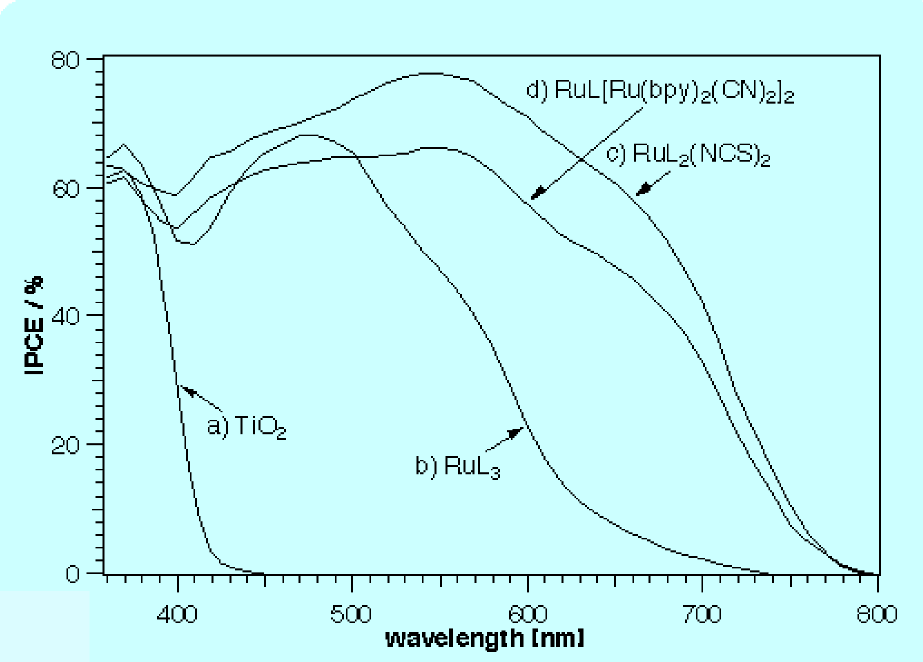

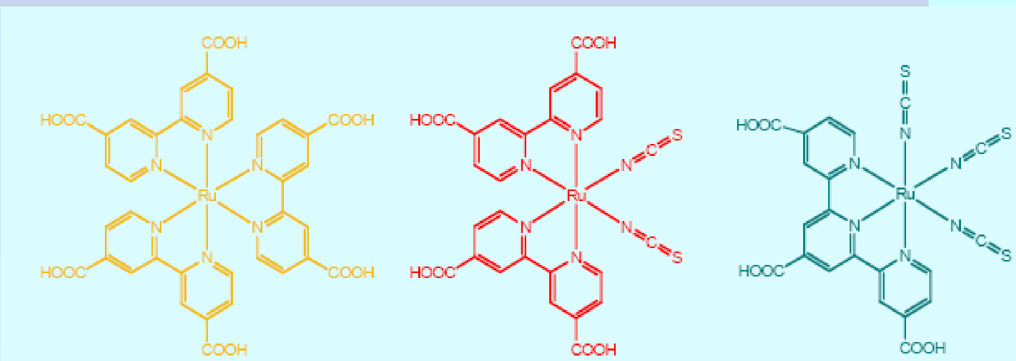

L. Spanhel

3. Cell kinetics !

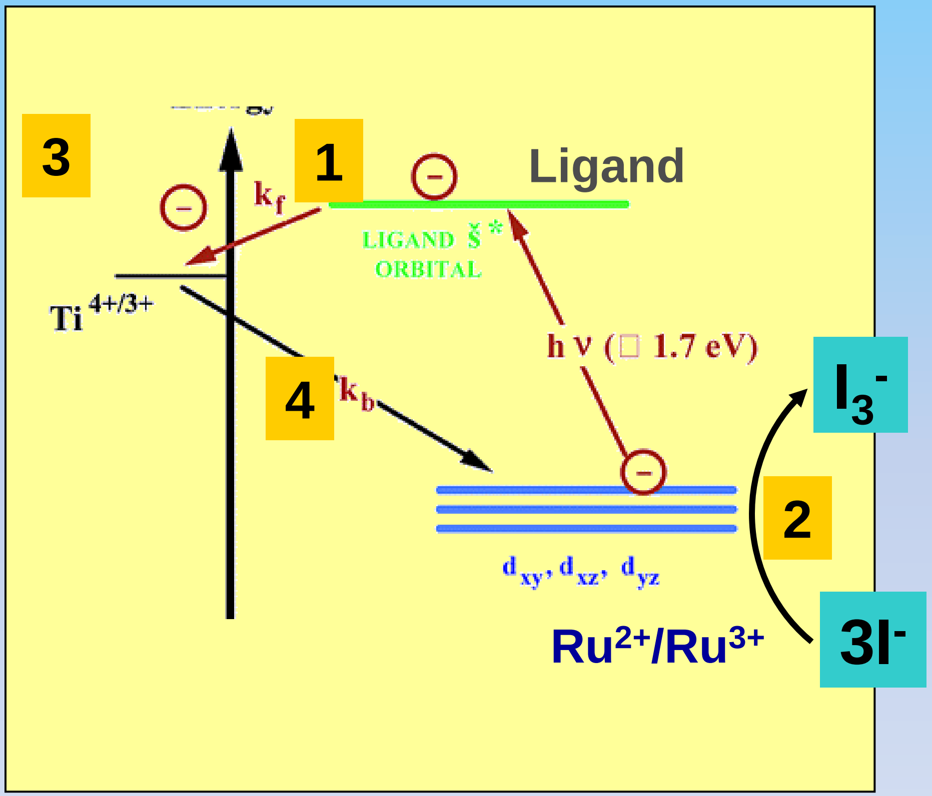

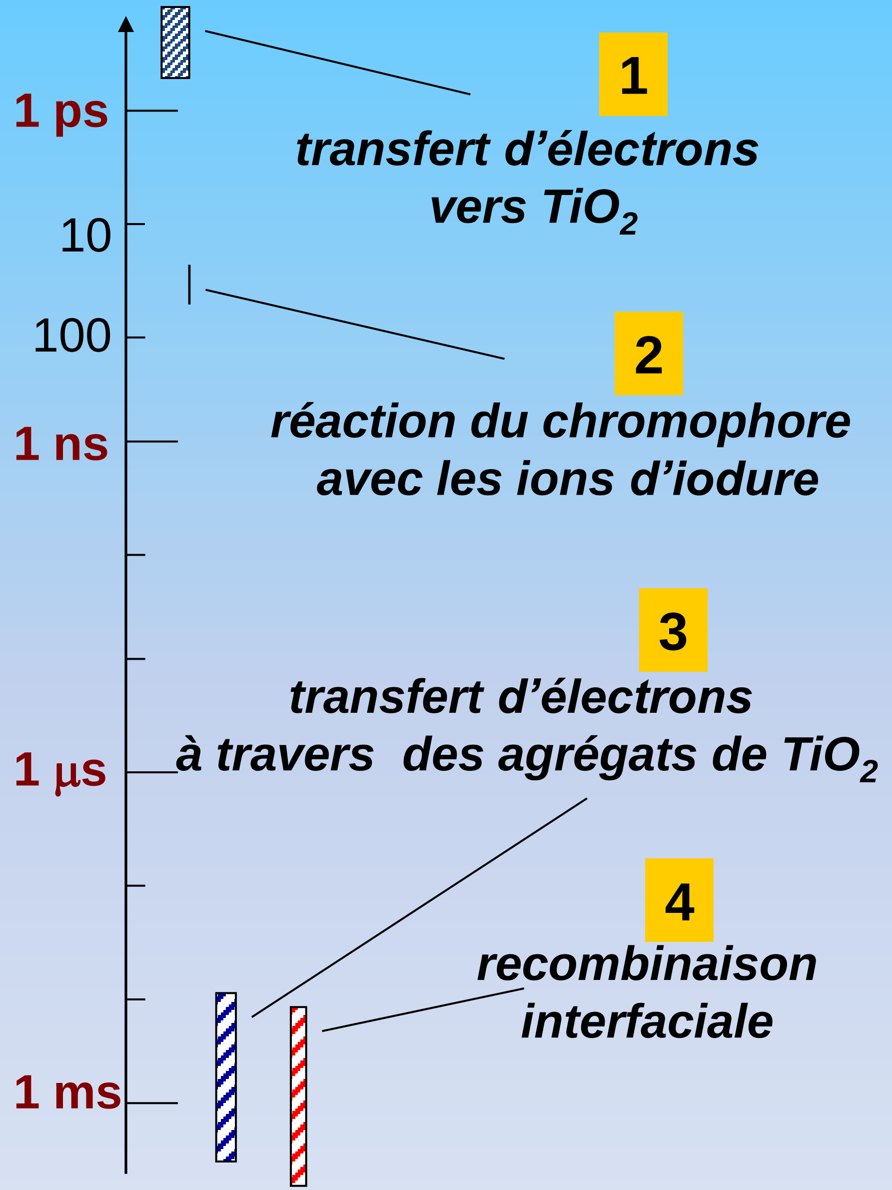

Construction d’une cellule d’après Grätzel

Degussa P 25 TiO_2

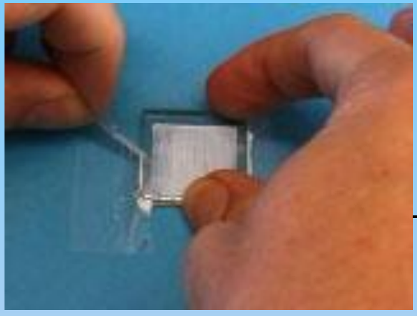

Verre avec FTO

Dye infiltration

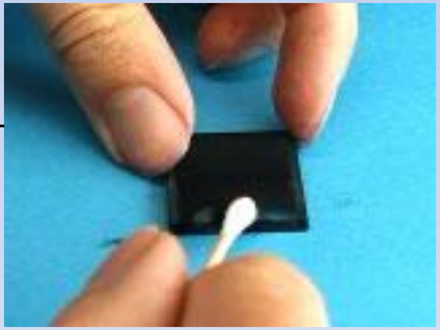

Carbone electrode

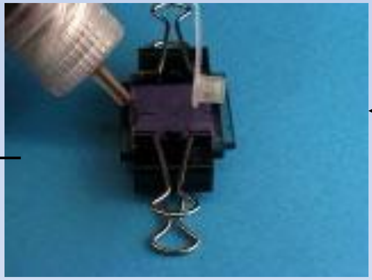

Infiltration du KI_3

Mesure photoélectrique

L. Spanhel

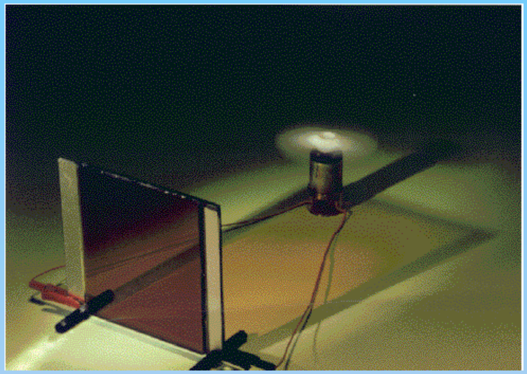

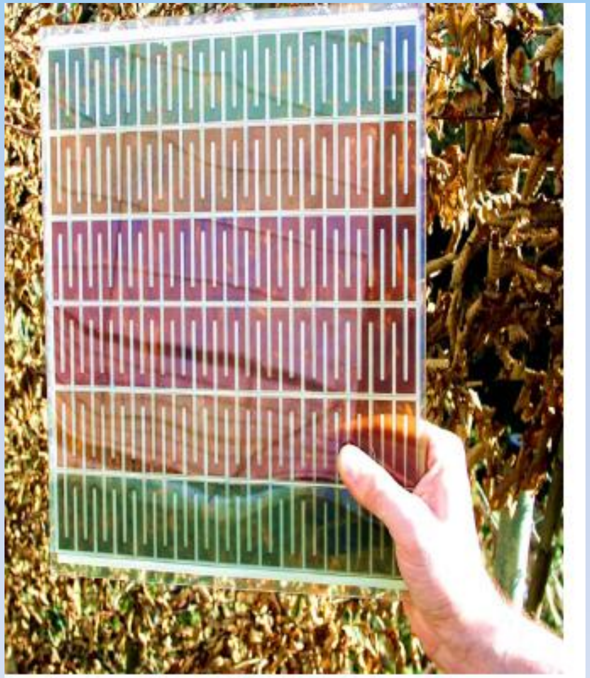

Dr. Andreas Hinsch, FHI, ISE Freiburg Germany

Courtesy Dr. Nam Gyu Park KIST

transparent, colorful, beautiful

Transparency: due to nano-sized (~20 nm) TiO_2 particle film

Color: due to visible light absorption by dye

* DSC costs lower than Si solar cell; 1/4 -1/5 of Si solar cell

L. Spanhel


ply for mobile
24

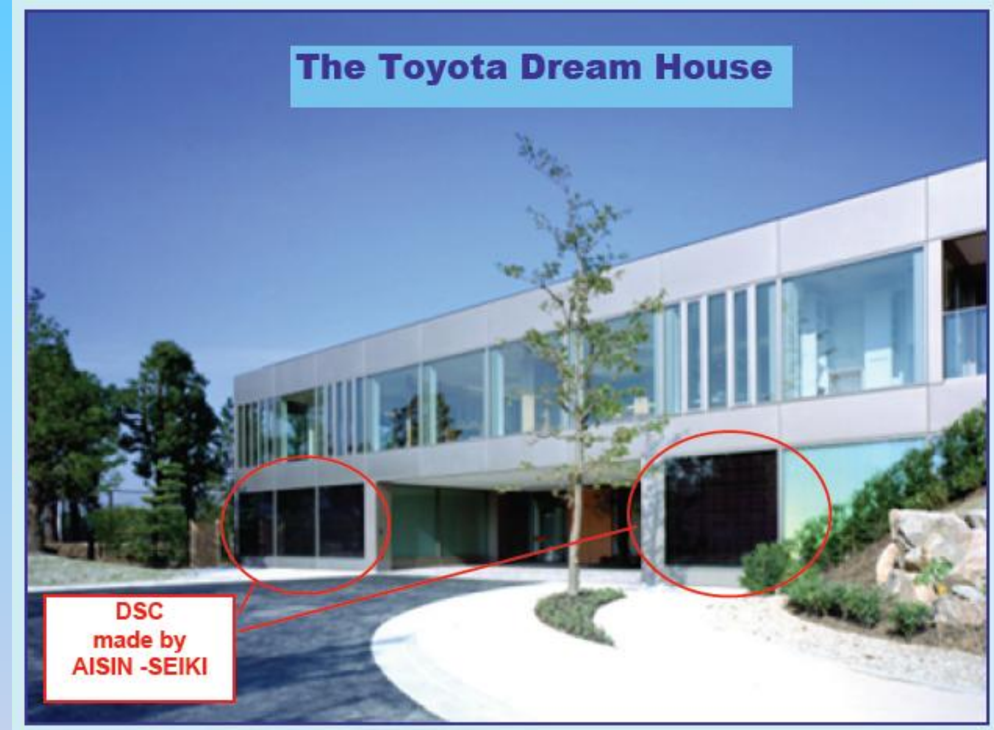
The Toyota Dream House
DSC
made by
AISIN -SEIKI


Kariya City at lat. 35°10'N,
Asimuthal angle: 0°
Facing due south, Tilted at 30°

10:00 – 11:45, 14:00 – 16:00H

2015	Dny v týdnu							Týden		
	Po	Út	St	Čt	Pá	So	Ne	Číslo týdne	Pracovních dnů	Č
Březen							**1**	9	0	
	2	3	4	5	6	**7**	**8**	10	5	
	9	10	11	12	13	**14**	**15**	11	5	
	16	17	18	19	20	**21**	**22**	12	5	
	23	24	25	26	27	**28**	**29**	13	5	
	30	31						14	2	
Duben			1	2	3 L	**4**	**5**	14	3	
	6	7	8	9	10	**11**	**12**	15	4	
	13	14	15	16	17 L	**18**	**19**	16	5	
	20	21	22	23	24	**25**	**26**	17	5	
	27	28	29	30				18	4	
Květen					**1**	**2**	**3**	18	0	
	4	5	6	7	**8**	**9**	**10**	19	4	
	11	12	13	14	15 LL	**16**	**17**	20	5	
	18	19	20	21	22	**23**	**24**	21	5	
	25	26	27	28	29	**30**	**31**	22	5	
Červen	1	2	3	4	5 E	**6**	**7**	23	5	
	8	9	10	11	12	**13**	**14**	24	5	
	15	16	17	18	19	**20**	**21**	25	5	
	22	23	24	25	26	**27**	**28**	26	5	
	29	30						27	2	